Spatial and temporal dependencies of the motion bridging effect: Investigations of an illusory motion

Dissertation

zur Erlangung des mathematisch-naturwissenschaftlichen Doktorgrades

"Doctor rerum naturalium"

der Georg-August-Universität Göttingen

im Promotionsprogramm Biologie

der Georg-August Universität School of Science (GAUSS)

vorgelegt von

Maximilian Stein

aus München

Göttingen, 2019

Betreuungsausschuss

Prof. Dr. Uwe Mattler, Abteilung für Experimentelle Psychologie, Georg-Elias-Müller-Institut für Psychologie, Georg-August-Universität Göttingen

Prof. Dr. Stefan Treue, Abteilung für Kognitive Neurowissenschaften, Deutsches Primatenzentrum

Mitglieder der Prüfungskommission

Referent/in: Prof. Dr. Uwe Mattler, Abteilung für Experimentelle Psychologie, Georg-Elias-Müller-Institut für Psychologie, Georg-August-Universität Göttingen

Korreferent/in: Prof. Dr. Stefan Treue, Abteilung für Kognitive Neurowissenschaften, Deutsches Primatenzentrum

Weitere Mitglieder der Prüfungskommission:

Prof. Dr. Alexander Gail, Abteilung für Kognitive Neurowissenschaften, Deutsches Primatenzentrum

apl. Prof. Dr. York Hagmayer, Abteilung für Kognitionswissenschaft und Entscheidungspsychologie, Georg-Elias-Müller-Institut für Psychologie, Georg-August-Universität Göttingen

Prof. Dr. Hannes Rakoczy, Abteilung für Biologische Entwicklungspsychologie, Georg-Elias-Müller-Institut für Psychologie, Georg-August-Universität Göttingen

Prof. Dr. Sascha Schroeder, Abteilung für Pädagogische Psychologie, Georg-Elias-Müller-Institut für Psychologie, Georg-August-Universität Göttingen

Acknowledgements

First, I wish to express my sincere appreciation to my supervisor, Professor Uwe Mattler. Without his persistent help, this thesis would not have been realized.

I would also like to recognize the invaluable help Professor Robert Fendrich provided during my study.

I am indebted to my department crew including all student assistants who proved monumental towards the success of this thesis.

I would also like to thank Professor Stefan Treue for his constructive suggestions in the thesis committee meetings and to thank him and all members of the examination board for taking the time to read this thesis and participate in the oral examination.

Lastly I wish to acknowledge the support and great love of my family, my mother, my father and my wonderful wife. Thank you for indulging me!

Abstract

The Motion Bridging Effect (MBE) is a visual illusion in which a motion that is not consciously visible creates a visible illusionary movement in a preceding or succeeding stationary ring of points. In the initial MBE study (Mattler & Fendrich, 2010), a ring of 16 points (the *inducing ring*) was rotated at an angular velocity of up to 2250°/s which entails that the point positions on the circumference of the ring were refreshed at temporal frequencies of up to 100 Hz. The observers only saw an uninterrupted outline circle and were unable to judge the rotation direction of the inducing ring. However, when the inducing ring was replaced by a ring of 16 stationary points (the *test ring*), the stationary ring seemed to visibly rotate to a standstill, mainly in the same direction as the inducing ring was rotating. This demonstrates that although the inducing ring rotation was not consciously perceived, its motion was processed by the visual system. Similar results were found when the test ring preceded the inducing ring: The test ring seemed to accelerate in this case. In this thesis the contributions of temporal frequency, retinal eccentricity, the separation between the points of the test ring, and the inducing ring start and stop position are discussed as mediators of the effect. Furthermore, it is considered that the illusionary movement in the MBE is caused by a new kind of apparent motion, the ring rotation illusion (RRI), whose spatial and temporal dependencies and differences to the MBE are demonstrated. Finally, it is shown that the MBE, which in all previous studies was only demonstrated on an analog oscilloscope, can also be reliably found with an LCD monitor.

Table of Contents

1. Introduction

Human perception of temporal changes is limited in everyday life. Very slow temporal changes, such as a sunset, are not perceived directly. The observer notices that it has suddenly become night, although the brightness has continuously decreased in the last few minutes. Similarly, very rapid temporal changes, such as the image change of a cathode ray tube monitor, cannot be detected. The viewer perceives a continuous image, although the monitor only displays a new image approximately every 17 ms when the refresh rate is set to 60 Hz.

The limits of human perception of temporal changes can be investigated by flicker fusion experiments. The best known flicker fusion experiment was conducted by Kelly (1961). He showed subjects a so-called "Ganzfeld" stimulus with a radius of 30° visual angle, which had no sharp edges and whose brightness was modulated sinusoidally over time with a certain frequency. The aim of the study was to use the method of adjustment to determine exactly the amplitude of the sinusoidal modulation at which the flickering stimulus was perceived as stationary. The data showed that the visual system was particularly sensitive to temporal frequencies from 5 to 30 Hz. Kelly's data also revealed the critical flicker frequency (CFF; Cornsweet, 1970). The CFF is the maximum frequency at which a flickering light starts to be perceived as stationary by test subjects. Kelly's flicker fusion threshold was approximately 40 Hz, but it can be higher in the periphery of the retina (Hartmann, Lachenmayer, & Brettel, 1979).

The CFF is only one of many temporal limitations of the visual system. Holcombe (2009) assigns the CFF to a group of fast temporal limits located at a temporal frequency of approximately 30 to 50 Hz. Another limit that can be assigned to this group is the limit of motion perception that could be based on similar neuronal mechanisms (Holcombe, 2009). In everyday life, the effects of this limit can be easily seen by looking at a rotating fan. At a low rotation level, its direction of rotation is clearly detectable. If the speed of rotation is increased by increasing the voltage, the fan blades appear to form a disc-shaped stationary surface, at least when illuminated by sunlight alone. The rotational speed of the fan changes the frequency with which the light rays reflected from the fan blades hit identical positions on the retina. If the temporal frequency of this periodicity is too high, movement can no longer be perceived.

The upper limit of the perception of movement is demonstrated by experiments carried out by Burr and Ross (1982). They showed subjects gratings that were sinusoidally modulated in intensity over space and time. By changing the contrast of the stimuli, test subjects were supposed to determine the threshold at which movement of the grating is barely perceptible by the method of adjustment. Interestingly, the perception of motion was not limited by the speed of motion, which was varied by adjusting the spatial and temporal sinusoidal modulation, but only by the temporal frequency of the stimulus (the frequency at which the sinusoidal grating returns to its initial position). The data from Burr and Ross also illustrate the temporal frequency limit at which a movement is perceived as stationary, and this limit is approximately 40 Hz, similar to the CFF. This limit of motion perception can be interpreted as the limit of neuronal coding of temporal distances. If, for example, cells on the retina are repeatedly stimulated with temporal frequencies above 40 Hz, the temporal signal could be lost and consequently no encoding of the temporal modulation and a subsequent perception of movement could take place.

In 2010, Mattler and Fendrich published a study questioning the previously proposed limits of encoding temporal change. Using the screen of an analog oscilloscope equipped with a particularly fast decaying phosphor, they first presented a rotating *inducing ring* of 16 points whose temporal frequency varied between 11.1 and 100 Hz. The temporal frequency of the inducing ring was defined by the time it took for the ring to return to its starting position. Subjects were instructed to judge the perceived direction of rotation (clockwise vs. counterclockwise). At temporal frequencies above about 40 Hz, this was no longer possible for subjects, as the points of the presented ring merged into a solid line. Interestingly, however, the direction of movement of the inducing ring could be made visible again by a second stimulus. When the authors presented a stationary *test ring* of 16 points shortly after the inducing ring, subjects reported to have seen an illusionary movement, which a quarter of the subjects spontaneously described as deceleration of the test ring. However, Mattler and Fendrich's new illusion does not only consist of the perception of the illusionary movement. Surprisingly, in up to 80% of the trials, the illusionary motion of the test ring was reported as going to the same direction in which the inducing ring rotated. Strikingly, subjects were unable to discriminate the rotation direction of the same inducing ring any better than chance, when the stationary test ring was not presented.

Moreover, the strength of the directional correspondence depended on the velocity of the inducing ring. Mattler and Fendrich (2010) varied the temporal frequency of the inducing

ring by changing its angular velocity in five steps (250, 750, 1250, 1500, and 2250 angular °/s corresponding to approximately 11.1, 33.3, 55.5, 66.7, and 100 Hz). In the condition in which only the inducing ring was shown, a pattern of results consistent with the limits for the detection of motion proposed by Burr and Ross (1982) was found. In Experiment 1 of the initial study, the rotation direction of the inducing ring is clearly detectable at a temporal frequency of 11.1 Hz. The discrimination performance of participants decreased steeply at 33.3 Hz and was only at chance level at frequencies of 55.5 Hz or higher. Fascinatingly, a similar pattern of results has been found in conditions in which the inducing ring was followed by the test ring: An increase of the temporal frequency led to a decrease in participants' discrimination performance. However, this decrease in discrimination performance was by no means as strong as when the inducing ring was presented alone. Even at the highest speed (2250 angular °/s), the illusory movement was perceived corresponding to the inducing ring direction in more than 50% of the trials. The perceived direction of the illusory motion thus also depends on the speed of the inducing ring and therefore its temporal frequency. Mattler and Fendrich concluded from these results that an unconscious encoding of the direction of motion of the inducing ring is possible despite its high temporal frequency, even if the motion cannot be consciously perceived. The conclusion of unconscious encoding of motion direction is supported by two decisive criteria of motion perception: The direction of the inducing ring appears to be encoded and this directional detection depends on the temporal frequency of the stimulus.

In another experiment of Mattler and Fendrich (2010) the stationary test ring was preceding the rotating inducing ring. Again, an illusionary movement was seen, which was described by some subjects as an acceleration of the test ring. Similarly, the direction of the illusory motion corresponded with the actual rotation direction of the inducing ring and the strength of this correspondence depended on the temporal frequency of the inducing ring. In their velocity updating hypothesis, the authors assume that the visual system tries to ensure continuity between a stimulus rotating at a very high velocity and the stationary stimulus whose velocity has a value of 0°/s. If this continuity is established, the test ring stops or speeds up visibly. Since a bridge is established between two stimulus states, Mattler and Fendrich called this illusionary motion the motion bridging effect (MBE). A critical aspect of the MBE is that there is a directional correspondence between the direction of rotation of the inducing ring and the direction of the illusionary motion. The strength of this directional correspondence is measured as sensitivity (d') in their investigation and in all investigations

presented in this thesis. Sensitivity (d') is defined as the difference of the Z-transformed rate of clockwise responses to a clockwise rotation when all clockwise rotations are considered and the rate of clockwise responses to a counter-clockwise rotation when all counter-clockwise rotations are considered (Macmillan & Creelman, 2005).

In their study, Mattler and Fendrich (2010) not only presented the discovered phenomenon, but also showed, that the MBE depends on temporal and spatial factors, such as the presentation duration of the inducing ring or the temporal and spatial distance between the two rings. For example, the direction correspondence shows a clear inverted U-shaped function when the temporal interval between the two rings (inter stimulus interval; ISI) is varied. With a small ISI, d' is low, increases to a maximum at 60 to 90 ms, and then drops again at an ISI of 180 ms. While the authors mention that there is a similar dependence on ISI for classical apparent motion (e.g., Korte, 1915), they interpret their results in the sense of intermediate perceptual stages generated during the brief temporal pause, which is consistent with the velocity updating hypothesis.

2. Studies

This thesis comprises four studies that were carried out in collaboration with Uwe Mattler and Robert Fendrich. A manuscript was written based on each of these investigations. The manuscripts are currently in different stages of editing: The first manuscript has already been published and the fourth manuscript will be submitted for publication shortly, whereas the second and third manuscripts may undergo more substantial editing before publication. All four manuscripts are appended to this thesis and each study is additionally summarized below.

In the four studies, numerous spatial and temporal parameters concerning the MBE were varied, some of them exploratively. Despite the exploratory character of some of the experiments, all results were evaluated using inferential statistics to uncover and clarify patterns in the collected data. I would like to emphasize that in our experiments the reliability of the collected data is warranted in particular by the fact that most of the investigated independent variables were parametrically varied and all findings remain stable throughout the investigations.

2.1 Results of the study "Stimulus dependencies of an illusory motion: Investigations of the Motion Bridging Effect"

In order to identify further temporal and spatial dependencies of the MBE, we systematically varied the number of points and the diameter of the inducing ring and test ring in three experiments. Increasing the number of points had the effect of increasing the temporal frequency of the inducing ring, since the increase in the number of points at constant angular velocity is accompanied by a reduction in the number of steps taken before the inducing ring returns to its starting position. The variation in diameter affected the retinal eccentricity of the stimuli as the larger rings are processed in more peripheral regions of the retina. Note that both manipulations led to an increase of the point distance in the test ring. The stimuli were presented on a smaller oscilloscope than in the original study (50 cm vs. 12.5 cm diameter; Mattler & Fendrich, 2010). The stimulus sequence was similar to the original study, but only the condition where the inducing ring is presented first was included in the present study. As in the original study, in each experiment the angular velocity of the inducing ring was varied over all conditions, but only in four steps (250°/s, 750°/s, 1500°/s, and 2250°/s).

In Experiment 1, we varied the number of points of the inducing ring and test ring in three steps (12, 16, and 20 points), with the inducing ring having as many points as the test ring in each trial. Both the condition in which only the inducing ring was shown and the MBE condition in which both rings were presented showed a decrease in sensitivity (d') with increasing number of points. This decrease in sensitivity can be attributed to the increase in the temporal frequency of the inducing ring. The result in the condition in which only the inducing ring was shown is consistent with the assumption of Burr and Ross (1982), because the direction of the inducing ring could no longer be detected above chance if the temporal frequency was greater than 40 Hz, regardless of whether the temporal frequency was determined by the number of points or the rotational speed. In the MBE condition, in which the test ring was also presented, it could be argued similarly that the reduction in performance is caused by the increased temporal frequency of the inducing ring. However, the limit of the MBE is higher than the limit of the conscious perception of motion (above 125 Hz).

In a second experiment we varied the diameter of the stimuli in three steps (3.5°, 5.5°, and 7.5° viewing angle), with the inducing ring being the same size as the test ring in each trial. It was found that the sensitivity increases significantly with higher ring diameters. This effect of diameter could be attributed to the fact that the periphery of the retina is more

sensitive to high temporal frequency changes (Breitmeyer & Ganz, 1976; Hartmann et al. 1979) and therefore shows a preference for the rapid motion of the inducing ring (Sekuler, 1975). However, we could not detect any effect of the stimulus diameter if only the inducing ring was shown. The results of Experiments 1 and 2 could, however, also be the result of a change in the spacing of the test ring points. Both an increase in the number of points and a reduction in the diameter of the rings reduce the distance between the points in the test ring. In order to evaluate the possibility that the results of Experiments 1 and 2 are due to a change in the distance between the points in the test ring, we performed Experiment 3.

In Experiment 3, we kept the distance between the points constant by simultaneously increasing the diameter of the rings when we increased their number of points. In this experiment there was no difference in sensitivity between the 12, 16 and 20 points condition at any level of velocity. The results of Experiment 3 can be interpreted in two ways. It is possible that the MBE is modulated by the temporal frequency of the inducing ring, both when manipulating the angular velocity and when varying the number of points. In addition, the MBE is larger the further the inducing ring is shown in the periphery of the retina. In Experiment 3, these two effects balance each other out. Another possibility is that the effect of the number of points and diameter is caused by the difference in spatial distance between the test ring points. I will return to this argument in my final discussion. The influence of the spatial distance between the test ring points brings up the possibility that the illusionary movement of the MBE is due to an apparent motion that occurs when the seemingly stationary inducing ring is transformed into an actually stationary test ring. This explanation makes a prediction regarding the stimuli of the MBE: if instead of a rotating ring an actual stationary ring is shown, the illusionary motion should still be visible.

2.2 Results and discussion of the study "Ring Rotation Illusion and the influence of heuristics on apparent motion"

Stein, Fendrich, and Mattler (2019) consider the possibility that the MBE is related to apparent motion, since the MBE is an apparent transformation from a seemingly stationary outline circle to a veridically stationary test ring. This explanation is supported by the fact that the MBE depends critically on both the temporal distance of the stimuli, which is influenced by the ISI (Mattler & Fendrich, 2010), and the spatial distance of the transformation, which is influenced by the point distance (Stein et al., 2019). Stein et al. even argue that the MBE consists of two processes: An ambiguous apparent motion perceived

from the inducing ring to the test ring and a directional signal that influences the direction of the ambiguous apparent motion percept. The two process approach makes a clear prediction: if the MBE is based on an apparent motion that is perceived independently of the direction signal, the illusory motion should also be visible if the rotating ring does not move, but an actually stationary continuous ring is shown. Preliminary observations showed that this was the case and that the generated illusionary motion is very similar to that of the MBE. The illusionary rotation, which occurs when a stationary ring of points is displayed after a stationary solid ring, we call ring rotation illusion (RRI). In the second investigation, we wanted to know whether the RRI shows similar dependencies on the ISI and point distance to investigate its relationship to apparent motion and to the MBE.

In the first experiment we therefore varied temporal (the ISI and the duration of stimuli) and spatial parameters (the number of points and the diameter of the rings) of the RRI. Due to the absence of a direction signal, it is impossible to determine the sensitivity (d') of subjects to the direction of rotation and use it as a dependent variable. Therefore, in this study we have determined the perceived clearness of the RRI (and in Experiment 2 also the motion distance) with the help of a rating scale because other studies have shown that rating scales can reliably reproduce typical dependencies of apparent motion (Downing & Treisman, 1997; Hubbard & Ruppel, 2011, 2018; Kahneman, 1967). The motion clearness judgments of the RRI were similarly influenced with respect to the ISI as the sensitivity measure (d') of the MBE. Motion is judged to be most pronounced when the ISI is 60 to 90 ms. However, the duration of the stimuli influences this dependence. The maximum motion clearness shifts to the ISI of 0 ms if the stimuli are shown for 500 ms. Interestingly, Kahneman (1967), who investigated classical apparent motion, similarly found a maximum of the perceived apparent motion at an ISI of 75 to 100 ms. This maximum shifted to 0 ms when the stimulus duration was increased to 800 ms. With small limitations, the results regarding the ISI can also be reconciled with results regarding the line motion illusion (LMI). Hubbard and Ruppel (2011; 2018) used a measure very similar to motion clearness they called motion strength and found that it decreases with increasing stimulus onset asynchrony (SOA). However, in their study the stimuli were presented overlapping in time, which could be the reason that the authors could not find an initial increase in motion strength.

With respect to the spatial parameters, the mean motion clearness behaves exactly opposite to the sensitivity of the MBE. The motion was judged to be most pronounced when the number of points was very large or the diameter of the rings was very small. In contrast to

the sensitivity of the MBE, the clearness of the RRI therefore increases with a smaller point distance. The results concerning the distance of the transformation cannot be reconciled with all results of other apparent motion phenomena. Although Korte (1915) finds a decrease of the perceived apparent motion with an increase of the spatial distance with small ISIs (in this case 183 ms) in classical apparent motion, Hubbard and Ruppel (2011) could not detect any change of the motion strength with regard to the line motion illusion if the line length is varied. However, they found an increase in perceived speed and suggested that this increase in perceived speed should be accompanied by a reduction in motion strength. Taken together, the results of Experiment 1 do not show a conclusive pattern, but they give first indications that the RRI, like e.g., classical apparent motion, depends on the temporal and spatial distance between the two stimuli. In the case of RRI, however, the spatial distance is defined by the distance of the transformation of the stationary continuous ring into the pointed ring.

In the other two experiments we compared the two phenomena, the MBE and the RRI. Experiment 2 aimed to investigate whether the motion signal in the rotating ring of the MBE has an effect on the perceived clearness of the RRI. We instructed subjects at both the MBE, where we chose a rotating ring speed of 1500°/s, and the RRI to judge the clearness of motion and distance traveled. In order to ensure that any differences were caused by the direction signal of the rotating inducing ring and not by a visible difference between the stationary inducer of the RRI and the rotating inducer of the MBE, subjects performed a discrimination task to ensure that the two stimuli could not be distinguished. In fact, there was a small but significant difference in the perceived motion clearness and distance. The motion of the MBE was judged to be both more distinct and traveling over a longer distance. This difference was especially found in trials where motion clearness was assessed and the illusionary motion of the MBE was perceived in the same direction as the rotating inducer.

In the third experiment, too, the clearness of the illusory motion produced by the rotating inducer was consistently judged to be higher than that produced by the stationary inducer. Since the number of points, the diameter and the ISI were also varied in this experiment, it was possible to investigate to what extent the motion clarity of the illusionary motion and the sensitivity measure (d') of the MBE are related. With regard to the spatial parameters, it was shown that the difference between the two conditions (stationary vs. rotating inducer) was particularly high whenever the MBE was high, i.e., at a low point number and a high diameter of the stimuli. The ISI had no significant influence on the difference in perceived motion clarity between the two conditions. In Experiment 3 we

further replicate the dependence of the RRI already found in Experiment 1 on spatial and temporal parameters, i.e., the RRI has a temporal optimum at about 60 ms and increases with a higher number of points and a smaller diameter, and replicate the dependencies of the MBE, which decreases with a larger number of points and increases with a larger diameter of the stimuli. For the MBE, we, as well as Mattler and Fendrich (2010), could determine an optimal ISI of 90 ms.

2.3 Results of the study "Spatiotemporal alignment and the Motion Bridging Effect"

The third investigation led us to fundamentally rethink the role of the directional information of the inducing ring. In all previous investigations, the start and stop position of the inducing ring was always identical to the position of the test ring. Mattler and Fendrich (2010) justified their decision with the fact that an apparent movement from the last points of the inducing ring to the test ring points is eliminated by this approach. As a consequence, the distances between the points of the inducing ring and the test ring always had a fixed spatiotemporal configuration. For example, if the inducing ring rotates clockwise, the most recent occupied positions when examining the test ring point at the 12 o'clock position were always to its left. If the inducing ring rotates counterclockwise, however, the most recent point positions were to the right of the test ring point at the 12 o'clock position. To investigate the influence of this spatiotemporal configuration, we systematically varied the start and stop positions of the inducing ring in three experiments.

In the first experiment, we parametrically varied the start and stop positions of the inducing ring by shifting them in 11 steps (plus the default position) across the circumference of the test ring. The center of the inducing ring was always on the same position as the center of the test ring and since the diameters of the two rings were identical, each point of the test ring was located on the circumference of the previously presented inducing ring. The speed of the inducing ring was also varied at each level of position displacement. Since the MBE is characterized by the directional correspondence between the inducing ring and the illusionary test ring motion, only velocities at which the MBE occurs were realized (750°/s, 1500°/s, and 2250°/s). Surprisingly, the MBE, defined by its sensitivity measure (d'), showed a sinusoidal course over the displacement manipulation. With increasing displacement of the start and stop position, the MBE decreased until the mean d' was equal to 0 when the start and stop positions of the inducing ring were offset by a quarter of the distance of the test ring points. If the start and stop positions of the inducing ring were exactly between two test ring point

positions, the illusionary movement was predominantly perceived in the opposite direction of the inducing ring. In this case the velocity manipulation did not have the effect of reducing *d'*, which could be expected if the direction of the inducing ring was discriminated increasingly worse with increasing velocities, but higher velocities brought the sensitivity closer to zero in all conditions of displacement.

The results of the first experiment show that the illusionary motion of the MBE corresponds to the direction of motion of the inducing ring only because a change in the direction of rotation changes the spatiotemporal relationship between the presented points of the inducing ring and the points of the test ring. These results partly contradict the interpretation that the motion of the inducing ring is encoded as a directional signal and suggest that the inducing ring is represented by the visual system as a spatiotemporal sequence that generates the directional correspondence only in interaction with the test ring. It is also conceivable, however, that the spatiotemporal sequence is carried by small gradations in the profile of the persisting retinal activations produced by the points as they advance. The activity at the retinal locations most recently stimulated by an advancing point will be higher than the activity at locations activated earlier and about to be re-stimulated by the next advancing point, although this difference will be small given the brevity of the temporal intervals between the successive stimulations. It is well known that fading luminance trails, visible as streaks behind a moving object convey motion information (Geisler, 1999; Geisler, Albrecht, Crane, & Stern, 2001; for a review see Burr & Thompson, 2011). Here we are suggesting that the fading in the streaks left by the moving points of the MBE display could also be conveying this motion information although that fading cannot be consciously discerned by observers.

To investigate whether the MBE is affected by fading luminance streaks, we enclosed the inducing ring with two 18 ms stationary ring masks, presented immediately before and after the inducing ring presentation. The ring masks looked exactly the same as the inducing ring because they differed from the inducing ring only in that they did not contain a spatiotemporal sequence because the point presentations in the stationary ring masks were randomized. As in Experiment 1, we varied the velocity of the inducing ring and the displacement of its start and stop positions. The same pattern of results were observed as in Experiment 1. The sensitivity (*d'*) of the MBE decreased with increasing displacements and became negative starting at a displacement over a quarter of the distance of the test ring points. Given these results we are tempted to conclude that the fading luminance streaks do

not play a role in the generation of the MBE, since the presentation of the ring mask after the inducing ring was presented should lead to the overwriting of these streaks. We were also interested in whether a similar course of sensitivity (d') could be observed if the test ring was preceding the inducing ring. Again, the results were similar to Experiment 1. Sensitivity (d') showed a sinusoidal course over the displacement of the start and stop position. Overall, however, more extreme d' values were found, confirming the original investigations by Mattler and Fendrich (2010), in which they demonstrated that the MBE is stronger when the test ring is shown before the inducing ring than when the test ring precedes it.

2.4 Results and discussion of the study "Encoding information from rotations too rapid to be consciously perceived as rotating: A replication of the motion bridging effect on a liquid crystal display."

The presentation of very high-frequency movements, such as the movement of the inducing ring in the MBE, requires a screen that updates with a very high temporal frequency. In all previous investigations of the MBE, the fast rotating ring was therefore presented on an analog oscilloscope. Similar to a CRT monitor, an analog oscilloscope consists of an electrode beam that can be deflected by magnetic fields and a phosphorous coated screen that produces visually perceptible light. In contrast to the CRT monitor, the analog oscilloscope has no fixed refresh rate, since the electron beam does not scan the screen in a fixed order, but the position of the beam, its dwell time and its intensity can be determined at any time by the connected computer, limited only by the speed of the digital-to-analog converter. The temporal frequency of the stimulus can thus be adjusted almost arbitrarily and is, for example, only limited by its complexity.

Nowadays, digital oscilloscopes are equipped with LCD screens and no longer offer the advantages of an analog oscilloscope. Therefore, an analog oscilloscope suitable for vision research can only be found in a few laboratories. In fact, the oscilloscope we used in the above investigations was the last analog model manufactured in Germany, but its production has been discontinued. In order to make MBE studies possible in laboratories that do not have access to an analog oscilloscope, the fourth study dealt with the question of whether the MBE can also be reproduced on another screen. Due to its high temporal frequency and its general suitability for vision research (Wang & Nikolić, 2011; Zhang et al., 2018), we opted for an LCD monitor whose temporal repetition rate of 240 Hz is so high that a replication of the MBE might be possible. For this, however, the characteristics of the original stimuli had to be changed. For example, a presentation of the inducing ring with a

temporal frequency as high as in the original study was only possible by reducing the number of steps the rotating ring takes during its rotation. The reduction of the number of steps, however, influences the character of the illusion, because if the inducing ring is presented with only a few intermediate steps, it no longer looks like a continuous circle, but like a dotted circle. Nevertheless, informal investigations have shown that an illusion can be created that looks very similar to the MBE.

The replication on the LCD was successful: Both when the inducing ring followed the test ring and when the inducing ring was shown first, subjects perceived an illusionary movement and the discrimination of the direction of the inducing ring was above chance. This was the case even though the direction of the inducing ring could no longer be perceived consciously at a temporal frequency of 40 Hz or higher. In addition, we illustrate that the MBE, as in the original study, depends on the velocity of the rotating ring. This indicates a high robustness of the phenomenon, since not only the step size was different from the original study, but also the size of the dots was enlarged. In addition, even though we reduced the brightness as much as possible, the backlight of the LCD monitor was always clearly visible, so that the retinal illumination was drastically increased. Despite these substantial modifications of the procedure, our results illustrate that the MBE works on a commercially available monitor. This supports the replicability of the effect and makes it accessible to scientific investigation by a broader range of researchers.

3. Final Discussion

In many respects, the investigations we have carried out lead to a more complete understanding of the MBE. First, we have shown that the MBE depends on the number of points and the diameter of the inducing ring and test ring. Both manipulations influence the spatial distance of the test ring points. One area of research where spatial distances play a role is the study of apparent motion. It has long been known that the relationship between the spatial and temporal separations of the successive stimuli used to produce apparent motion determine the optimal perception of that motion (Wertheimer, 1912). Korte (1915), for example, proposed that as the spatial distance between two stimuli increases, their temporal distance also needs to increase to sustain an apparent motion percept (assuming constant stimulus intensities; Korte's third law). A similar relationship has been shown for path-guided apparent motion (Shepard & Zare, 1983). In path-guided apparent motion a curved

grey path is shown between the two stimuli producing the apparent motion. The perceived apparent motion follows this path, and the minimal temporal interval needed to produce this effect depends upon the length of the path.

At first glance, it seems difficult to reconcile apparent motion and the MBE. In classic apparent motion, two spatially distant stimuli are presented in temporal succession, and the observer perceives an apparent movement of the object over the distance separating the two stimuli. The MBE, on the other hand, is perceived as a transition from an apparently continuous ring to a pointed ring. One type of apparent motion that gives credence to the possibility that the MBE is connected to apparent motion is the line motion illusion (LMI; Downing & Treisman, 1997). Downing and Treisman showed subjects a square followed by an adjacent line. In this stimulus configuration, the line is perceived as expanding out of the square. In another experiment, the authors reversed the order of the stimuli. If the line was shown before the square, one sees the line shrinking into the square. This is reminiscent of the MBE, because the illusionary motion of the MBE can be interpreted as 16 curved lines shrinking into one of the nearest test ring points (in the inducing ring first condition) or 16 test ring points expanding to the 16 curved line segments (in the test ring first condition). A demonstration reported by Downing and Treisman makes the percept of multiple lines contracting in tandem to their neighboring points credible. When these investigators presented a line and then two points adjacent to each end of the line, the points were "seen to disappear from the center outward" (p. 771). However, when a second line was presented to the right of the rightward point, the "dual lines were seen to shrink laterally, each toward just one of the cues" (p.771). Note that in contrast to this demonstration of the LMI, the spatial transition that produces the MBE is highly ambiguous in respect to which direction the lines will transform.

Similar to apparent motion, the LMI and the MBE are both sensitive to variations of temporal distance. Downing and Treisman (1997), for example, found that LMI mean motion ratings decreased with an increase in stimulus onset asynchrony (SOA) between the successive display elements. Kawahara et al. (1996) also found an adverse effect of increasing the inter stimulus interval (ISI) when participants searched for a LMI target, and Hubbard and Ruppel (2011) found that the perceived LMI velocity decreased with an increase in SOA. A similar dependency on the temporal separation of between the inducing and test rings has been reported for the MBE. Performance first increases with short ISI (up to 90 ms) and then decreases steeply (Mattler & Fendrich, 2010). While no initial rise of

performance has been reported for the LMI, differences in the nature of the measurements made (the MBE is measured by a congruency in direction judgments rather than perceived motion strength) and the range of temporal intervals investigated (the shortest SOA employed by Kawahara et al., 1996, was 400 ms and the shortest employed by Downing & Treisman, 1997, was 195 ms) make the importance of this discrepancy hard to evaluate.

As noted above, the strength of apparent motion percepts depends on the spatial distance between the sequentially presented objects. Some evidence has been reported that the LMI also exhibits spatial distance dependencies. Hubbard and Ruppel (2011), for example, found that ratings of perceived velocity are increased when the line length is increased. Downing and Treisman (1997) did not find a significant effect on the reported strength of the motion percept when they varied the distance between the square and the line, but report the effect of distance "approached significance" (p = .08; p. 772). This potential effect appears to be due to a trend towards increased motion ratings with increased distance. However, a spatial dependency in the reverse direction was found in a variant of the LMI first reported by Kanizsa in 1951 (as described in Kanizsa, 1979), which he termed Polarized Gamma Motion. In this variant one of two adjacent shapes is sequentially flashed and observers perceive the flashing shape as smoothly extending from and retracting back into the other. In this case, increasing the spatial gap between the two shapes weakened the polarization. Interestingly, Kanizsa further investigated the phenomenon and found a similar effect when varying the length of the flashed rectangle: When the flashed rectangle is longer (becomes less square-like and more similar to the LMI displays), the reports of polarized movements decrease.

These similarities between the dependencies of the MBE and other apparent motion phenomena suggest that the MBE can be interpreted as an apparent motion, more precisely as an RRI. This alternative approach to accounting for the perceived motion of the test ring does not however, explain the MBE's defining attribute — the test ring's motion direction tends to match the inducing ring's motion direction, although the inducing ring's motion is not consciously visible. Thus, even if the motion generated by the transition of the inducing ring to the test ring represents a case of an RRI, the spatiotemporal properties of the inducing ring motion are being registered by the visual system and these properties might convey a direction signal to the test ring. This could involve the transfer of high temporal frequency motion signals from the retina to higher cortical motion processing regions, as Mattler and Fendrich (2010) proposed.

However, with regard to the rotation direction that affects the perceived motion of the RRI, we found evidence that it is not the direction of motion of the inducing ring that is decisive for the directional correspondence in the MBE, but the spatiotemporal relationship between the points of the inducing ring and the test ring. The results of the third study suggest that the RRI of the MBE is perceived the direction of the inducing ring only because a change in the direction of rotation is accompanied by changes in the spatiotemporal distances between the points of the inducing ring and the test ring. This dependence on the spatiotemporal relationship of the stimuli could be explained by the possibility that the MBE is generated by spatiotemporal receptive fields (Adelson & Bergen, 1985; Burr, Ross, & Morrone, 1986; McLean, Raab, & Palmer, 1994; Reid, Soodak, & Shapley, 1991). These spatiotemporal receptive fields could span over both stimuli and signal a movement starting from the rotating ring and stopping at the test ring point positions. If the motion of the MBE is considered to be caused by spatiotemporal receptive fields, a correspondence problem arises, because each of the points in the inducing ring could be associated with each of the points shown in the test ring as long as a spatiotemporal receptive field exists that can detect this motion. This problem is known in simpler form as the correspondence problem of motion perception (Dawson, 1991; Ullman, 1979). Since there is evidence that the correspondence problem is solved in favor of the slowest velocity (Dawson, 1991; Weiss, Simoncelli, & Adelson, 2002), a highly speculative weighing model of multiple receptive fields based on the velocity of inducing and test ring point correspondences is proposed.

The model consists of three computational steps and is explained here only for a two-dimensional representation of the inducing ring — test ring transition. The computation is also illustrated in Figure 1. In the first step, for each possible correspondences between the points of the inducing ring and its two adjacent test ring points, the velocity it takes to travel to the neighboring test ring point is calculated. Since each point of the inducing ring in Figure 1 can correspond to two possible test ring points, two arrays of velocities are produced: One corresponding to clockwise movement and one to counterclockwise movement. Points on the inducing ring that are located at the same position as the test ring points will be assigned a velocity of 0°/s. In the second step, the mean value of the velocity is determined separately for the array of clockwise and counterclockwise motions. In a final step, the difference between the two mean values is calculated (mean value of counterclockwise velocity — mean value of clockwise velocity) such that if the difference is positive, the mean value of

clockwise motion is the slowest and if the difference is negative, the mean value of counterclockwise motion is the slowest.

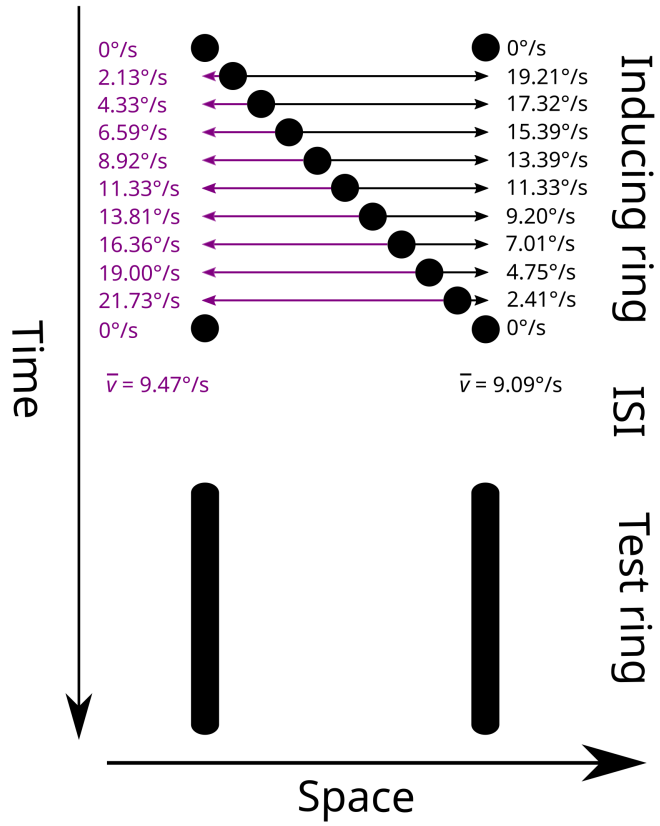

Figure 1. Spatiotemporal illustration of the inducing ring points presented between two test ring point positions at 12 O'clock on the inducing ring circumference. The stimulus sequence was reduced to one spatial dimension, so that a global clockwise rotation corresponds to a spatial shift to the right and a global counter-clockwise rotation to a spatial shift to the left. The stimuli sequence corresponds to a 11 ms clockwise rotating inducing ring with a velocity of 2250°/s preceding the test ring. The arrows indicate in which direction the inducing ring point has to move to produce the velocity indicated in the arrays on the left and right side of to the inducing ring points (clockwise movements are printed black, counter-clockwise movements are printed purple). The mean value of velocity is calculated for both arrays. Because the mean value of velocity is slower for the clockwise movements, the MBE may be perceived in the same direction as the inducing ring was rotating.

Figure 1 demonstrates that for a clockwise 11 ms inducing ring rotating at a velocity of 2250°/s, the model predicts that the mean value of velocity of the clockwise rotation is lower and therefore the illusion is perceived in the same direction as the inducing ring. Analogous to Figure 1, this computation can be performed for the conditions realized in Mattler and Fendrich (2010), Stein et al. (2019) and the third manuscript of this thesis, and the predictions of the model can be compared with the actual results (the calculations for the values reported in the figures are appended to this thesis). Figure 2 shows the simulated data for the first experiment of the initial study (Mattler & Fendrich, 2010). Interestingly, the decrease of the calculated difference with increasing velocity is similarly pronounced as the decrease of the mean sensitivity in the original study. This might indicate that the dependence of the MBE on angular velocity, caused by differences in temporal frequency, can as well be explained by the temporal and spatial distance of the points of the rotating ring and the test ring, if it is assumed that slow velocities are preferred by the visual system.

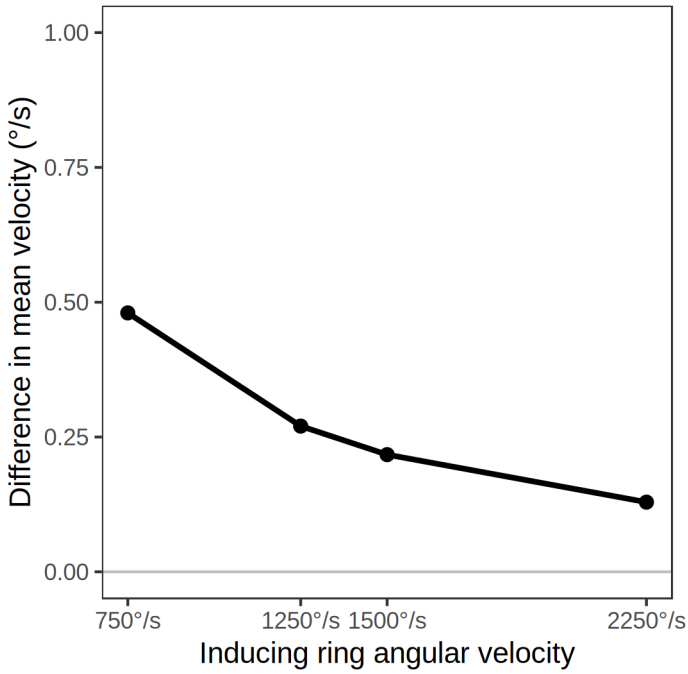

Figure 2. Difference in mean velocity for clockwise and counter-clockwise motion as a function of inducing ring angular velocity in Experiment 1 of Mattler and Fendrich (2010).

With regard to the experiments of Stein et al. (2019), the results are somewhat vague. Just as in the original study, the difference in mean velocity decreases with increasing

number of points (Figure 3A) and increases with increasing diameter (Figure 3B), but the effect of number of points and diameter is not exactly equalized when co-varied (Figure 3C). However, there is a noticeable reduction in the effect of the number of points on the difference of mean velocity, which gives credence to the possibility that the manipulation of the ring diameter and the number of points can also be traced back to the spatiotemporal relationship of the induction ring and test ring.

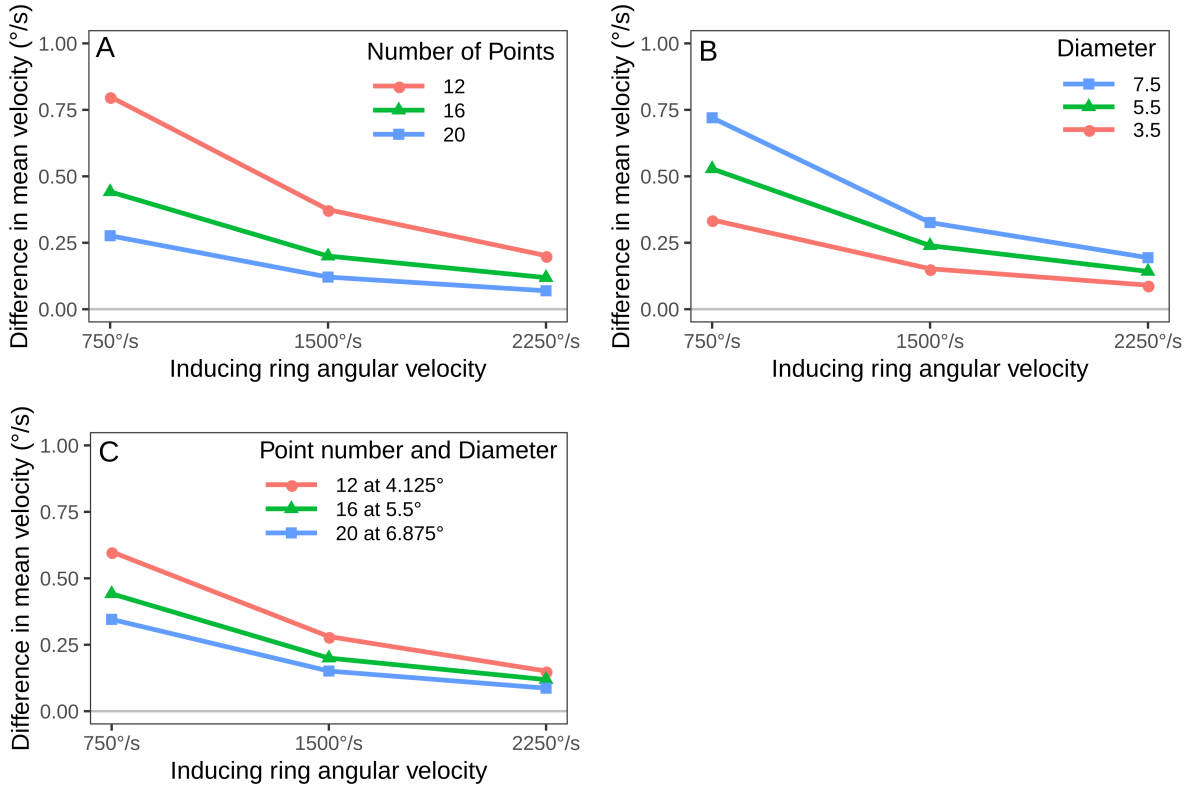

Figure 3. Difference in mean velocity for clockwise and counter-clockwise motions as a function of inducing ring angular velocity, point number and diameter in Experiment 1 to 3 of Stein et al. (2019).

Finally, if the results of the third manuscript, in which we varied the start and stop position of the inducing ring, are modeled, then a similar pattern can be found as with mean sensitivity (see Figure 4). With increasing displacements, the difference of the mean values of the velocity decreases, reverses and is most negative at an offset of 50%. However, in contrast to the original data, the curve loses its sinusoidal character and the effect is reversed much earlier than in the original data (at 15% displacement).

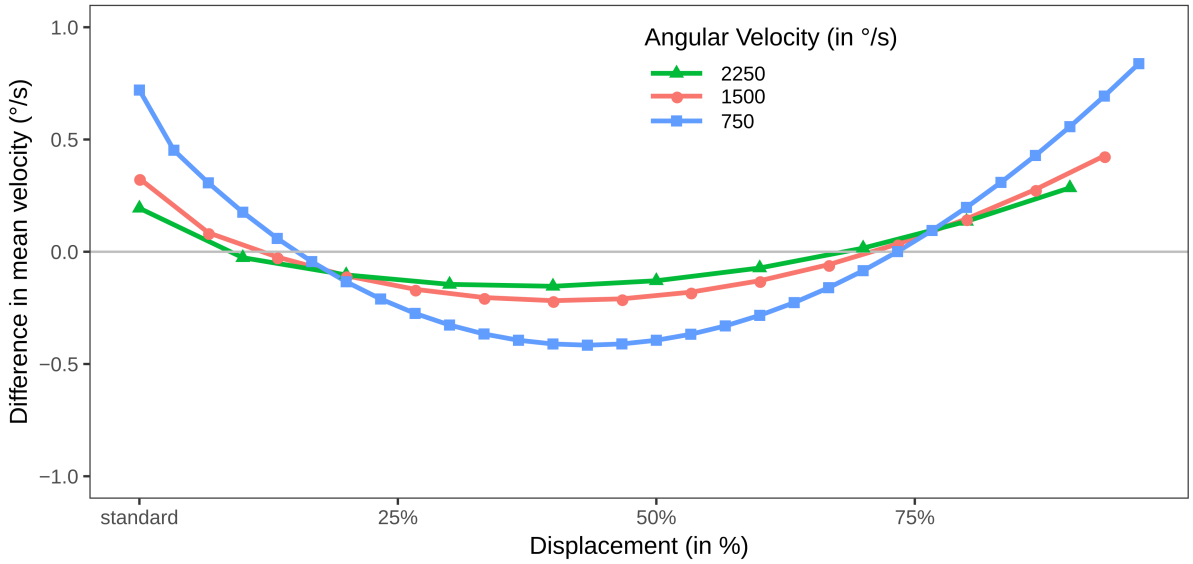

Figure 4. Difference in mean velocity for clockwise and counter-clockwise motions as a function displacement of the inducing ring and test ring position (third manuscript).

The computational model predicts some aspects of the directional correspondence, the velocity dependence, the dependence of the MBE on the displacement of the start and stop position of the inducing ring, and to some degree the dependence of the MBE on spatial parameter variations. However, there are crucial shortcomings: the model lacks the temporal and spatial resolution limits associated with the visual system, and therefore the difference in mean velocity between the two competing directions of motion is preserved, no matter how small (or large) the ISI and how short the spatial displacement is. In an experiment that is not included in this thesis, the inducing ring and test ring were presented very briefly and the ISI was minimized. Under these conditions we were not able to reproduce the MBE. With these short temporal intervals, there may no longer be any cells that are able to detect the motion of the inducing ring – test ring transition, since their receptive fields do not cover such short temporal distances. If combined with spatiotemporal filter models (e.g., Adelson & Bergen, 1985), however, the predictions of the introduced computational model may improve drastically.

4. Conclusion

In the first study we uncovered the dependence of the MBE on the number of points and the diameter of the inducing ring and test ring. We are inclined to interpret this as the MBE depending on the inter-point distance of the test ring, as this increases the spatial distance of the transformation from the seemingly stationary solid ring to the pointed test ring. These results might indicate that the MBE is closely related to apparent motion, which is known to be strongly dependent on changes in spatial distance. In addition, we illustrate that the spatiotemporal information of the inducing ring is not necessary to perceive an illusionary motion very similar to the MBE, since we could also create a similar illusion with an actually stationary solid ring. We called this new illusion "ring rotation illusion" and have illustrated similarities and differences to the MBE and to other apparent motion phenomena. This study also demonstrates that the MBE is at least partly due to an apparent motion, namely the RRI. By varying the start and stop positions of the inducing ring, we were able to reveal that the MBE is not perceived in the same direction as the inducing ring because direction of rotation is coded, but because a spatiotemporal sequence of the inducing ring is represented in the visual system that seems to interact with the test ring producing the directional correspondence in the standard condition of the MBE. Finally, we successfully replicated the MBE on an LCD monitor. This makes the MBE accessible to scientific investigations by a broader range of researchers.

5. References

Adelson, E. H., & Bergen, J. R. (1985). Spatiotemporal energy models for the perception of motion. *Journal of the Optical Society of America A*, *2*, 284–299. https://doi.org/10.1364/JOSAA.2.000284

Breitmeyer, B. G., & Ganz, L. (1976). Implications of sustained and transient channels for theories of visual pattern masking, saccadic suppression, and information processing. *Psychological Review*, *83*, 1–36. https://doi.org/10.1037/0033-295X.83.1.1

Burr, D. C., Ross, J., & Morrone, M. C. (1986). Seeing objects in motion. *Proceedings of the Royal Society B: Biological Sciences*, *227*, 249–265. https://doi.org/10.1098/rspb.1986.0022

Burr, D. C., & Ross, J. (1982). Contrast sensitivity at high velocities. *Vision Research*, *22*, 479–484. https://doi.org/10.1016/0042-6989(82)90196-1

Burr, D. C., & Thompson, P. (2011). Motion psychophysics: 1985–2010. *Vision Research*, *51*, 1431–1456. https://doi.org/10.1016/j.visres.2011.02.008

Cornsweet, T. N. (1970). *Visual perception*. New York, NY: Academic Press.

Dawson, M. R. (1991). The how and why of what went where in apparent motion: Modeling solutions to the motion correspondence problem. *Journal of Neurophysiology*, *52*, 1106–1130. https://doi.org/10.1037/0033-295X.98.4.569

Downing, P. E., & Treisman, A. M. (1997). The line-motion illusion: Attention or impletion? *Journal of Experimental Psychology: Human Perception and Performance*, *23*, 768–779. https://doi.org/10.1037/0096-1523.23.3.768

Geisler, W. S. (1999). Motion streaks provide a spatial code for motion direction. *Nature*, *400*, 65–69. https://doi.org/10.1038/21886

Geisler, W. S., Albrecht, D. G., Crane, A. M., & Stern, L. (2001). Motion direction signals in the primary visual cortex of cat and monkey. *Visual Neuroscience*, *18*, 501–516. https://doi.org/10.1017/S0952523801184014

Hartmann, E., Lachenmayr, B., & Brettel, H. (1979). The peripheral critical flicker frequency. *Vision Research*, *19*, 1019–1023. https://doi.org/10.1016/0042-6989(79)90227-X

Holcombe, A. O. (2009). Seeing slow and seeing fast: Two limits on perception. *Trends in Cognitive Sciences*, *13*, 216–221. https://doi.org/10.1016/j.tics.2009.02.005

Hubbard, T. L., & Ruppel, S. E. (2011). Effects of temporal and spatial separation on velocity and strength of illusory line motion. *Attention, Perception, & Psychophysics*, *73*, 1133–1146. https://doi.org/10.3758/s13414-010-0081-7

Hubbard, T. L., & Ruppel, S. E. (2018). Does allocation of attention influence relative velocity and strength of illusory line motion? *Frontiers in Psychology*, *9*, 1–13. https://doi.org/10.3389/fpsyg.2018.00147

Kahneman, D. (1967). An onset-onset law for one case of apparent motion and metacontrast. *Perception & Psychophysics*, *2*, 577–584. https://doi.org/10.3758/BF03210272

Kanizsa, G. (1979). *Organization in vision: Essays on gestalt perception*. New York, NY: Praeger.

Kawahara, J., Yokosawa, K., Nishida, S., & Sato, T. (1996). Illusory line motion in visual search: Attentional facilitation or apparent motion? *Perception*, *25*, 901–920. https://doi.org/10.1068/p250901

Kelly, D. H. (1961). Visual responses to time-dependent stimuli. I. Amplitude sensitivity measurements. *Journal of the Optical Society of America*, *51*, 422–429. https://doi.org/10.1364/JOSA.51.000422

Korte, A. (1915). Kinematoskopische Untersuchungen [Kinematoscopic studies]. *Zeitschrift Für Psychologie*, *72*, 193–296.

Macmillan, N. A., & Creelman, C. D. (2005). Detection theory: A user's guide (2nd ed.). Mahwah, NJ: Lawrence Erlbaum Associates.

Mattler, U., & Fendrich, R. (2010). Consciousness mediated by neural transition states: How invisibly rapid motions can become visible. *Consciousness and Cognition*, *19*, 172–185. https://doi.org/10.1016/j.concog.2009.12.015

McLean, J., Raab, S., & Palmer, L. A. (1994). Contribution of linear mechanisms to the specification of local motion by simple cells in areas 17 and 18 of the cat. *Visual Neuroscience*, *11*, 271–294. https://doi.org/10.1017/S0952523800001632

Reid, R. C., Soodak, R. E., & Shapley, R. M. (1991). Directional selectivity and spatiotemporal structure of receptive fields of simple cells in cat striate cortex. *Journal of Neurophysiology*, *66*, 505–529. https://doi.org/10.1152/jn.1991.66.2.505

Sekuler, R. (1975). Visual motion perception. In E. C. Carterette & M. P. Friedman (Eds.), *Handbook of perception V: Seeing* (pp. 387–430). New York, NY: Academic Press.

Shepard, R. N., & Zare, S. L. (1983). Path-guided apparent motion. *Science*, *220*, 632–634. https://doi.org/10.1126/science.6836307

Stein, M., Fendrich, R., & Mattler, U. (2019). Stimulus dependencies of an illusory motion: Investigations of the Motion Bridging Effect. *Journal of Vision*, *19*, 1–23. https://doi.org/10.1167/19.5.13

Ullman, S. (1979). *The interpretation of visual motion*. Cambridge, MA: MIT Press.

Wang, P., & Nikolić, D. (2011). An LCD monitor with sufficiently precise timing for research in vision. *Frontiers in Human Neuroscience*, *5*, 1–10. https://doi.org/10.3389/fnhum.2011.00085

Weiss, Y., Simoncelli, E. P., & Adelson, E. H. (2002). Motion illusions as optimal percepts. *Nature Neuroscience*, *5*, 598–604. https://doi.org/10.1038/nn0602-858

Wertheimer, M. (1912). Experimentelle Studien über das Sehen von Bewegung [Experimental studies on seeing movement]. *Zeitschrift für Psychologie*, *61*, 161–265.

Zhang, G.-L., Li, A.-S., Miao, C.-G., He, X., Zhang, M., & Zhang, Y. (2018). A consumer-grade LCD monitor for precise visual stimulation. *Behavior Research Methods*, *50*, 1496–1502. https://doi.org/10.3758/s13428-018-1018-7

6. Appendices

The following manuscripts are attached to this thesis:

Stein, M., Fendrich, R., & Mattler, U. (2019). Stimulus dependencies of an illusory motion: Investigations of the Motion Bridging Effect. *Journal of Vision*, *19*, 1–23. https://doi.org/10.1167/19.5.13

Mattler, U., Stein, M., & Fendrich, R. (in preparation). Ring Rotation Illusion and the influence of heuristics on apparent motion.

Stein, M., Fendrich, R., & Mattler, U. (in preparation). Spatiotemporal alignment and the Motion Bridging Effect.

Stein, M., Fendrich, R., & Mattler, U. (in preparation). Encoding information from rotations too rapid to be consciously perceived as rotating: A replication of the motion bridging effect on a liquid crystal display.

The following document is attached to this thesis:

Octave code to calculate the differences in mean velocity.

Stimulus dependencies of an illusory motion: Investigations of the Motion Bridging Effect

Maximilian Stein Department of Experimental Psychology, University of Goettingen, Goettingen, Germany

Robert Fendrich Program in Cognitive Neuroscience, Dartmouth College, Hanover, NH, USA

Uwe Mattler Department of Experimental Psychology, University of Goettingen, Goettingen, Germany

The Motion Bridging Effect (MBE) is an illusion in which a motion that is not consciously visible generates a visible motion aftereffect that is predominantly in the same direction as the adapter motion. In the initial study of the MBE (Mattler & Fendrich, 2010), a ring of 16 points was rotated at angular velocities as high as 2250°/s so that observers saw only an unbroken outline circle and performed at chance when asked to report the ring's rotation direction. However, when the rotating ring was replaced by a veridically stationary ring of 16 points, the stationary ring appeared to visibly spin to a halt, principally in the same direction as the initial ring's rotation. Here we continue to investigate the stimulus dependencies of the MBE. We find the MBE, measured by the correspondence between the direction of the invisible rotation of the spinning ring and perceived rotation of the stationary ring, increases as the number of points used to construct the rings decreases and grows stronger as the diameter of the rings get larger. We consider the potential contributions of temporal frequency, retinal eccentricity, luminance levels, and the separation between the points forming the rings as mediators of these effects. Data is discussed with regard to the detection of real movement and apparent motion. We conclude that the detection of the rapid rotation of the spinning ring is likely to be modulated by temporal frequency of luminance changes along the ring perimeter while the point-distance may modulate an apparent motion produced by the transition from the perceptually unbroken spinning ring to the point-defined stationary ring.

Introduction

A wealth of vision research has addressed the abilities and limits of the human visual system, and a direct approach to exploring these limits has been to focus on the reported perceptual experiences of participants. However, there is evidence for the processing of visual information, which is not accessible to conscious reports. Much of this evidence is based on priming and adaptation effects produced by unconscious information (e.g., Lin & He, 2009; Vorberg, Mattler, Heinecke, Schimdt, & Schwarzbach, 2003). Two of the present authors previously reported evidence for the processing of unconscious motion information. Mattler and Fendrich (2007) employed a ring of points that rotated so rapidly observers saw only a fused static ring, but viewing this ring primed direction judgments when observers subsequently viewed a visibly rotating ring. In 2010 Mattler and Fendrich extended their observations by reporting that viewing such a rapidly rotating ring can produce an illusory rotation in the same direction as the invisible rapid rotation in a stationary ring of points that precedes or follows the rotating ring.

In the investigations reported in the 2010 paper, the rotating ring was 5° of visual angle in diameter, constructed of 16 points, and presented on the CRT screen of a fast phosphor oscilloscope. This "inducing ring" was rotated at angular velocities as high as 2250°/s. When the inducing ring simply appeared and vanished, observers perceived it as a flashed continuous outline circle and performed at chance when asked to report if the rotation had been clockwise or counterclockwise. However, when the inducing ring was replaced by a stationary "test ring" of 16 points, this stationary ring appeared to visibly spin to a halt, primarily in the same direction the inducing ring had been spinning. This illusionary spin was seen although the initial and final positions of the inducing ring points and the display positions of the test ring points were

Citation: Stein, M., Fendrich, R., & Mattler, U. (2019). Stimulus dependencies of an illusory motion: Investigations of the Motion Bridging Effect. *Journal of Vision*, *19*(5):13, 1–23, https://doi.org/10.1167/19.5.13.

https://doi.org/10.1167/19.5.13 Received January 3, 2019; published May 17, 2019 ISSN 1534-7362

identical. Because the illusory rotation of the test ring usually corresponded to the direction of the inducing ring, observers were able to report this direction at substantially greater than chance levels. Subsequently, Mattler and Fendrich (2010) found there was a similar effect when the stationary test ring preceded the inducing ring. In this case, the test ring appeared to launch into motion in the direction of the inducing ring. Because these illusory motions linked the actual (although invisible) rotation of the inducing ring to the veridically stationary test ring, Mattler and Fendrich labeled this illusion the Motion Bridging Effect (MBE).

Whereas other studies have reported ways of making a moving stimulus invisible, these studies used methods like crowding (e.g., Moutoussis & Zeki, 2006), binocular rivalry (e.g., Lehmkuhle & Fox, 1974), or continuous flash suppression (e.g., Maruya, Watanabe, & Watanabe, 2008) to mask or suppress the stimulus motion. The MBE differs from these studies because it demonstrates a motion *inherently* inaccessible to consciousness is not only encoded by the visual system but can subsequently manifest itself as a visible attribute. A similar phenomenon has been previously demonstrated in a different domain. Stationary gratings can be made invisible by crowding (He, Cavanagh, & Intriligator, 1996) or interocular suppression (Blake & Fox, 1974) and still generate an aftereffect. It has been shown that this is also possible if the grating is inherently inaccessible to consciousness because of its high spatial frequency (He & MacLeod, 2001).

Although the processes underlying the MBE are still uncertain, a number of its characteristics are known. Mattler and Fendrich (2010) found the MBE, assessed by the congruence of the actual inducing ring and reported test ring spin directions, declined as the inducing ring's angular velocity increased but was still present at 2250°/s, the highest velocity they tested. They also found the MBE was maximal when there was a 90 ms ISI between the inducing and test ring presentation, and was observable with inducing ring durations as short as 15 ms, reaching an asymptotic level with durations of 60 ms. In addition, they noted that the MBE was degraded by a small (1° of visual angle) spatial mismatch between the inducing and test ring positions (produced by an expansion or upward shift of the test ring) and this degradation was complete when the spatial mismatch was increased to 3°. This outcome suggests the MBE depends on interactions that occur at an early stage of the visual pathway where neural representations map closely onto retinal locations.

More than one factor might be responsible for the decline in the MBE as the inducing ring velocity increases. An increase in the rotation rate increases not only the linear velocity of the inducing ring but also the temporal frequency at which points cross a given position along the circumference of that ring. Temporal frequency is one basic feature that affects the detection of motion. Due to limitations in the rate at which the human visual system can track luminance changes, objects that stimulate retinal locations at high temporal frequencies may be perceived as static forms or outlines (e.g., a rotating fan blade may look like a blurred disk). The upper limit of the system's temporal response capabilities can be investigated with a flicker detection paradigm in which an observer reports the perceived flicker of a luminous patch that has its intensity modulated sinusoidally in time. Experiments using this paradigm show that sensitivity to flicker initially rises with increasing modulation frequencies and then falls off steeply (Kelly, 1961). This pattern indicates that the visual system acts like a band-pass filter that is most sensitive to frequencies ranging from approximately 10 to 30 Hz (Cornsweet, 1970), with lower and higher frequencies attenuated (see Kaufman, 1974, for a summary of early research on flicker perception).

The temporal frequency at which a flickering light is perceived as steady is termed critical flicker frequency (CFF). While the CFF is influenced by a number of stimulus conditions, including the luminance, size, chromaticity, and sharpness of the test patch, as well as variables such as an observer's light adaptation level (Kelly, 1959; Landis, 1954), the maximum value of the CFF in humans is about 60 Hz. The apparently steady appearance of stimuli that flicker faster than the CFF can be taken to be indicative of the stability in the activity of neurons responding to the flickering stimulus. The visual system is, in effect, integrating luminance variations over short periods of time (see Barlow, 1958), with neural persistence acting to fill in the activity troughs. This filling in may occur as early as the photoreceptor level but could also be occurring at higher levels in the visual system (see Coltheart, 1980).

However, flicker detection paradigms measure only the conscious perception of flicker and therefore only demarcate limits of conscious perception. A variety of studies indicate that some neurons can encode luminance modulation frequencies higher than the CFF. Cells in the monkey lateral geniculate nucleus respond to flicker rates well beyond the human CFF (Spekreijse, van Norren, & van den Berg, 1971), and neurons in the primary visual cortex (V1) of monkeys respond to flicker rates as high as 100 Hz when high contrast patterns are used (Williams, Mechler, Gordon, Shapley, & Hawken, 2004). In addition, macaque monkey V1 neurons respond to heterochromatic flicker at 30 Hertz (Gur & Snodderly, 1997) although macaques do not discriminate isoluminant red/green flicker at 15 Hz (Schiller, Logothetis, & Charles, 1990). In human observers, Regan (1968) has reported that stimuli with temporal frequency modulations higher than the CFF evoke potentials in the EEG (for similar findings, see Herrmann, 2001; Krolak-Salmon et al., 2003; Lyskov,

Ponomarev, Sandström, Mild, & Medvedev, 1998). Akin to the results for chromatic flicker in monkeys, in a human fMRI study, Jiang, Zhou, and He (2007) found activity in visual cortical areas related to chromatic flicker at 30 Hz even when participants were unable to distinguish the presented stimulus from a static control stimulus. Moreover, Shady, MacLeod, and Fisher (2004) showed that temporal frequency modulations above the CFF can have an impact on perception. These investigators found in an adaptation experiment that patches flickering above an observer's CFF influenced sensitivity to subsequent flickering patches.

The limited ability of observers to consciously perceive rapid rates of temporal change also sets limits on their ability to perceive rapid rates of motion. Holcombe, in a 2009 review of the visual system's temporal processing capabilities, has in fact argued that flicker can be regarded as "a degenerate case of motion" (p. 217). In the case of rapidly moving stimuli, neural persistence can generate percepts of spatially extended lines and areas rather than stimuli that are spatially displacing. This neural persistence also sets limits to the perception of apparent motion: If presented at a sufficiently rapid rate, advancing or alternating points will be seen as simultaneously present rather than advancing or jumping back and forth (Wertheimer, 1912).

The visual system's spatial resolving capabilities with static stimuli can be evaluated by determining the minimum luminance contrast required for the detection of sinusoidal gratings of increasing spatial frequency. This determination yields the human contrast sensitivity function (e.g., Campbell & Robson, 1968). Kelly (1979) extended this method to obtain spatio-temporal contrast-sensitivity functions for moving sinusoidal gratings. He found the sensitivity function remains similar in shape but shifts to a lower spatial frequency as the grating is presented at higher velocities, and notes that at velocities greater than 100°/s there is probably no spatial frequency within the range of normal human vision that would allow a grating to have a detectable contrast. Using a direction detection task, Burr and Ross (1982) likewise found the contrast sensitivity function of moving gratings shifted towards lower spatial frequencies as the grating's velocity increases. However, Burr and Ross (1982) challenged the 100°/s limitation: They found that gratings with velocities as high as 800°/s could be detected when the spatial frequency was lowered to 0.01 c/°. They proposed that the limiting factor of motion detection, as is the case with flicker perception, is the temporal frequency of intensity modulations. In their experiment this frequency was approximately 30 Hz. Above this critical rate, motion could no longer be perceived. Thus, the sensitivity of local motion processing seems to depend on temporal rather than spatial frequency.

Like measurements of the CFF, however, these investigations depend upon the conscious percepts of observers. They therefore do not rule out the possibility that stimulus motions with higher temporal frequencies are being encoded at the retinal level and processed at postretinal levels of the visual system although they cannot be consciously detected or discriminated. Thus, just as Shady et al. (2004) reported the processing of flicker rates above the flicker-fusion threshold, motion inaccessible to consciousness could still be processed and have an impact on perception.

Overview

In the present study, we report four experiments that further investigate functional dependencies of the MBE. In Experiment 1 we varied the number of points used to construct the inducing and test ring. Increasing the number of points had the effect of increasing the temporal frequency of point presentations at each position along the inducing ring circumference while leaving its linear and angular velocity unchanged. In Experiment 2 we varied the diameter of the inducing and test rings. In addition to altering their retinal eccentricity, this manipulation modified the linear velocity of the inducing ring points but left the temporal frequency of point presentations along the ring circumference unchanged. In Experiment 3 we investigated the possibility that the observed effects of varying the number of points and the diameter of the rings are both mediated by a common factor: the distance between the points that formed the rings. By changing the diameter of the rings together with the number of points, we kept the point distance constant but varied temporal frequency. In Experiment 4 we addressed the effect of the inducing and test ring luminance on the MBE and found no effect of these variables.

General methods

Participants

The participants were students at University of Goettingen with a mean age of 24.5 years. They were compensated €7 per hour for their participation. All participants undertook a visual acuity test using the Landolt ring chart and had normal or corrected-to-normal vision. In Experiments 1–3 participants completed three, 1 hr sessions; in Experiment 4 they

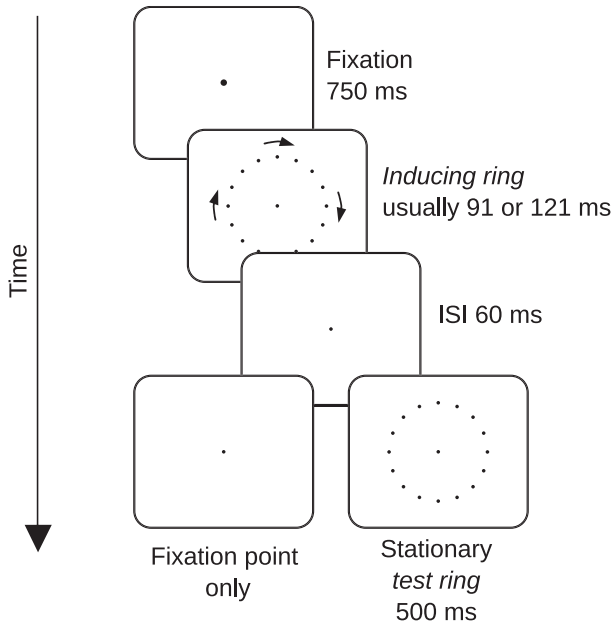

Figure 1. Display sequence in Experiments 1–4. On a given trial the inducing ring rotated either clockwise (as shown in the figure) or counterclockwise. Note the points on the oscilloscope were bright on a dark background.

completed two, 1 hr sessions. Sessions were always run on separate days. We examined 12 students in each experiment, with no student taking part in more than one. However, in Experiment 1, the data of one of the 12 students was subsequently excluded from data analyses because it was found her vision was impaired, so data from 11 subjects is reported for this experiment.

Apparatus

Stimuli were presented on a cathode-ray oscilloscope (HAMEG HM 400) controlled by a PC with a 12-bits Digital-Analog converter. The 8 × 10 cm oscilloscope display was customized with a fast P15 phosphor (50 μs luminance decay time to 0.1%). The experiment was run in a dark room, and participants had their head positions stabilized 57 cm from the oscilloscope by a chin and forehead rest.

Stimuli

Stimuli are illustrated in Figure 1. Participants were presented with a rapidly rotating inducing ring of luminous points and a stationary test ring of luminous points. The points were slightly blurred because pilot observations had shown this enhanced the illusionary motions being investigated.

In all the reported experiments, 12, 16, or 20 equally spaced points were used to construct the inducing and test rings. The position of these points could be adjusted in steps of 0.25 angular degrees, allowing them to be placed in 1440 potential positions along the ring circumference. The inducing ring was rotated by advancing all of its points by a specified number of positions every millisecond, so that it was updated with an effective frame rate of 1000 Hz. When the inducing ring was formed from 16 or 20 points, it could be rotated clockwise or counterclockwise with angular velocities of 250°, 750°, 1500°, and 2250°/s. These velocities entailed sequential point position advances of 1, 3, 6, and 9 steps. Due to programming constraints, when the inducing ring was constructed from 12 points, the highest angular velocity was 2500°/s rather than 2250°/s which entailed a step size of 10. The rotation of the inducing ring always started and ended with points placed at the same set of ring circumference positions. These were also the positions of the test ring points when the test ring was presented. At the higher rotation velocities (above 250°/s) the inducing ring appeared to be an unbroken outline circle. To produce a display free of visible switching artifacts, the CRT electron beam was switched off during its transit between the successive point positions. The diameter of the rings, number of points used to form the rings, and actual rotation rates employed in each experiment are described in each experiment's specific methods sections.

As indicated in Figure 1, the inducing ring duration was usually 121 ms. However, in Experiments 1 and 3 when the inducing ring velocity was 250°/s, this duration was 91 ms when 16 points were displayed and 145 ms when 20 points were displayed. These deviations from the standard display time were necessitated by the combined constraints imposed by the relatively slow inducing ring rotation and the need to end its display interval when its point positions matched the position of the test ring points. Note that these variations in the inducing ring display time had no effect on our measures of the MBE since at the 250°/s velocity the MBE could not be measured because the inducing ring rotation was visible even when no test ring was presented.

Statistical analysis

In all the experiments, we used signal detection methods to analyze performance (Macmillan & Creelman, 2004). We defined hits as clockwise responses to a clockwise rotation and false alarms as clockwise responses to a counterclockwise rotation. Hit and false alarm rates were estimated separately for each subject in each condition and corrected with the log-linear rule (Hautus, 1995). We evaluated d' measures of the discrimination ability of participants with repeated

	Angular velocity (in °/s)			
Point number	250	750	1500	2250/2500
12	0.012	0.037	0.072	0.124
16	0.017	0.050	0.099	0.149
20	0.017	0.051	0.101	0.149

Table 1. Time averaged brightness of inducing ring points in Experiments 1 and 3 in cd/m^2. *Note*: The replication of the point refresh rates in the 250°/s angular velocity conditions necessitated time averaging across flicker rates that were below the flicker fusion frequency.

measures analyses of variances (ANOVAs). All reported ANOVA p values were corrected using Greenhouse-Geisser estimates of sphericity but for the sake of readability, the uncorrected degrees of freedom are reported. Differences between specific conditions were evaluated with posthoc Bonferroni-corrected two-tailed t tests. Performance levels in specific conditions were compared to a chance level of 50% with one-tailed Bonferroni-corrected t tests that evaluated whether d' exceeded zero.

Luminance of the stimuli

Because of its small size, special methods are required to measure the brightness of a point on an oscilloscope screen. We employed a Minolta LS-100 luminance meter with a close-up lens that allowed us to focus on a small region of the oscilloscope display. To obtain a measurable luminance signal, we presented a rectangular matrix of 12, 16, or 20 contiguous points with their intensity, on-time, and repetition rates set to match the intensity, on-time, and repetition rates of the points in our inducing ring or test ring displays. Luminance estimates of the time averaged brightness of our display points were obtained by measuring the luminance of these matrices.

The brightness of the test ring points in the 12 and 16 point display conditions was about 1.50 cd/m^2 on a dark background. Point luminance in the 20 point condition was slightly lower (1.20 cd/m^2). The time averaged brightness of the inducing ring points varied with point number and velocity (see Table 1). We address the possible effect of these luminance variations in Experiment 4.

Experiment 1

In this experiment we confirmed the previously reported Motion Bridging Effect (Mattler & Fendrich, 2010) and investigated the effect of varying the number of points used to form the inducing and test rings. Changing the number of points effectively changes the temporal frequency of point presentations at each position along the inducing ring circumference (see Table 2) while keeping the linear and angular velocity constant.

	Angular velocity (in °/s)			
Point number	250	750	1500	2250/2500
12	8.33	25	50	83.33
16	11.11	33.33	66.67	100
20	13.89	41.67	83.33	125

Table 2. Temporal frequency of point presentations at each position along the circumference of the inducing ring in Experiments 1 and 3 in Hz.

The limiting factor in the perception of the direction of sinusoidal gratings is the temporal modulation rate of the stimulus (e.g., Burr & Ross, 1982). This might hold true for the MBE as well, although the MBE is found when the temporal frequency of point presentations along the inducing ring circumference substantially exceeds conventional flicker fusion thresholds (de Lange Dzn, 1958; Kelly, 1961). A decrease in the MBE as the number of points increases, with the consequent increase in their temporal frequency, would support this premise.

Method

Stimuli

Twelve, 16, or 20 equally spaced points formed the circumference of the inducing and test rings (see Figure 2). The point separations for these three point numbers were respectively 1.44, 1.08, and 0.86° of visual angle measured along the ring circumference. The number of points in the inducing and test rings was identical in any given trial. The diameter of the rings was 5.5° of visual angle. Rotation rates of 250°, 750°, 1500°, and 2250°/s (2500°/s in the 12 point condition) were employed.

Task

Participants reported the direction of any perceived rotation (clockwise or counterclockwise). Responses were registered with the arrow keys of a conventional computer keyboard, with the right arrow indicating a clockwise rotation and the left arrow a counterclockwise rotation. Trial blocks were started with a press of the space key. No feedback was given about the correctness of responses.

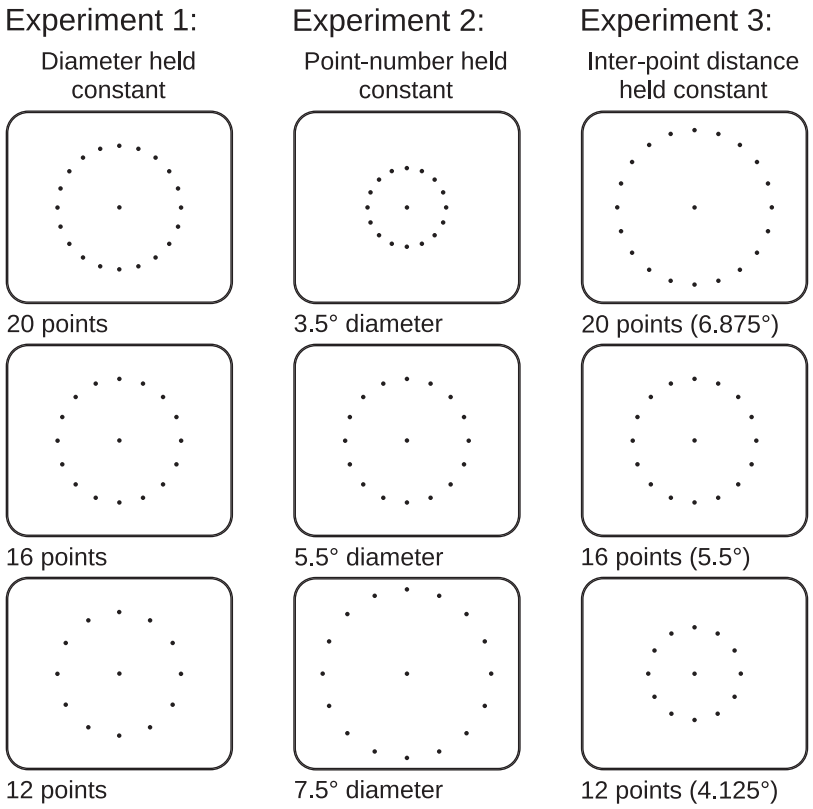

Figure 2. The various display conditions in Experiment 1–3. When the diameter of the rings was varied, the visual angle of its diameter is indicated. Note that the sizes of the rings depicted here are not precisely scaled to their sizes in the actual displays. Also note the points on the oscilloscope were bright on a dark background.

Procedure

Participants were instructed to maintain their gaze on a central fixation point during the trials. This fixation point brightened for 750 ms at the start of each trial to indicate that the inducing ring was about to appear. In the conditions in which the test ring was presented, it followed the inducing ring after a 60 ms interstimulus interval (ISI) and remained visible for 500 ms. Subjects' reports of the inducing ring direction were recorded starting 300 ms after the offset of the test ring. A response was required for the experiment to proceed. A new trial started 1 second after the response.

Design

Fourteen trial blocks were run in each session with the first two treated as practice and excluded from data analysis. The number of points in the inducing ring was changed in the seventh and 11th blocks following a Latin Square design. There were 48 trials in each block, with an additional eight practice trials (which were not analyzed) added at the start of the seventh and 11th blocks. Blocks in which only the inducing ring was presented were alternated with blocks in which the inducing ring was followed by the test ring. The angular velocity and the rotation direction of the inducing ring were varied quasirandomly within each block.

The combination of two test ring states (present vs. absent), four inducing ring angular velocities (250°, 750°, 1500°, 2250°/2500°/s) and three point numbers (12, 16, 20) produced 24 experimental conditions. There were 72 trials in each of these conditions: 36 with a clockwise inducing ring rotation and 36 in counter-clockwise rotation.

Results

Results and confidence intervals for sensitivity to the inducing ring direction in all the conditions of Experiment 1 are presented in Figure 3A. This data is also presented as mean percent correct accuracy rates in Appendix Table A1. To take into account the very different response profiles found when the test ring is present and absent, we calculated two separate, two-way ANOVAs, one for each of the test ring conditions (present vs. absent). These analyses are presented in Table A2 in the Appendix. They evaluate the effect of angular velocity and the number of points that formed the inducing and test ring on observers' sensitivity (d')

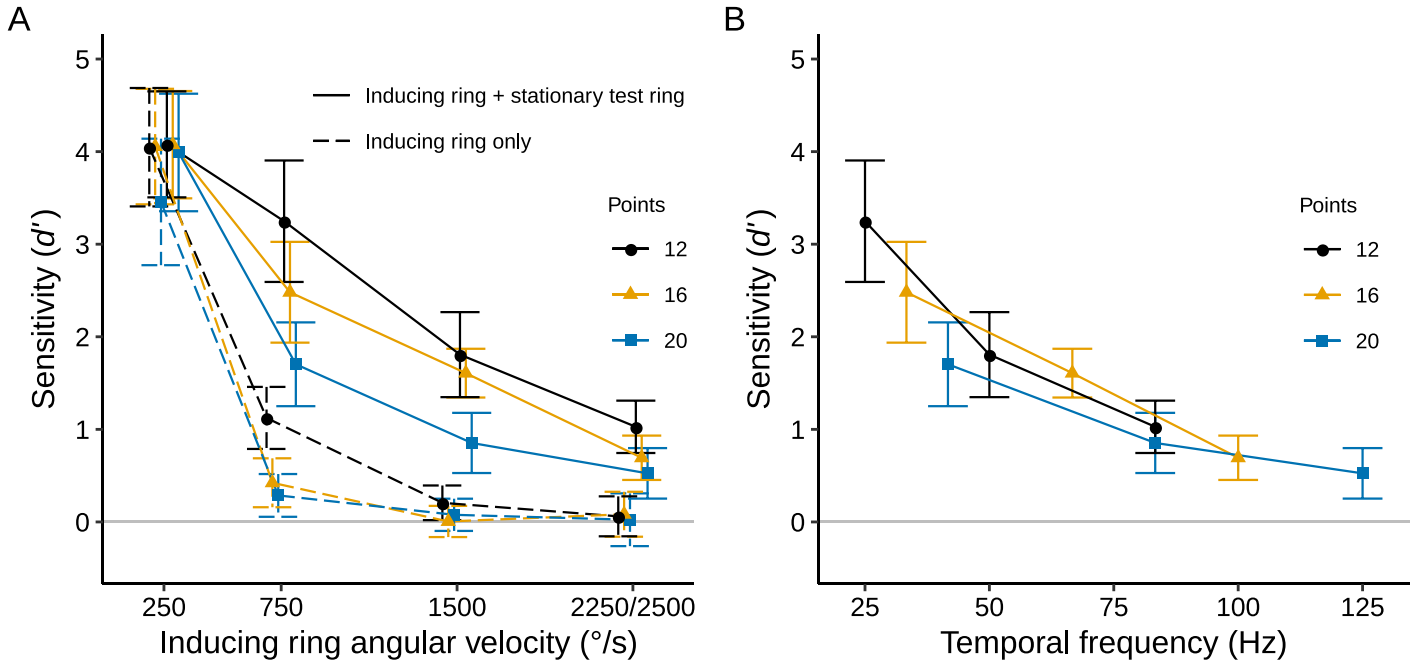

Figure 3. (A) Mean sensitivity (d') for 11 participants of Experiment 1 as a function of inducing ring velocity and point-number in the inducing ring only conditions (the dashed lines) and the inducing ring + test ring conditions (the solid lines). (B) Mean d' values from the inducing ring + test ring conditions for rotation rates of 750°/s and greater as a function of temporal frequency. The solid gray line indicates the chance level of accuracy ($d' = 0$). The error bars show 95% CI. Points and confidence intervals are slightly offset horizontally to improve their visibility in (A).

to the inducing ring rotation. We will refer to these factors as *Velocity* and *Point-number*.

Inducing ring only

When the inducing ring was presented alone, the main effects of both Velocity and Point-number were significant and there was a significant Velocity × Point-number interaction (Appendix Table A2). Mean sensitivity declined as Velocity increased ($d' = 3.85$, $d' = 0.61$, $d' = 0.10$, and $d' = 0.06$ at 250°, 750°, 1500°, and 2250°/2500°/s, respectively) and as Point-number increased ($d' = 1.36$, $d' = 1.14$, and $d' = 0.96$ with 12, 16, and 20 points, respectively). As can be seen in Figure 3A, sensitivity rates were high in the 250°/s condition, dropped precipitously in the 750°/s condition, and were at chance in the two high velocity conditions. This pattern of outcomes accords with informal reports that the inducing ring perimeter fused into a visually unbroken outline circle at the higher velocities but was perceived as a set of spinning points at the lowest velocity (250°/s).

	Angular velocity (in °/s)			
Diameter	250	750	1500	2250/2500
3.5°	7.64	22.91	45.82	68.72
5.5°	12.00	36.00	72.00	108.00
7.5°	16.36	49.09	98.18	147.26

Table 3. Linear velocity of the rotating points in the 3 diameter conditions of Experiment 2 in degrees of visual angle per second.

The effect of Point-number was restricted to the two lower ring velocities. At the higher velocities, sensitivity remained near zero irrespective of the point number, accounting for the Point-number × Velocity interaction. Two-tailed t tests (with a Bonferroni-corrected alpha level of 0.0042) were performed to compare the across subject mean values of d'. These tests indicate that with the 250°/s velocity the sensitivity was lower in the 20 point condition than in the 16 point condition, whereas with the 750°/s velocity the sensitivity was lower in both the 20 and 16 point conditions than the 12 point condition. With the 1500°/s and 2250°/2500°/s velocities, the point conditions did not produce any significant differences in d'.

A fundamental aspect of the MBE is that the improvement in sensitivity produced by the test ring presentation occurs even when subjects perform at chance in the inducing ring only condition. To investigate the velocity and point-number levels at which subjects were unable to discriminate the rotation direction of the inducing ring, we directly compared the discrimination ability of participants in the inducing ring only condition to a chance level of 50% ($d' = 0$). To do this we calculated 12 one-tailed t tests (with a Bonferroni adjusted alpha level of 0.0042), one for each

combination of velocity and point-number. We found that mean sensitivity was significantly greater than zero with every point-number when the angular velocity was 250°/s ($p < 0.0001$ in all cases), and with the 750°/s velocity when the inducing ring was formed by 12 or 16 points ($p < 0.0001$ and $p = 0.0026$, respectively). The mean d' did not exceed zero in the 20 point 750°/s condition or with any point number in the two high velocity rotation conditions. Except for the 12 point 1500°/s condition, this was the case with the two high velocities even when we employed an uncorrected 0.05 significance level.

Inducing ring + test ring

To address the characteristics of the MBE, similar analyses were carried out with the inducing ring + test ring conditions. However, it is only meaningful to speak of the MBE when the appearance of the test ring enables the discrimination of the inducing ring direction. The 250°/s velocity therefore was excluded from these analyses since at this velocity the inducing ring rotation is readily visible even when no test ring is presented.

In a 3 × 3 ANOVA with Velocity (750°, 1500°, 2250°/2500°/s) and Point-number (12, 16, 20 points) as factors the main effects of both Velocity and Point-number were significant as well as the Velocity × Point-number interaction (Appendix Table A2). As in the inducing ring only conditions, mean sensitivity declined with increasing angular velocities ($d' = 2.48$, $d' = 1.42$, and $d' = 0.75$ for the 750°, 1500°, and 2250°/2500°/s velocities, respectively), and with increasing point numbers ($d' = 2.03$, $d' = 1.59$, and $d' = 1.03$ with 12, 16, and 20 points, respectively). However, it can be seen in Figure 3A that the pattern of the data is very different from that found when no test ring was present. Rather than plummeting towards zero, observer's sensitivity rates remained quite high at the 750°/s velocity and declined in a relatively linear fashion as the velocity increased, remaining well above zero at 1500°/s and 2250°/2500°/s. In addition, point number continued to have an effect at all three velocities, although there is a reduction in this effect as the velocity increased, accounting for the Velocity × Point-number interaction.

The reliability of the observed pattern of effects was evaluated with two-tailed posthoc t tests that compared specific values of d' in the various point-number conditions (using a Bonferroni-corrected alpha level of 0.0056). In all three velocity conditions sensitivity was significantly poorer in the 20 point condition than in the 12 point condition (see Figure 3A). In addition, d' values were significantly lower in the 20 point condition than in the 16 point condition with the 750°/s and 1500°/s velocities. No difference between the 12 point and the 16 point condition was found at any velocity when we used the Bonferroni-corrected α values. However, d' values were lower in the 16 point condition than in the 12 point condition at 750°/s, and at 2250°/2500°/s when we employed an uncorrected 0.05 significance level.

Velocity and Point-number both modulate the temporal frequency of the point presentations at specific localities on the inducing ring circumference: As the rotation rates go up, points cross a given locality more frequently, and as the point number goes up, fewer steps are needed for successive points to cross a given locality. To address the hypothesis that the decline in the strength of the MBE as the inducing ring velocity increases and point-number decreases, is attributable to the increased temporal frequency of point presentations, we calculated the temporal frequency for each combination of point number and angular velocity (see Table 2) and correlated these rates with observer's mean sensitivity (d') in that condition. A significant relationship between the MBE and the temporal frequency of the inducing ring was found, $r = -0.92$, $p < 0.001$, with the MBE decreasing as temporal frequency increased (see Figure 3B).

Summary and discussion: Experiment 1

In Experiment 1 we replicated the MBE and confirmed its dependence on angular velocity (Mattler & Fendrich, 2010). When the inducing ring was presented by itself, observers' ability to detect its rotation fell to chance at velocities of 1500°/s and higher, but remained well above chance at velocities of up to 2500°/s when the rotating ring was followed by the stationary test ring. Interestingly, at these high velocities the temporal frequency of point presentations along the circumference of the inducing ring could be as high as 125 Hz, which not only exceeds conventional estimates of the CFF (Kaufman, 1974) but also exceeds the reported limits for the conscious detection of motion (Burr & Ross, 1982; Kelly 1979).

Experiment 1 also demonstrates that the conscious perception of motion in the inducing ring only conditions and the MBE in the inducing ring + test ring conditions were dependent on the number of points that formed the rings. Increasing the number of points reduced an observer's ability to discriminate the inducing ring's rotation direction both when it was presented by itself and when it was followed by the test ring, though in the latter case performance remained better than chance at every tested velocity and point-number. Because increasing the point number acted to increase the temporal frequency without altering velocity, the effect of point number is consistent with the premise that the conscious perception of motion was limited by the temporal frequency of the point

presentations along the inducing ring circumference. When only the inducing ring was presented, this effect was largely overridden by ceiling effects at the 250°/s velocity (since participant's responses were mostly correct) and basement effects at the 1500°/s and higher velocities (since participants always performed at chance), but at the 750°/s velocity, performance in the 12 point (25 Hz) condition was substantially better than in the 16 (33 Hz) and 20 (42 Hz) point conditions (see Figure 3A). These results are consistent with Burr and Ross's study (1982) in which the detection of the motion of sinusoidal gratings begins to deteriorate at around 10 Hz and completely breaks down at around 30 Hz.

When both the inducing and test rings were presented, the effect of point-number was far more pervasive, clearly demonstrating that the illusory motion of the MBE, like the actual inducing ring motion, is modulated by the number of points in the inducing ring. Increasing the number of points reliably reduced the MBE with the 750°, 1500°, and 2250°/2500°/s velocities. As is the case for the percepts of the actual motion, this effect may be attributable to an increase in the temporal frequency. However, in the case of the MBE the upper limit of the effective range of temporal frequency would be above 125 Hz, considerably higher than it is in the case for flicker and motion perception.

Varying the point number has the additional effect of generating complex changes in the inducing ring's spatial frequency spectrum. The effect of altering the point-number could therefore also be attributed to a dependency of the MBE on the inducing ring's spatial frequency composition. While we cannot rule out the spatial frequency spectrum of the inducing ring as a factor that contributes to the observed effects, we regard this issue as unlikely. Burr and Ross (1982) regarded spatial frequencies as meaningful for motion detection only because they determined the temporal frequency of the intensity modulations that occurred when their grating stimuli moved. Moreover, when the inducing ring rotates at a high velocity, there is little opportunity for the spatial frequency components associated with the number of inducing ring points to have any effect because the inducing ring fuses due to visual persistence into an apparently continuous outlined circle irrespective of point separation. This implies the moving points are rendered visually simultaneous at every position where they are displayed so that the amplitude of the spatial frequency components associated with the inducing ring point separations will be reduced to virtually zero. Based on these considerations, the findings of Experiment 1 are more likely to be the effect of temporal frequency changes rather than any change in the spatial frequency spectrum of the inducing ring.

Experiment 2

In this experiment we investigated the effect of changing the diameter of the inducing and test ring on the illusory motion percept. Changing the diameter of the inducing ring has two major effects: It changes both the retinal eccentricity of the points that form the ring and changes their linear velocity as the ring rotates (see Table 3). However, the change in ring diameter will not change the angular velocity of the rotating points or the temporal frequency of the point presentations at specific positions along the ring circumference.

While the MBE occurs at rotational velocities so high that visual persistence prevents motion from being consciously perceived, this rotation may nevertheless be capable of driving speed-selective cortical cells (Simoncelli & Heeger, 1998) tuned to high velocity motions. Velocity-tuned cells in the medial temporal cortex of monkeys that are specifically responsive to rotational movements have been reported by Tanaka and Saito (1989). If such cells play a role in mediating the MBE, increasing the linear velocity of the inducing ring points could decrease the MBE by raising velocities above the response limits of these cells. Alternatively, the MBE could increase with increasing eccentricity because the modulation sensitivity of the visual system increases with eccentricity (Hartmann, Lachenmayr, & Brettel, 1979; Tyler, 1985, 1987).

Method

Stimuli and procedures were similar to those described for Experiment 1 with the following changes: In Experiment 2 the inducing and test rings were always constructed from 16 points, but the diameter of the rings was varied block-wise in three steps: 3.5°, 5.5°, and 7.5° of visual angle (see Figure 2). The point-distance was respectively 0.69°, 1.08°, and 1.47° of visual angle (measured along the ring circumference) for the three diameters. The diameter of the test ring always matched that of the inducing ring. As in the first experiment, 14 trial blocks were run in each session with the first two treated as practice and excluded from data analysis. The diameter of the inducing ring was changed after the sixth and 10th blocks following a Latin Square design. There were 48 trials in each block, with an additional eight practice trials (which were not analyzed) added at the start of the seventh and 11th blocks.

The inducing ring duration was always 91 ms and the test ring duration 500 ms. Inducing ring rotation velocities of 250°, 750°, 1500°, and 2250°/s were presented within each block in a quasirandom order. For the corresponding linear velocities see Table 3. The

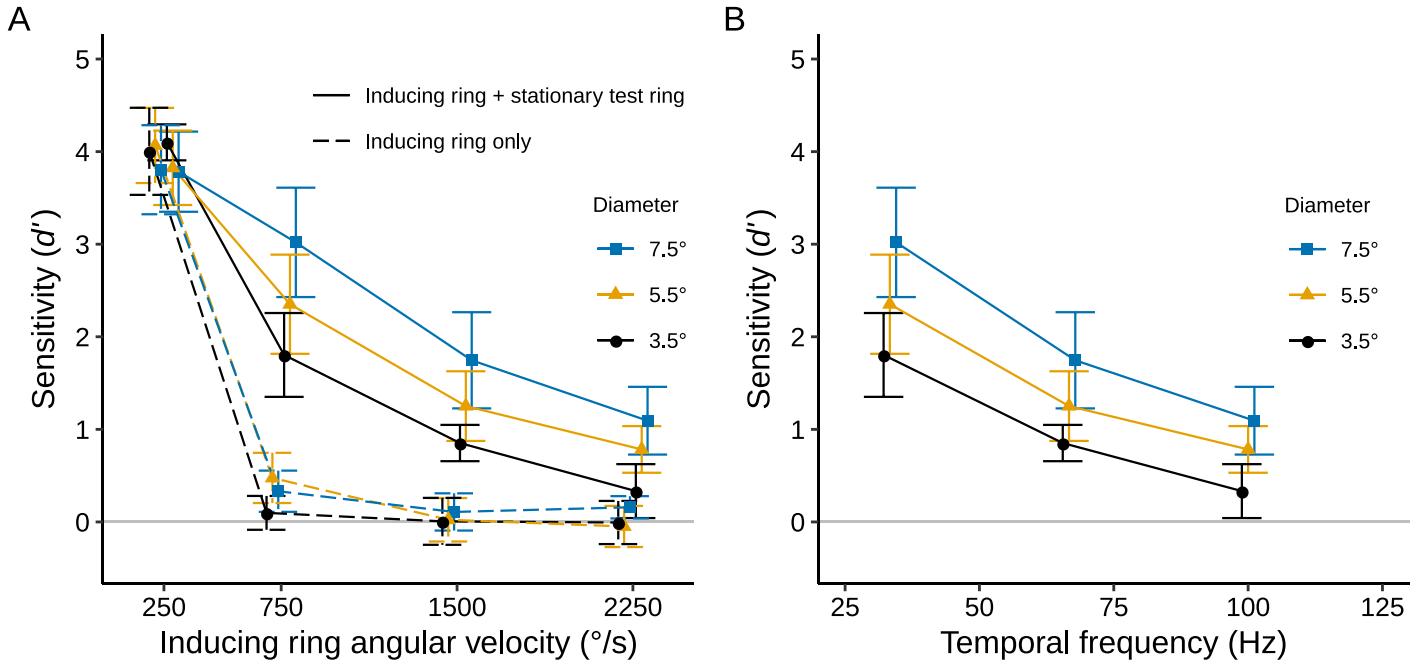

Figure 4. (A) Mean sensitivity (d') for 12 participants of Experiment 2 as a function of inducing ring velocity and ring diameter in the inducing ring only conditions (the dashed line) and the inducing ring + test ring conditions (the solid line). (B) Mean d' values from the inducing ring + test ring conditions for rotation rates of 750°/s and greater as a function of temporal frequency. The solid gray line indicates the chance level of accuracy ($d' = 0$). The error bars show 95% confidence intervals. Points and confidence intervals are slightly offset horizontally to improve their visibility.

combination of two test ring states (present vs. absent), four inducing ring angular velocities, and three diameters produced 24 experimental conditions. There were 72 trials in each of these conditions: 36 with a clockwise inducing ring rotation and 36 in counter-clockwise rotation.

Results

Results and confidence intervals for all the conditions of Experiment 2 are presented as d' values in Figure 4A. Figure 4B shows the relationship between the MBE and temporal frequency. Mean percentage correct performance values are presented in Appendix Table A3. As in Experiment 1, separate ANOVAs were calculated for the test ring present and test ring absent conditions. These ANOVAs are presented in Appendix Table A4.

Inducing ring only

When only the inducing ring was presented, the across subject sensitivity (d') to the rotation direction was examined with a 4×3 ANOVA with Velocity and Diameter as the factors. The main effect of Velocity was significant, but we found no significant main effect of Diameter and no significant interaction between Velocity and Diameter (Appendix Table A4). The effect of Velocity followed the pattern observed in Experiment 1, as shown in Figure 4A. Sensitivity rates were high in the 250°/s condition, abruptly dropped in the 750°/s condition, and fell to chance levels in the two high velocity conditions.

Twelve one-tailed t tests (with a Bonferroni-corrected alpha level of 0.0042) confirmed the consistent above chance performance in the 250°/s velocity conditions ($p < 0.0001$ in all cases) and chance performance in the high velocity 1500° and 2250°/s conditions. In the 750°/s condition, d' was slightly but significantly greater than zero with the two larger ring diameters ($d' = 0.48$ and $d' = 0.33$, $p = 0.0013$ and $p = 0.0037$, for the 5.5° and 7.5° rings, respectively). Performance did not differ from chance for any ring diameter in the two high velocity conditions. Except for the 7.5° ring diameter in the 2250°/s condition ($p = 0.0073$), which we regard as a false positive, this was the case even when we employed an uncorrected 0.05 significance level.

Inducing ring + test ring

Similar analyses were carried out for the inducing ring + test ring conditions to address the characteristics of the MBE. As in Experiment 1, trials with 250°/s velocity were excluded from these analyses because at this velocity discrimination of the inducing ring rotation did not depend upon the test ring presentation. In a 3×3 ANOVA with Velocity and Diameter as factors, the

main effect of both these factors was significant but they did not interact (Appendix Table A4).

As in Experiment 1, the pattern of the data is very different from that found when no test ring was present. As expected, mean sensitivity declined with increasing angular velocities in a relatively linear fashion ($d' = 2.39$, $d' = 1.28$, and $d' = 0.74$ at 750°, 1500°, and 2250°/s, respectively). In addition, as the ring diameter increased the MBE grew stronger ($d' = 1.00$, $d' = 1.46$, and $d' = 1.95$ at 3.5°, 5.5°, and 7.5° of visual angle). However, despite the fact that the 3.5° diameter ring produced the lowest accuracy rates at all velocities, only with the 2250°/s velocity did that rate come close to chance. The reliability of the effect of ring diameter was confirmed by Bonferroni-corrected two-tailed posthoc t tests ($\alpha = 0.0056$) which indicated that at all three velocities the MBE was significantly weaker with the 3.5° ring diameter than the 7.5° ring diameter. Additionally, the MBE was weaker with the 5.5° ring diameter than with 7.5° ring diameter in the 750°/s condition and weaker with 3.5° ring diameter than the 5.5° diameter in the 2250°/s condition.

Discussion: Experiment 2

In Experiment 2 we found that the MBE depends on the diameter of the inducing and test ring, with a larger ring diameter producing a stronger MBE. Increasing the diameter of the rings both increased the retinal eccentricity of the points that formed the rings and increased the linear velocity of the points as the inducing ring rotated. The increase in linear velocity produced by increases in the inducing ring's angular velocity is reliably associated with a decrease in the MBE. Therefore, it would be reasonable to expect any effect of the increase produced by the larger ring diameter would also be a reduction of the MBE. Since we observed the reverse—larger ring diameters increased the MBE—we think it is likely that the increase in retinal eccentricity was responsible for this effect. While it is possible that the increase in velocity did in fact act to reduce the MBE but this reduction was overwhelmed by an opposing effect produced by the eccentricity change, our data suggest that the increase in linear velocity had no effect at all. When we calculated the linear velocity for each combination of diameter and angular velocity (see Table 3) and correlated these rates with observers' mean sensitivity (d') no significant relationship between the MBE and linear velocity was found ($r = -0.41$, $p > 0.05$).

The ring diameters we employed placed the ring circumferences in two anatomically distinct regions of the retina. Because the foveal region has an anatomical diameter of approximately 5° (Millodot, 2018; Schubert, 2014; Wandell, 1995), the inducing and tests rings were foveal in the 3.5° diameter condition but parafoveal in the 7.5° condition. Therefore, the increase in the MBE with increasing ring size might be attributable to the para- and perifoveal areas being more capable of processing rapid motions due to the increased dominance of transient cells in these regions relative to the fovea (for Y cell dominance in cats, see Hoffmann, Stone, & Sherman, 1972; for the M cell increase in monkeys, see Schein & de Monasterio, 1987; on the implications for human perception see Breitmeyer & Ganz, 1976). While there is data indicating that sensitivity to motion is similar in the fovea and more peripheral regions of the retina (McKee & Nakayama, 1984) or that the fovea is actually more sensitive to motion than the periphery (Finlay, 1982), Sekuler (1975) concluded that the periphery has a distinct preference for high rates of temporal modulation. One can construe this as a shift in the temporal frequency response function for moving stimuli towards higher values as retinal eccentricity increases. Along with other evidence, Sekuler notes that when Armstrong (reported in Sekuler, 1975) presented targets with linear velocities up to 100°/s on an oscilloscope, the motion of these targets was only perceived when the target was 10° eccentric. Baker and Braddick (1985) argue, based on an increase of the spatial limit of apparent motion (d_{max}) with eccentricity, that high velocity motions that are not visible in central vision can become visible in the periphery of the retina. The argument that the periphery of the retina is sensitive for high temporal modulation is further supported by findings from flicker research. Tyler (1985), for example, reports the peripheral CFF can be substantially higher than the foveal CFF (see also Hartmann et al., 1979; and Tyler, 1987). If the temporal frequency is a primary determinant of the strength of the MBE, as our Experiment 1 results suggest (see also Figure 4B), these findings make a higher temporal sensitivity in the peripheral retina a likely candidate for the reported effect of ring diameter.

There is, however, an additional factor that needs to be considered. In both Experiments 1 and 2 the stimulus conditions that led to an increase in the MBE were associated with an increase in the spatial separation between the points that formed the inducing and test rings. This finding raises the possibility that the observed effects were attributable to this increased point separation. In Experiment 3 we examined this possibility.

Experiment 3

In Experiment 1 we found reducing the number of points in the inducing and test rings increased the strength of the MBE. In Experiment 2 we found that enlarging the rings increased the MBE. The fact that

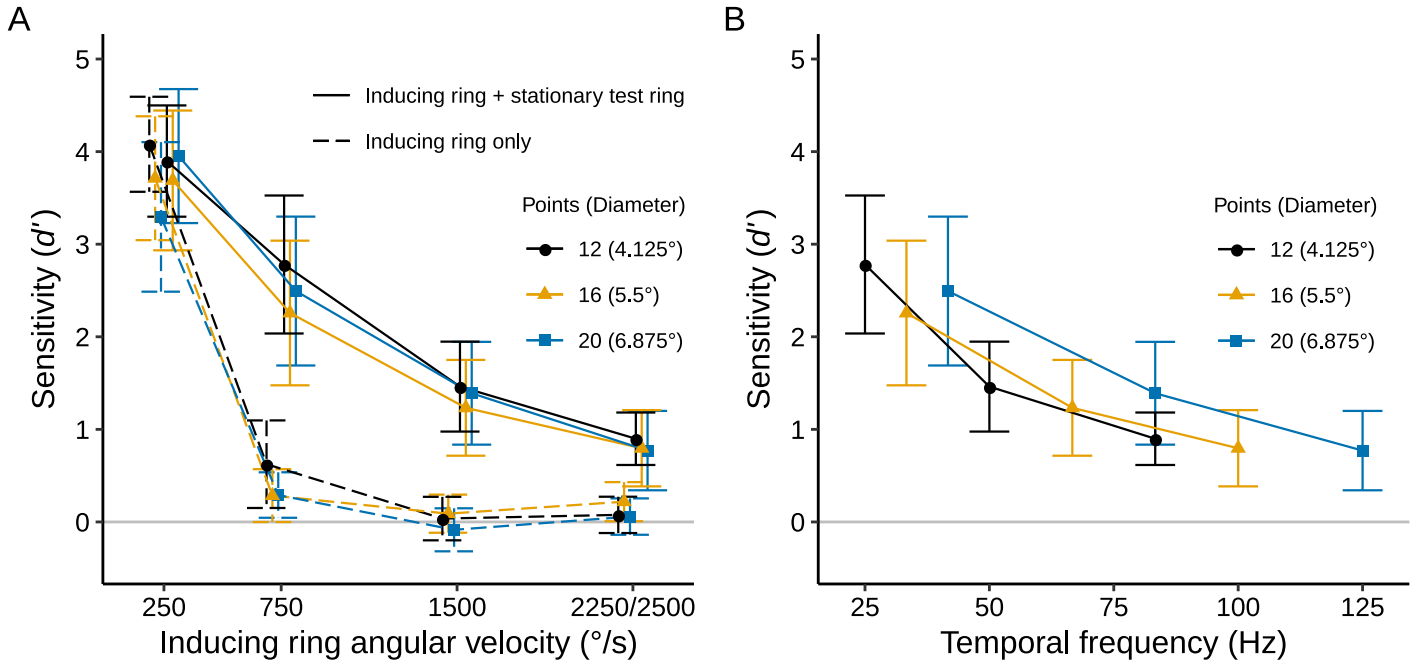

Figure 5. (A) Mean sensitivity (d') for 12 participants of Experiment 3 as a function of inducing ring velocity and point-number/diameter combination in the inducing ring only (the dashed line) and inducing ring + test ring conditions (the solid line). (B) Mean d' values from the inducing ring + test ring conditions for rotation rates of 750°/s and greater as a function of temporal frequency. The solid gray line indicates the chance level of accuracy ($d' = 0$). The error bars show 95% CI. Points and confidence intervals are slightly offset horizontally to improve their visibility in (A).

both these manipulations increased the spatial separation between the points forming these rings raised the possibility that this change in separation was mediating the change in performance in both cases. In the discussion of Experiment 1 we noted that the spatial frequency components associated with the separation of the points that form the inducing ring do not seem likely to directly impact the MBE because when its rotation is rapid, visual persistence transforms the ring into a visually continuous outline. Nevertheless, because point spacing was a confounding variable in both Experiments 1 and 2 we felt its potential contribution to the experimental outcomes needed to be empirically evaluated. This was done in Experiment 3 by covarying the diameter and the number of points in the inducing and test rings in a manner that caused the spacing between the points forming the rings to remain constant. Experiment 3 is therefore akin to Experiment 1 in that at each tested angular velocity, temporal frequency is varied, but this is accomplished while holding point separations constant.

Method

Fourteen trial blocks of 48 trials, half with the inducing ring followed by the test ring, were run in each of three sessions, following the sequence and procedures described for Experiment 1. Stimuli were similar to those employed in Experiment 1 with the following modifications. As in the first Experiment, 12, 16, or 20 equally spaced points formed the circumference of the inducing and test rings, with changes in the point number at the start of the seventh and 11th block following a Latin-square design. However, these changes were coupled with changes to the inducing ring diameter so that an interpoint separation of 1.08° of visual angle on the circumference of the ring was maintained. The required ring diameters were 4.125°, 5.5°, and 6.875° of visual angle in the 12, 16, and 20 point conditions, respectively (see Figure 2). As in Experiments 1 and 2, clockwise and counterclockwise inducing ring rotation directions with angular velocities of 250°, 750°, 1500°, and 2250°/s (2500°/s in the 12 point condition) were presented in a quasirandom fashion.

The combination of two test ring states (present vs. absent), four inducing ring angular velocities, and three point-number/diameters produced 24 experimental conditions. There were 72 trials in each of these conditions: 36 with a clockwise inducing ring rotation and 36 in counterclockwise rotation.

Results

Results and confidence intervals for all conditions of Experiment 3 are presented in Figure 5A. Figure 5B shows the relationship between the MBE and temporal

frequency. Mean percent correct rates are presented Appendix Table A5. As in the previous experiments, separate ANOVAs were calculated for the test ring present and test ring absent conditions. These analyses are presented in Appendix Table A6.

Inducing ring only

When the inducing ring was presented alone, the effect of Velocity replicated the pattern found in the previous experiments with mean sensitivity declining sharply to chance levels as the inducing ring Velocity increased. A 4×3 ANOVA with Velocity and Point-number/diameter as factors revealed a significant main effect of Velocity and a significant main effect of Point-number/diameter (Appendix Table A6). The effect of Point-number/diameter reflects a decline in performance as Point-number/diameter increased. However, while sufficient to produce a significant main effect in the ANOVA, the effect of Point-number/diameter was quite small and could not be confirmed at any velocity with Bonferroni-corrected two-tailed posthoc t tests ($\alpha = 0.0042$). When we employed an uncorrected 0.05 significance level, point-number/diameter did produce significant posthoc d' differences but only when the inducing ring velocity was 250°/s, with performance in the 20 point condition poorer than in the 12 and 16 point conditions. Posthoc comparisons at the higher velocities all failed to yield significant differences even at 0.05 level.

Bonferroni-corrected one-tailed t tests ($\alpha = 0.0042$) confirmed that sensitivity was significantly greater than zero with every point-number when the angular velocity was 250°/s ($p < 0.0001$ in all cases), but did not differ from chance for any point number at any of the higher velocities. When we employed an uncorrected 0.05 significance level, d' exceeded 0 in every 750°/s velocity condition, but at higher velocities the only case of a data point exceeding chance was in the 16 point condition when the ring diameter was 5.5° and velocity was 2250°/s, $t(11) = 2.28$, $p = 0.0217$. We regard this outcome as a probable false positive.

Inducing ring + test ring

To evaluate the effect of point separations on the MBE, a similar ANOVA was performed on data of conditions where the test ring followed the inducing ring (Appendix Table A6). As in the first two experiments, the 250°/s condition was excluded from these analyses because it was not appropriate for measuring the MBE, so there were three Velocity and three Point-number/diameter conditions. As expected, the main effect of Velocity was significant with a profile similar to that observed in the inducing + test ring conditions of the previous experiments. Sensitivity to the inducing ring direction was high in the 750°/s condition, and declined relatively smoothly with increasing angular velocities ($d' = 2.51$, $d' = 1.36$, and $d' = 0.82$ at 750°, 1500°, and 2250°/2500°/s velocities, respectively), but remained well above chance at the two highest velocity. However, there was no significant main effect of Point-number/diameter and no significant interaction between Velocity and Point-number/diameter.

Thus, despite the fact that point-number (Experiment 1) and diameter (Experiment 2) both modulated the strength of the MBE when presented separately, when covaried so that the interpoint distance remained constant, they seemed to have no effect. This result supports the hypothesis that the interpoint distance was the critical variable in the previous experiments, although, as discussed below, this hypothesis raises problems and other interpretations are feasible.

Discussion: Experiment 3

Experiment 1 suggested that the increases in the temporal frequency of activations on the inducing ring circumference might be a critical determinant of the MBE's decline with increasing angular velocity. In Experiment 2 it was found that increasing the retinal eccentricity of the inducing ring circumference enhanced the MBE. In Experiment 3, when these variables were covaried to keep the separation between the points that formed the inducing and test rings constant, the magnitude of the MBE did not change. As this manipulation required the pairing of an increase in the ring diameter with an increase in the number of points forming the rings, the simplest way to account for this result is to posit that the enhancement produced by the increase in diameter and decrement produced by the increase in point number simply canceled. This account seems unlikely because it requires that the cancelation be coincidentally perfect when the interplay of point-number and diameter also holds the interpoint distance constant. We return to this consideration in our final discussion. Here, we note that the alternative hypothesis that the distance between the inducing ring points was directly responsible for the effects observed in Experiments 1 and 2 also needs to be considered.

Accepting this premise, however, implies that the changes in temporal frequency produced by our point number manipulations in Experiment 3 played little or no role in determining the MBE strength (see Figure 5B). This implication does not fit well with the existing evidence (e.g., Burr & Ross, 1982) that motion perception is in general dependent on the processing of temporal frequencies. There must, in

fact, be some temporal frequency at which neural persistence makes the neural responses to intensity changes too shallow to differentiate a rotating from a stationary ring. The absence of an effect of point-number in Experiment 3 suggests that with temporal frequencies as high as 125 Hz (see Table 2) the flattening of neural modulations is not yet sufficient to degrade the MBE. This is a surprising outcome. Moreover, in combination with the implication of Experiment 2 that linear velocity does not affect the MBE, it leaves the relatively steady decline in the MBE with increasing angular velocity unaccounted for. The results of Experiment 3 therefore raise puzzling issues that need to be addressed. We will return to these issues in our final discussion.

Experiment 4

In Experiments 1 and 3, a side effect of varying the number of points in the inducing ring was a change in the time-averaged luminance of the inducing ring and test ring points. Because luminance changes flicker sensitivity (Kelly, 1961), these luminance variations could in principle have contributed to the observed effects of point-number. Experiment 4 evaluated this possibility by varying the luminance of inducing and test rings to determine what effect, if any, these luminance changes might have had on the experimental outcomes. Two experimental sessions were run on separate days. In Session 1, the luminance of the inducing ring points was varied in four steps and the test ring luminance was held constant. In session 2, there were two inducing ring luminances combined with four test ring luminances. Across the two sessions we employed luminance levels that encompassed all the measured test ring point luminances (1.20 to 1.50 cd/m^2) and time averaged inducing ring luminances in the 1500° and 2250°/2500°/s angular velocity conditions of Experiments 1 and 3 (0.072 to 0.149 cd/m^2; cf. Table 1).

Method: Session 1

Eighteen blocks of 32 trials were run during the first session. Participants were presented with inducing rings and test rings like those employed in the previous experiments (see Figure 1). The inducing rings were always constructed from sixteen equally spaced points, 5.5° in diameter, and presented for 91 ms. As in the previous experiments, the test ring was presented for 500 ms. There were four time-averaged inducing ring luminances: 0.073, 0.094, 0.118, and 0.188 cd/m^2. The luminance was constant within each block but varied across the trial blocks using a repeated Latin Square design. The luminance of the test ring points was held constant at 1.088 cd/m^2. Two inducing ring velocities were presented within each block: On 25% of the trials (16 total in each condition) there was a slow 250°/s rotation, and on 75% of the trials (48 in each condition) there was a rapid 1500°/s ring rotation. No test ring was presented in the initial block; then blocks in which the test ring was presented and blocks with no test ring were alternated. The first two blocks and the slow rotation rate trials were treated as practice and not analyzed.

Method: Session 2

Seventeen trial blocks with 32 trials per block were run. The test ring luminance was varied in four steps (0.733, 1.088, 1.441, and 1.779 cd/m^2,) and each test ring luminance level was presented with two inducing ring luminance levels (0.073 and 0.188 cd/m^2). The inducing ring-test ring luminance combinations were varied quasirandomly between blocks. Two inducing ring velocities were presented within each block: On 25% of the trials (16 total in each condition) there was a slow 250°/s ring rotation, and on 75% of the trials (48 in each condition) there was a rapid 1500°/s ring rotation. The first block and the slow rotation rate trials were treated as practice and were not analyzed.

Results

Results and confidence intervals for all conditions of Session 1 are presented in Figure 6. The across subject sensitivity (d') to the rotation direction was calculated for each condition and examined with a 2×4 ANOVA with Test ring (inducing ring only vs. inducing ring + test ring condition) and Inducing ring luminance as the factors. As expected, the main effect of Test ring was significant, $F(1, 11) = 100.37$, $p < 0.001$. The mean sensitivity was higher when the inducing ring was followed by the test ring ($d' = 1.67$ compared to $d' = 0.25$) but we found no significant main effect of Inducing ring luminance, $F(3, 33) = 0.34$, $p = 0.759$, and no interaction between Test ring and Inducing ring luminance, $F(3, 33) = 0.06$, $p = 0.944$. As can be seen in Figure 6, accuracy rates were stable across the full range of inducing ring luminances. This is true both when the inducing ring is presented on its own (54.1% to 55.4%) and when it is followed by the test ring (77.1% to 78.3%).

Results and confidence intervals for session 2 are shown in Figure 7. We once again performed a 2×4 ANOVA with Inducing ring luminance and Test ring

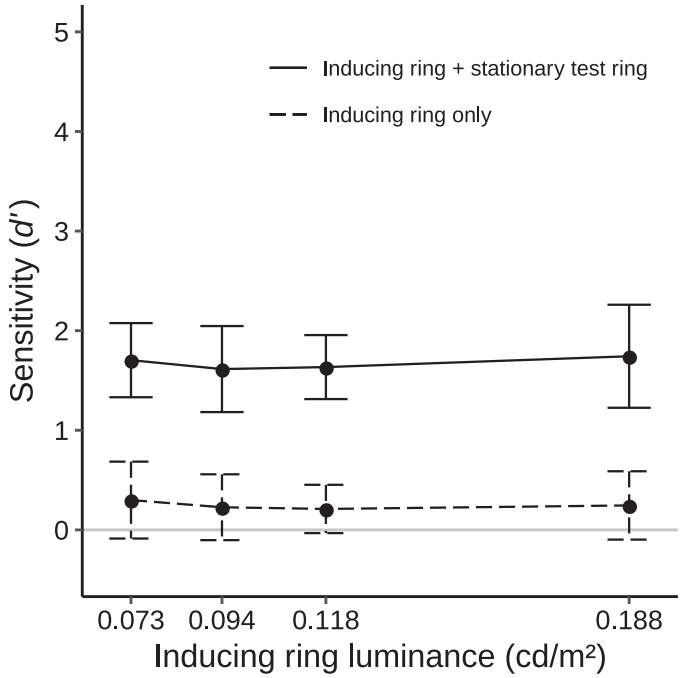

Figure 6. Mean sensitivity (d') for 12 participants of Experiment 4 (Session 1) as a function of time averaged inducing ring luminance levels in the inducing ring only conditions (the dashed line) and the inducing ring + test ring conditions (the solid line). The error bars show 95% CI. The solid gray line indicates the chance level of accuracy ($d' = 0$).

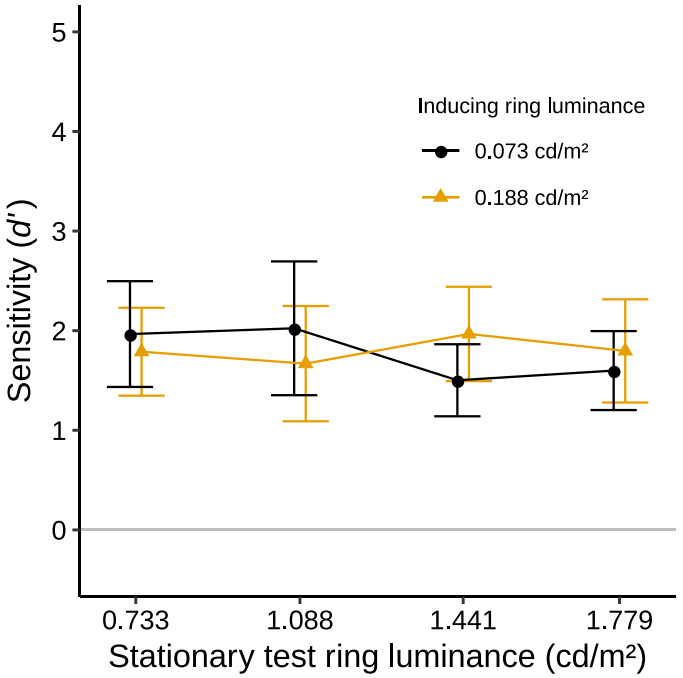

Figure 7. Mean sensitivity (d') for 12 participants of Experiment 4 (Session 2) as a function of test ring luminance levels with each of two time averaged inducing ring luminance levels. The error bars show 95% CI. Only the inducing ring + test ring conditions are shown. The solid gray line indicates the chance level of accuracy ($d' = 0$).

luminance as factors. Neither of these factors had a significant main effect and there was no significant interaction between them: $F(1, 11) = 0.11$, $p = 0.751$ for the main effect of Inducing ring luminance, $F(3, 33) = 0.95$, $p = 0.398$ for the main effect of Test ring luminance, and $F(3, 33) = 2.82$, $p = 0.064$ for the interaction. The nonsignificant interaction might point to a slight trend towards larger MBEs in conditions in which inducing ring and test ring have comparable luminances. Overall, however, Figure 7 shows that neither the inducing ring nor test ring luminance had any effect on accuracy rates.

Discussion: Experiment 4

Although the luminance variations associated with the number of points displayed could in principle have confounded the results of Experiments 1 and 3, in Experiment 4 we found that luminance changes that encompassed the full range of these variations had no effect on participants' performance. We conclude that luminance was not a confounding factor. It needs to be noted, though, that the range of luminance levels we investigated was quite small. It is therefore entirely possible that luminance variations over a wider range could modulate the MBE.

General discussion

When participants judged the rotation direction of a rapidly rotating ring of points (the inducing ring), they performed at chance when the investigated angular velocities were 1500°/s and higher. However, when an additional stationary ring (the test ring) was presented after a short delay, an illusory rotation of this test ring allowed them to report the inducing ring's rotation direction at rates substantially better than chance even at the highest velocity employed (2500°/s). This effect was previously reported by Mattler and Fendrich (2010) and termed the Motion Bridging Effect. The experiments reported here examine the effect of two variables on the MBE: the number of points that made up the inducing and test rings and the diameter of those rings. We found an increase in the MBE (measured by the accuracy of reports of the inducing ring direction) when the number of points used to construct the rings was reduced. In addition, we found an increase in the MBE when the diameter of the rings was increased. However, both of these manipulations influenced the distance between the points that formed the inducing and test rings. When this distance was held constant by covarying the point number and ring diameter, no effect on the MBE was observed. We will speculate that

processes related to the perception of both real and apparent motion may be contributing to this pattern of results.

Burr and Ross (1982) have proposed that all motion perception is limited by the temporal frequency of intensity modulations on the retina. If the temporal frequency is too high (e.g., over 30 Hz for sinusoidal gratings), the spatial-temporal properties of the stimulus cannot be translated into visible motion. If this argument is extended to the MBE, then both the decline in the MBE with increasing angular velocity and the decline with an increase in the number of points used to form the inducing ring can be explained. However in the case of the MBE, the temporal frequency limit must be at least 125 Hz, which is well above the rates that normally mediate motion detection and substantially above the human flicker fusion frequency. In addition, to account for the performance gain in the MBE when the diameter of the rings is increased, one must also posit that its dependence on temporal frequency is scaled by retinal eccentricity, with high temporal frequencies more readily processed at more peripheral positions. This scaling can also explain the stability of the MBE in Experiment 3 if one accepts that the decline in the MBE produced by the increase in point-number is canceled by the improved processing of high temporal frequencies as the ring diameter is increased. However, this explanation requires that the decline and improvement in the MBE balance one another almost perfectly when a combined effect of these variables also acts to hold the separation between the points that form the inducing ring constant. The presumption that these effect null-points co-occur by chance strains the credibility of this account.

Apparent motion

An alternative approach to explaining the observed pattern of outcomes is to propose that the MBE is modulated by the spatial separation between the test ring rather than inducing ring points. In our experiments, the separation of the points that formed the test ring always matched the separation of the points in the inducing ring, and because the test ring was always veridically stationary, this separation was visually salient irrespective of the inducing ring velocity. We speculate that an essential component of the MBE is an apparent motion percept generated by the inducing ring to test ring transition.

In their 2010 paper, Mattler and Fendrich (2010) linked the MBE to apparent motion because the MBE consists of an intermediate visual percept that is synthesized from the sequence of two rings, one with a continuous outline and the other constructed of points. They note that a synthesis of the two rings by an updating process could account for both the deceleration when the continuous ring precedes the pointed ring and the acceleration when the pointed ring precedes the continuous outlined ring. Here we consider the link to apparent motion in more detail.

It has long been known that the spatial separation between the successive stimuli used to produce apparent motion can modulate the motion percepts (e.g., Korte, 1915; Wertheimer, 1912). Korte proposed that as the spatial distance between two stimuli increases their temporal distance also needs to increase to sustain an apparent motion percept (Korte's third law). More recent proposals have argued that depending on the presentation conditions, the relationship between spatial and temporal distance needed to maintain optimal apparent motion can be either a positive coupling or a tradeoff, so that an increase in spatial distance must be coupled with a decrease in temporal distance (Gepshtein & Kubovy, 2007).

A phenomenon related to apparent motion in which there is also an interplay of spatial and temporal factors has been termed *Singularbewegung* (Wertheimer, 1912), polarized gamma movement (Kanizsa, 1979), or the line-motion illusion (LMI; Downing & Treisman, 1997). In LMI experiments, a square flashed on a screen precedes the presentation of an adjacent line that appears as smoothly expanding outward from the square. Contemporary research on the LMI was initiated by Hikosaka, Miyauchi, and Shimojo (1993) who proposed that the square draws attention to its spatial location and facilitates neural processing at the end of the line adjacent to that location leading to the precept of expansion. Downing and Treisman (1997) discounted the attentional explanation of the LMI by showing a complementary phenomenon in which the line appears to shrink into a square. This result cannot be accounted for by attention because no cue to bias attention to a specific location was presented. The authors therefore interpret the LMI as an apparent motion linking two successive states that are treated as representations of a single object, making the LMI an instance of what Tse, Cavanagh, and Nakayama (1998) have termed "transformational" apparent motions. The LMI, like more traditional instances of apparent motion, exhibits spatial distance dependencies: Ratings of perceived velocity are increased when the line length is increased (Hubbard & Ruppel, 2011).

There are noteworthy similarities between the displays used to demonstrate the LMI and our MBE displays. In the case of the LMI, there is an immediate transition between a stationary line and one or more stationary markers, and a smooth illusory motion links the two stationary states, ensuring perceptual continuity. In case of the MBE, there is a transition from a perceptually stationary outline ring to multiple verid-

ically stationary points. We propose that when this transition happens, the segments of the inducing ring flanking the points of the test ring contract into those points.

Given this hypothesis, a question that arises is why observers see all the test ring points rotate together, rather than seeing the inducing ring segments adjacent to each of the test ring points, contract locally into those points. One possible explanation for the common direction of the test ring points in the MBE is that it represents an instance of the apparent motion yoking effect initially reported by Ramachandran and Anstis (1983). These investigators presented bistable dots pairs that could be seen to be undergoing either a horizontal or vertical oscillation when repetitively switched between their alternative states. When groups of these dot pairs are presented and switched simultaneously, the perceived direction of the oscillation is identical in all the pairs. In addition, other investigations have shown that when multiple line-motion stimuli are presented together, their motion signals can pool and be integrated to form a joint global motion percept (Tang, Dickinson, Visser, Edwards, & Badcock, 2013; Tse & Logothetis, 2002). These yoking and integration effects could result in all the inducing ring segments contracting in the same direction to generate the rotation percept.

The hypothesis that the test ring motion is a case of transformational apparent motion leaves, however, a core aspect of the MBE unexplained: It does not explain why the test ring generally rotates in the same direction as the inducing ring's invisible rotation. The transition from the continuous inducing ring to the point-defined test ring is ambiguous in respect to which direction the line will transform, so one might expect the test ring's rotation direction to be random. The fact that its direction usually matches the direction of the inducing ring indicates the inducing ring direction must have been encoded somewhere in the visual system and acted to bias the perceived rotation of the test ring. As we have previously noted, this implies the registration of temporal frequencies well beyond the range that the human visual system is conventionally thought to be able to process. The hypothesis that the test ring motion is a form of transformational apparent motion does not alter these implications. The MBE would therefore represent a case where a motion that is inherently inaccessible to consciousness is nevertheless modifying subsequent percepts. We note that if the biasing effect of the inducing ring acts on every test ring point this would support the percept that these points all move in a common direction. Moreover, if the ability of the inducing ring to bias the direction of the test ring motion varies with the spacing of the test ring points, this could account for the potential dependence of the MBE on that spacing. While this idea is speculative, the spatial dependencies found with apparent motion and the LMI lend credence to the supposition that the perceived rotation of the test ring could be a function of spacing of the points in that ring.

Conscious and unconscious motion processing

The processing of movement is generally thought to rest upon direction selective cells that have been found in the visual cortex of macaque and owl monkeys (Albright, 1984; Zeki, 1980). A well-known phenomenon that can be related to the reduced responsiveness of direction selective cells in V1 is the motion aftereffect (MAE; see Anstis, Verstraten, & Mather, 1998, for a review). The MAE is characterized by an illusory percept of a motion in the reverse direction of a previously inspected actual linear or rotary motion. It is generally attributed to a damping by neural adaptation of the activity of the direction sensitive cells that mediate the perception of the inspected motion, creating an imbalance that favors cells tuned to motion in opposite direction. The rotating dot displays used in the present experiments can produce a MAE if the rate of rotation is sufficiently slow (Mattler & Fendrich, 2010) but we think the origins of MAE and MBE are likely to be quite different. Besides the obvious difference in the direction of the perceived illusory motion, the build-up and decay of the MBE is far more rapid than the MAE. The MAE typically builds during extended exposures to the adapting stimulus and slowly fades away (Hershenson, 1989, 1993). In contrast, Mattler and Fendrich found the MBE occurred with exposures to the inducing ring as brief as 30 ms and reached its maximum strength after only 60 ms. While the duration of the MBE was not formally measured, they note that it generally "braked to a standstill" in the course of their 500 ms test ring presentation. Additionally the temporal frequencies of the stimuli presented in MBE experiments clearly exceed the temporal frequency limits of adapting stimuli in MAE experiments. The duration of the MAE is highest when the adapter frequency is 1–5 Hz, begins to rapidly decline at 20 Hz, and when the adapter is presented with a temporal frequency of 50 Hz, no MAE is seen (Pantle, 1974). These considerations lead us to conclude that the MBE and MAE are not related effects.

Studies of the MAE and other phenomena, however, show (as does the MBE) that movement can be processed without awareness of the motion direction. In a functional MRI study, Moutoussis and Zeki (2006) found a drifting grating at 15° eccentricity generated motion specific activations in brain areas as high as MT. Surprisingly, this was also the case when the grating was crowded by two additional flickering gratings and participants could no longer judge the

direction of movement of the target grating. Additional evidence is provided by binocular rivalry studies demonstrating that the duration of the MAE does not depend on whether the drifting adaptation grating is binocularly suppressed (Lehmkuhle & Fox, 1974, O'Shea & Crassini, 1981). Other studies have shown that the MAE still occurs in reduced form when the adapter is rendered unconscious by continuous flash suppression (Kaunitz, Fracasso, & Melcher, 2011; Maruya et al., 2008).

Apparent motion has also been investigated in the context of binocular rivalry: Wiesenfelder and Blake (1991) showed that subjects still perceived apparent motion when the first frame of a two-frame sequence was suppressed. Blanco and Soto (2009) have reported an instance of the LMI in which the flashed stimulus that generates the illusion is not consciously visible. In their experiment, a gray circle was displayed in one of four positions, followed by a mask in all four of these positions. When only the circle and masks were shown, participants were unable to report the position where the circle had been presented. However, when a gray line was presented subsequent to the masks, it was perceived as moving outward from the circle's location. All of these cases differ from the MBE, however, in that they involve an inherently detectable stimulus that only fails to reach consciousness because it is masked or suppressed.

An instance where an inherently invisible moving stimulus has been shown to have perceptual consequences has, however, been reported by Glasser, Tsui, Pack, and Tadin (2011), but in this case the motion was undetectable because of its brevity rather than velocity. In this study a high contrast 1 cycle/° sinusoidal grating drifted across a 16° diameter Gabor patch at 15°/s for intervals as short as 25 ms. Even when the presentations were too brief to allow observers to identify the drift direction of this grating, they produced a brief but detectable motion aftereffect in a subsequently low contrast stationary grating. However, this aftereffect corresponds to a classic MAE—a perceived motion in the direction opposite the preceding real motion—whereas the aftereffect in the case of the MBE is in the same direction as the preceding real motion. In addition, the aftereffect reported by Glasser et al. decreased steadily as the ISI between the moving and subsequent stationary stimulus grew larger than zero. The MBE, in contrast, increases with ISI from zero up to 90 ms (Mattler & Fendrich, 2010). These differences suggest that the neural mechanisms responsible for the aftereffects reported by Glasser et al. and those responsible for the MBE are fundamentally different.

In addition, global motion percepts that would otherwise be apparent become imperceptible when the number of motion directions shown becomes too high (e.g., Greenwood & Edwards, 2009). Lee and Lu (2014) demonstrated that such imperceptible global motions can elicit a motion aftereffect. Observers viewed a doughnut shaped field of drifting Gabor patches. Subsets of these Gabors conveyed global motion directions (e.g., expansion) but because a multiplicity of motion directions was shown, these global motions were not consciously detectable. Nevertheless, when a set of stationary Gabors replaced a subset of the drifting Gabors that had signified a specific global motion direction, a motion aftereffect that reversed the global motion direction was seen. Like the MBE, the MAE reported by Lee and Lu demonstrates the processing of motion information that is not consciously seen due to visual system processing limitations. However, in the case of the global motions addressed by Lee and Lu, these limitations occur at a stage where visible motions are integrated. Although observers are not able to link the displayed Gabors to derive a conscious global motion percept, the grating drift within each individual Gabor can be readily seen. In contrast, the motion responsible for the MBE fails to reach consciousness because of limitations in ability of the visual system to process a primary sensory attribute—luminance modulations. The MBE demonstrates that motion information can be derived from stimuli with temporal frequencies that have generally been regarded as beyond the range of human sensory encoding.

We have argued that two processes contribute to the MBE: (a) a transformational apparent motion generated by the transition from the perceptually continuous outline of the rapidly rotating inducing ring to the discrete stationary points of the test ring, and (b) a direction biasing process mediated by the inducing ring motion. This view of the MBE makes an interesting prediction. If the motion seen when the inducing ring is replaced by the test ring is a form of transformational apparent motion, then one would expect a motion percept to be present even if the inducing ring is a genuinely stationary outline. Under these conditions there can, of course, be no MBE because the MBE is defined by congruence between the inducing and test ring motion directions. Nevertheless, if observers see a coherent rotational motion of the test ring points similar to that observed with the MBE displays, this effect would argue strongly that the motion seen in the case of the MBE displays is mediated by a transformational component. On the other hand, if no motion or a directionally incoherent motion is seen, this would argue against the role of a transformational component in the MBE. In addition, studies in which the character of the inducing stimulus is changed could provide further information about the generality of the MBE and the suggested connection to apparent motion. Displays which produce linear or radial apparent motions might also be capable of giving rise to MBE

like percepts. We are currently exploring these possibilities.

Summary

The MBE demonstrates the neutral encoding of direction information from a ring of points that spins so rapidly its rotation is not consciously detectable (Mattler & Fendrich, 2010). When this spinning ring (the inducing ring) is followed by a stationary ring of points (the test ring), observers report seeing the test ring to rotate. This rotation is primarily in the same direction as the inducing ring, although this direction is not detectable when the inducing ring is presented by itself. The present study reveals that the MBE, indexed by the congruence of the inducing and test ring's rotation directions, weakens as number of points used to form the rings is increased. This finding supports the premise that the MBE is limited by the temporal frequency of point presentations produced as the points of the inducing ring advance around the ring perimeter. In addition, we found the MBE strengthens as the diameter of the rings is increased, which can be attributed to the more efficient registration of high temporal frequencies at more peripheral retina locations. However, when we covaried the number of points and the ring diameter in a manner that maintained a constant separation between the points that formed the inducing and test rings, the strength of the MBE was also constant. To account for this pattern of results, we propose that the MBE reflects the joint action of two processes, one that registers the direction of the inducing ring's rotation (and declines as a function of temporal frequency) and one that generates the illusory test ring spin (and is sensitive to the spacing between the points that form the test ring). We further propose that the second process represents an instance of a transformational apparent motion, generated by the transition from the inducing ring's perceptually continuous outline to the discrete stationary points of the test ring. We think the directional congruence that defines the MBE is produced by a biasing of the test ring direction by registered inducing ring direction information. Finally, we suggest the spacing of the test ring points (which was always the same as the spacing of the inducing ring points) may modulate the ability of the encoded inducing ring direction information to influence the perceived test ring direction, accounting for the dependence of the MBE on the point separations. Research to evaluate this speculative analysis is now in progress.

Keywords: motion aftereffects, motion perception, unconscious perception, apparent motion, temporal frequency

Acknowledgments

The authors thank Johannes Bommes and Marilena Reinhardt for their valuable support in recruiting participants and collecting data.

We acknowledge support by the Open Access Publication Funds of Goettingen University.

Data from Experiment 2 were presented at the 39th European Conference on Visual Perception, Barcelona, Spain.

Commercial relationships: none.
Corresponding author: Uwe Mattler.
Email: uwe.mattler@psych.uni-goettingen.de.
Address: Department of Experimental Psychology, University of Goettingen, Goettingen, Germany.

References

Albright, T. D. (1984). Direction and orientation selectivity of neurons in visual area MT of the macaque. *Journal of Neurophysiology*, *52*, 1106–1130, https://doi.org/10.1152/jn.1984.52.6.1106.

Anstis, S., Verstraten, F. A. J., & Mather, G. (1998). The motion aftereffect. *Trends in Cognitive Sciences*, *2*, 111–117, https://doi.org/10.1016/S1364-6613(98)01142-5.

Baker, C. L., Jr., & Braddick, O. J. (1985). Eccentricity-dependent scaling of the limits for short-range apparent motion perception. *Vision Research*, *25*, 803–812, https://doi.org/10.1016/0042-6989(85)90188-9.

Barlow, H. B. (1958). Temporal and spatial summation in human vision at different background intensities. *The Journal of Physiology*, *141*, 337–350, https://doi.org/10.1113/jphysiol.1958.sp005978.

Blake, R., & Fox, R. (1974). Adaptation to invisible gratings and the site of binocular rivalry suppression. *Nature*, *249*, 488–490, https://doi.org/10.1038/249488a0.

Blanco, M. J., & Soto, D. (2009). Unconscious perception of a flash can trigger line motion illusion. *Experimental Brain Research*, *192*, 605–613, https://doi.org/10.1007/s00221-008-1564-9.

Breitmeyer, B. G., & Ganz, L. (1976). Implications of sustained and transient channels for theories of visual pattern masking, saccadic suppression, and information processing. *Psychological Review*, *83*, 1–36, https://doi.org/10.1037/0033-295X.83.1.1.

Burr, D. C., & Ross, J. (1982). Contrast sensitivity at high velocities. *Vision Research*, *22*, 479–484, https://doi.org/10.1016/0042-6989(82)90196-1.

Campbell, F. W., & Robson, J. G. (1968). Application of Fourier analysis to the visibility of gratings. *The Journal of Physiology*, *197*, 551–566, https://doi.org/10.1113/jphysiol.1968.sp008574.

Coltheart, M. (1980). Iconic memory and visible persistence. *Perception & Psychophysics*, *27*, 183–228, https://doi.org/10.3758/BF03204258.

Cornsweet, T. N. (1970). *Visual perception*. New York, NY: Academic Press.

de Lange Dzn, H. (1958). Research into the dynamic nature of the human fovea→cortex systems with intermittent and modulated light. I. Attenuation characteristics with white and colored light. *Journal of the Optical Society of America*, *48*, 777–784, https://doi.org/10.1364/JOSA.48.000777.

Downing, P. E., & Treisman, A. M. (1997). The line-motion illusion: Attention or impletion? *Journal of Experimental Psychology: Human Perception and Performance*, *23*, 768–779, https://doi.org/10.1037/0096-1523.23.3.768.

Finlay, D. (1982). Motion perception in the peripheral visual field. *Perception*, *11*, 457–462, https://doi.org/10.1068/p110457.

Gepshtein, S., & Kubovy, M. (2007). The lawful perception of apparent motion. *Journal of Vision*, *7*(8):9, 1–15, https://doi.org/10.1167/7.8.9. [PubMed] [Article]

Glasser, D. M., Tsui, J. M. G., Pack, C. C., & Tadin, D. (2011). Perceptual and neural consequences of rapid motion adaptation. *Proceedings of the National Academy of Sciences, USA*, *108*, E1080–E1088, https://doi.org/10.1073/pnas.1101141108.

Greenwood, J. A., & Edwards, M. (2009). The detection of multiple global directions: Capacity limits with spatially segregated and transparent-motion signals. *Journal of Vision*, *9*(1):40, 1–15, https://doi.org/10.1167/9.1.40. [PubMed] [Article]

Gur, M., & Snodderly, D. M. (1997). A dissociation between brain activity and perception: Chromatically opponent cortical neurons signal chromatic flicker that is not perceived. *Vision Research*, *37*, 377–382, https://doi.org/10.1016/S0042-6989(96)00183-6.

Hartmann, E., Lachenmayr, B., & Brettel, H. (1979). The peripheral critical flicker frequency. *Vision Research*, *19*, 1019–1023, https://doi.org/10.1016/0042-6989(79)90227-X.

Hautus, M. J. (1995). Corrections for extreme proportions and their biasing effects on estimated values of *d′*. *Behavior Research Methods, Instruments, & Computers*, *27*, 46–51, https://doi.org/10.3758/BF03203619.

He, S., Cavanagh, P., & Intriligator, J. (1996). Attentional resolution and the locus of visual awareness. *Nature*, *383*, 334–337, https://doi.org/10.1038/383334a0.

He, S., & MacLeod, D. I. A. (2001). Orientation-selective adaptation and tilt after-effect from invisible patterns. *Nature*, *411*, 473–476, https://doi.org/10.1038/35078072.

Herrmann, C. S. (2001). Human EEG responses to 1–100 Hz flicker: Resonance phenomena in visual cortex and their potential correlation to cognitive phenomena. *Experimental Brain Research*, *137*, 346–353, https://doi.org/10.1007/s002210100682.

Hershenson, M. (1989). Duration, time constant, and decay of the linear motion aftereffect as a function of inspection duration. *Perception & Psychophysics*, *45*, 251–257, https://doi.org/10.3758/BF03210704.

Hershenson, M. (1993). Linear and rotation motion aftereffects as a function of inspection duration. *Vision Research*, *33*, 1913–1919, https://doi.org/10.1016/0042-6989(93)90018-R.

Hikosaka, O., Miyauchi, S., & Shimojo, S. (1993). Focal visual attention produces illusory temporal order and motion sensation. *Vision Research*, *33*, 1219–1240, https://doi.org/10.1016/0042-6989(93)90210-N.

Hoffmann, K.-P., Stone, J., & Sherman, S. M. (1972). Relay of receptive-field properties in dorsal lateral geniculate nucleus of the cat. *Journal of Neurophysiology*, *35*, 518–531, https://doi.org/10.1152/jn.1972.35.4.518.

Holcombe, A. O. (2009). Seeing slow and seeing fast: Two limits on perception. *Trends in Cognitive Sciences*, *13*, 216–221, https://doi.org/10.1016/j.tics.2009.02.005.

Hubbard, T. L., & Ruppel, S. E. (2011). Effects of temporal and spatial separation on velocity and strength of illusory line motion. *Attention, Perception, & Psychophysics*, *73*, 1133–1146, https://doi.org/10.3758/s13414-010-0081-7.

Jiang, Y., Zhou, K., & He, S. (2007). Human visual cortex responds to invisible chromatic flicker. *Nature Neuroscience*, *10*, 657–662, https://doi.org/10.1038/nn1879.

Kanizsa, G. (1979). *Organization in vision: Essays on gestalt perception*. New York, NY: Praeger.

Kaufman, L. (1974). *Sight and mind: An introduction to visual perception*. New York, NY: Oxford University Press.

Kaunitz, L., Fracasso, A., & Melcher, D. (2011). Unseen complex motion is modulated by attention and generates a visible aftereffect. *Journal of Vision*, *11*(13):10, 1–9, https://doi.org/10.1167/11.13.10. [PubMed] [Article]

Kelly, D. H. (1959). Effects of sharp edges in a flickering field. *Journal of the Optical Society of America*, *49*, 730–732. https://doi.org/10.1364/JOSA.49.000730

Kelly, D. H. (1961). Visual responses to time-dependent stimuli. I. Amplitude sensitivity measurements. *Journal of the Optical Society of America*, *51*, 422–429, https://doi.org/10.1364/JOSA.51.000422.

Kelly, D. H. (1979). Motion and vision. II. Stabilized spatio-temporal threshold surface. *Journal of the Optical Society of America*, *69*, 1340–1349, https://doi.org/10.1364/JOSA.69.001340.

Korte, A. (1915). Kinematoskopische Untersuchungen [Cinematoscopic studies]. *Zeitschrift für Psychologie*, *72*, 193–296.

Krolak-Salmon, P., Hénaff, M.-A., Tallon-Baudry, C., Yvert, B., Guénot, M., Vighetto, A., ... Bertrand, O. (2003). Human lateral geniculate nucleus and visual cortex respond to screen flicker. *Annals of Neurology*, *53*, 73–80, https://doi.org/10.1002/ana.10403.

Landis, C. (1954). Determinants of the critical flicker-fusion threshold. *Physiological Reviews*, *34*, 259–286, https://doi.org/10.1152/physrev.1954.34.2.259.

Lee, A. L. F., & Lu, H. (2014). Global-motion aftereffect does not depend on awareness of the adapting motion direction. *Attention, Perception, & Psychophysics*, *76*, 766–779, https://doi.org/10.3758/s13414-013-0609-8.

Lehmkuhle, S. W., & Fox, R. (1975). Effect of binocular rivalry suppression on the motion aftereffect. *Vision Research*, *15*, 855–859, https://doi.org/10.1016/0042-6989(75)90266-7.

Lin, Z., & He, S. (2009). Seeing the invisible: The scope and limits of unconscious processing in binocular rivalry. *Progress in Neurobiology*, *87*, 195–211, https://doi.org/10.1016/j.pneurobio.2008.09.002.

Lyskov, E., Ponomarev, V., Sandström, M., Mild, K. H., & Medvedev, S. (1998). Steady-state visual evoked potentials to computer monitor flicker. *International Journal of Psychophysiology*, *28*, 285–290, https://doi.org/10.1016/S0167-8760(97)00074-3.

Macmillan, N. A., & Creelman, C. D. (2005). *Detection theory: A user's guide* (2nd ed.). Mahwah, NJ: Lawrence Erlbaum Associates.

Maruya, K., Watanabe, H., & Watanabe, M. (2008). Adaptation to invisible motion results in low-level but not high-level aftereffects. *Journal of Vision*, *8*(11):7, 1–11, https://doi.org/10.1167/8.11.7. [PubMed] [Article]

Mattler, U., & Fendrich, R. (2007). Priming by motion too rapid to be consciously seen. *Perception & Psychophysics*, *69*, 1389–1398, https://doi.org/10.3758/BF03192954.

Mattler, U., & Fendrich, R. (2010). Consciousness mediated by neural transition states: How invisibly rapid motions can become visible. *Consciousness and Cognition*, *19*, 172–185, https://doi.org/10.1016/j.concog.2009.12.015.

McKee, S. P., & Nakayama, K. (1984). The detection of motion in the peripheral visual field. *Vision Research*, *24*, 25–32, https://doi.org/10.1016/0042-6989(84)90140-8.

Millodot, M. (2018). *Dictionary of optometry and vision science* (8th ed.). Philadelphia, PA: Elsevier.

Moutoussis, K., & Zeki, S. (2006). Seeing invisible motion: A human fMRI study. *Current Biology*, *16*, 574–579, https://doi.org/10.1016/j.cub.2006.01.062.

O'Shea, R. P., & Crassini, B. (1981). Interocular transfer of the motion after-effect is not reduced by binocular rivalry. *Vision Research*, *21*, 801–804, https://doi.org/10.1016/0042-6989(81)90177-2.

Pantle, A. (1974). Motion aftereffect magnitude as a measure of the spatio-temporal response properties of direction-sensitive analyzers. *Vision Research*, *14*, 1229–1236, https://doi.org/10.1016/0042-6989(74)90221-1.

Ramachandran, V. S., & Anstis, S. M. (1983). Extrapolation of motion path in human visual perception. *Vision Research*, *23*, 83–85, https://doi.org/10.1016/0042-6989(83)90044-5.

Regan, D. (1968). A high frequency mechanism which underlies visual evoked potentials. *Electroencephalography and Clinical Neurophysiology*, *25*, 231–237, https://doi.org/10.1016/0013-4694(68)90020-5.

Schein, S. J., & de Monasterio, F. M. (1987). Mapping of retinal and geniculate neurons onto striate cortex of macaque. *The Journal of Neuroscience*, *7*, 996–1009, https://doi.org/10.1523/JNEUROSCI.07-04-00996.1987.

Schiller, P. H., Logothetis, N. K., & Charles, E. R. (1990). Functions of the colour-opponent and broad-band channels of the visual system. *Nature*, *343*, 68–70, https://doi.org/10.1038/343068a0.

Schubert, H. D. (2014). Structure of the neural retina. In M. Yanoff & J. S. Duker (Eds.), *Ophthalmology*

(4th ed., pp. 419–422). Philadelphia, PA: Elsevier Saunders.

Sekuler, R. (1975). Visual motion perception. In E. C. Carterette & M. P. Friedman (Eds.), *Handbook of perception V: Seeing* (pp. 387–430). New York, NY: Academic Press.

Shady, S., MacLeod, D. I. A., & Fisher, H. S. (2004). Adaptation from invisible flicker. *Proceedings of the National Academy of Sciences, USA*, *101*, 5170–5173, https://doi.org/10.1073/pnas.0303452101.

Simoncelli, E. P., & Heeger, D. J. (1998). A model of neuronal responses in visual area MT. *Vision Research*, *38*, 743–761, https://doi.org/10.1016/S0042-6989(97)00183-1.

Spekreijse, H., van Norren, D., & van den Berg, T. J. T. P. (1971). Flicker responses in monkey lateral geniculate nucleus and human perception of flicker. *Proceedings of the National Academy of Sciences, USA*, *68*, 2802–2805, https://doi.org/10.1073/pnas.68.11.2802.

Tanaka, K., & Saito, H. (1989). Analysis of motion of the visual field by direction, expansion/contraction, and rotation cells clustered in the dorsal part of the medial superior temporal area of the macaque monkey. *Journal of Neurophysiology*, *62*, 626–641, https://doi.org/10.1152/jn.1989.62.3.626.

Tang, M. F., Dickinson, J. E., Visser, T. A. W., Edwards, M., & Badcock, D. R. (2013). The shape of motion perception: Global pooling of transformational apparent motion. *Journal of Vision*, *13*(13):20, 1–20, https://doi.org/10.1167/13.13.20. [PubMed] [Article]

Tse, P. U., Cavanagh, P., & Nakayama, K. (1998). The role of parsing in high-level motion processing. In T. Watanabe (Ed.), *High-level motion processing: Computational, neurobiological, and psychophysical perspectives* (pp. 249–266). Cambridge, MA: MIT Press.

Tse, P. U., & Logothetis, N. K. (2002). The duration of 3-D form analysis in transformational apparent motion. *Perception & Psychophysics*, *64*, 244–265, https://doi.org/10.3758/BF03195790.

Tyler, C. W. (1985). Analysis of visual modulation sensitivity. II. Peripheral retina and the role of photoreceptor dimensions. *Journal of the Optical Society of America A*, *2*, 393–398, https://doi.org/10.1364/JOSAA.2.000393.

Tyler, C. W. (1987). Analysis of visual modulation sensitivity. III. Meridional variations in peripheral flicker sensitivity. *Journal of the Optical Society of America A*, *4*, 1612–1619, https://doi.org/10.1364/JOSAA.4.001612.

Vorberg, D., Mattler, M., Heinecke, A., Schmidt, T., Schwarzbach, J. (2003). Different time courses for visual perception and action priming. *Proceedings of the National Academy of Sciences, USA*, *100*, 6275–6280, https://doi.org/10.1073/pnas.0931489100.

Wandell, B. A. (1995). *Foundations of vision*. Sunderland, MA: Sinauer Associates.

Wertheimer, M. (1912). Experimentelle Studien über das Sehen von Bewegung [Experimental studies on seeing movement]. *Zeitschrift für Psychologie*, *61*, 161–265.

Wiesenfelder, H., & Blake, R. (1990). The neural site of binocular rivalry relative to the analysis of motion in the human visual system. *The Journal of Neuroscience*, *10*, 3880–3888, https://doi.org/10.1523/JNEUROSCI.10-12-03880.1990.

Williams, P. E., Mechler, F., Gordon, J., Shapley, R., & Hawken, M. J. (2004). Entrainment to video displays in primary visual cortex of macaque and humans. *The Journal of Neuroscience*, *24*, 8278–8288, https://doi.org/10.1523/JNEUROSCI.2716-04.2004.

Zeki S. (1980). The response properties of cells in the middle temporal area (area MT) of owl monkey visual cortex. *Proceedings of the Royal Society of London. Series B, Biological Sciences*, *207*, 239–248, https://doi.org/10.1098/rspb.1980.0022.

Appendix

	Angular velocity (in °/s)			
Points	250	750	1500	2250/2500
Inducing ring only condition				
12	97.3	70.0	53.9	51.3
16	97.5	58.2	50.1	51.5
20	94.3	55.4	51.3	50.4
Inducing ring + test ring condition				
12	97.9	93.6	79.7	68.1
16	97.8	87.0	76.9	62.6
20	97.2	77.3	65.8	59.8

Table A1. Mean percentage of correct direction reports in Experiment 1.

Effect	dfn/dfd	*F*	*p*
Inducing ring only condition			
Velocity	3/30	164.13	< 0.001
Point-number	2/20	15.35	< 0.001
Velocity × Point-number	6/60	6.97	< 0.001
Inducing ring + test ring condition			
Velocity	2/20	84.60	< 0.001
Point-number	2/20	46.99	< 0.001
Velocity × Point-number	4/40	8.04	= 0.001

Table A2. ANOVA outcomes for Experiment 1. dfn = numerator *df*; dfd = denominator *df*.

	Angular velocity (in °/s)			
Diameter	250	750	1500	2250/2500
Inducing ring only condition				
3.5°	97.9	51.0	50.7	50.0
5.5°	98.5	58.8	50.7	48.7
7.5°	97.3	56.5	51.5	53.6
Inducing ring + test ring condition				
3.5°	99.1	79.4	65.9	54.2
5.5°	97.6	85.8	70.8	63.9
7.5°	97.5	92.1	79.1	70.1

Table A3. Mean percentage of correct direction reports in Experiment 2.

Effect	dfn/dfd	*F*	*p*
Inducing ring only condition			
Velocity	3/33	347.41	< 0.001
Diameter	2/22	1.73	0.203
Velocity × Diameter	6/66	2.17	0.089
Inducing ring + test ring condition			
Velocity	2/22	113.92	< 0.001
Diameter	2/22	27.63	< 0.001
Velocity × Diameter	4/44	1.26	0.305

Table A4. ANOVA outcomes for Experiment 2. dfn = numerator *df*; dfd = denominator *df*.

	Angular velocity (in °/s)			
Points / diameter	250	750	1500	2250/2500
Inducing ring only condition				
12 / 4.125°	97.9	60.7	50.3	51.2
16 / 5.5°	95.5	54.7	51.4	53.9
20 / 6.875°	91.8	55.0	49.1	50.7
Inducing ring + test ring condition				
12 / 4.125°	96.8	87.8	72.9	65.5
16 / 5.5°	95.0	81.8	69.7	63.4
20 / 6.875°	96.1	83.9	71.9	62.6

Table A5. Mean percentage of correct direction reports in Experiment 3.

Effect	dfn/dfd	*F*	*p*
Inducing ring only condition			
Velocity	3/33	149.55	< 0.001
Point-number/diameter	2/22	5.13	0.034
Velocity × Point-number/diameter	6/66	2.63	0.062
Inducing ring + test ring condition			
Velocity	2/22	61.05	< 0.001
Point-number/diameter	2/22	3.37	0.063
Velocity × Point-number/diameter	4/44	1.34	0.282

Table A6. ANOVA outcomes for Experiment 3. dfn = numerator *df*; dfd = denominator *df*.

Ring Rotation Illusion and the influence of heuristics on apparent motion

Uwe Mattler
University of Goettingen
Maximilian Stein
University of Goettingen
Robert Fendrich
Dartmouth College

Author Note

Uwe Mattler, Department of Experimental Psychology, University of Goettingen; Maximilian Stein, Department of Experimental Psychology, University of Goettingen; Robert Fendrich, Department of Psychological and Brain Sciences, Dartmouth College.

Correspondence concerning this article should be addressed to Uwe Mattler, Georg-Elias-Mueller Institute of Psychology, Georg August University Goettingen, Gosslerstr. 14, 37073 Goettingen, Germany. E-mail: uwe.mattler@psych.uni-goettingen.de

Abstract

We report a new visual illusion we designate *Ring Rotation Illusion* (RRI). When the outline of a circle is replaced by a ring of stationary points, the ring of points appears to rotate to a halt, even though no motion is actually present in either of the displays. In three experiments we examined the RRI, measured by participants' reports of the clearness of the illusory rotation, and compared the RRI to a closely related illusion, the Motion Bridging Effect (MBE; Matter & Fendrich, 2010; Stein et al., 2019). Experiment 1 reveals that the clearness of the RRI increases as the diameter of the rings decreases and as the number of points forming the second ring increases. In addition, we found that the optimum interstimulus interval (ISI) between the outline circle and the ring of points depends on the duration the stimuli. Experiment 2 compares the RRI to the MBE, which occurs when a ring of points, that rotates so rapidly it appears to be a stationary outline, is replaced by a stationary ring of points. This produces an illusory rotation of the stationary ring of points that generally matches the direction of the rotating ring's invisible spin. We found participants could not distinguish between the rotating ring that produces the MBE and the outline ring that produces the RRI, but report a slightly clearer motion percept when the spinning ring is presented. Experiment 3 compares the effects of point number, ring diameter, and ISI on the motion percept in the RRI and MBE. These functional relationships are found to be similar in the two illusions, suggesting a common mechanism produces the perceived rotation in both cases. We suggest with both the RRI and MBE, the visual system employs a heuristic, which holds that in the real world the transition from an outline circle to a pointed ring is plausibly explained by a rapidly spinning pointed ring decelerating to a halt. However, in case of the MBE the correspondence between the direction of the spinning ring's invisible rotation and stationary ring's illusory rotation demonstrates a motion dependent mechanism also operates, which may enhance the clearness of the illusory rotation.

Keywords: Ring Rotation Illusion, motion bridging effect, unconscious perception, apparent motion, heuristics

Ring Rotation Illusion: A new type of apparent motion

In 2010 Mattler and Fendrich reported an illusion of motion, which implied the processing of motion information beyond the range of velocities the human visual system is generally regarded as capable of encoding. A ring of 16 luminous points (the *inducing ring*) was rotated so rapidly, observers perceived a continuous circular outline and performed at chance when asked to report the rotation direction. However, when this rapidly rotating ring was replaced by a static ring of 16 points (the *test ring*), the static ring appeared to briefly spin in the direction that the rotating ring had spun. Because this illusionary rotation formed a link between the veridically rotating but apparently static inducing ring and the veridically static and apparently rotating test ring, Mattler and Fendrich termed this illusion the *Motion Bridging Effect* (MBE). The congruence between the actual inducing ring and illusory test ring rotations implies the direction of the consciously invisible inducing ring spin must have been somehow encoded by the visual system. This was the case despite the fact that the advancing inducing ring points were refreshed at rates well above the normal human flicker-fusion threshold.

While the measure of the MBE was the congruence between the inducing and test ring rotations, Mattler and Fendrich presumed that the percept of the test ring motion per se, and not just the rotation direction, was derived from the signals conveyed by the inducing ring spin. However, a continued investigation of the MBE's functional dependencies by Stein et al. (2019) raised the possibility that the motion percept and motion direction information were in fact dissociable signals. Stein et al. suggested that while the direction signal necessarily had to derive from the inducing ring spin, the actual motion percept could be treated as a case of transformational apparent motion (TAM; Tse, Cavanagh, & Nakayama, 1995).

TAM occurs when two successive stimuli that differ in color and/or shape are presented sequentially, and the first appears to transform to the second in a continuous manner. This transformation can arguably be taken to reflect the operation of a visual heuristic, which adjusts motion percepts to reflect the fact that in the external world object features change progressively rather than instantaneously (Hsieh, Caplovitz, & Tse, 2005). A particular instance of TAM, germane to the MBE, has been termed Singularbewegung (Wertheimer, 1912), polarized gamma movement (Kanizsa, 1979) or the line-motion illusion (LMI; Downing & Treisman, 1997). In LMI experiments, a square flashed on a screen precedes the presentation of an adjacent line.

Interestingly, the line is perceived as smoothly expanding outward from the square. Contemporary research on the LMI was initiated by Hikosaka, Miyauchi, and Shimojo (1993a) who regarded it as an attention related phenomenon. However, subsequent investigations have indicated that the LMI is more likely to be related to apparent motion (Kawahara, Yokosawa, Nishida, & Sato, 1996; Downing & Treisman, 1997). Downing & Treisman found that if they reversed the order of the line and square participants continued to perceive a smooth illusory motion, with the line shrinking into the square. This result cannot be accounted for by attention because no cue to bias attention to a specific location is presented. The authors therefore interpreted the LMI as a transformational apparent motion, in which a dot transforms into a line (or vice-versa). The motion percept in the case of the MBE can be viewed as a global version of the LMI in which multiple segments contract in unison into a circular array of points. According to this view, the visual system pools the motion signals of the multiple line-motion stimuli and integrates them to form a joint global motion percept with a unitary motion direction.

An implication of this view is that the actual motion of the inducing ring should not be necessary for the motion percept to occur. That is, if a truly continuous static outline circle replaces the spinning inducing ring a motion percept should still be seen. In the experiments we report here, this prediction is confirmed. We term the illusion of motion generated in this case *Ring Rotation Illusion* (RRI). We report a series of experiments in which we investigated how manipulations of the diameter of the rings, the number of points used to form the test ring and the ISI between the continuous and pointed ring presentation affect the RRI. In addition, we evaluate the ability of participants to distinguish between the MBE and RRI displays and compare the effects of the aforesaid stimulus manipulations on the MBE and RRI.

To the extent that the rapidly rotating inducing ring of the MBE and the continuous outline circle shown in RRI displays are indistinguishable, it might be argued that they would be expected to generate the same illusion. We believe, however, that there are strong grounds for distinguishing between the MBE and RRI. A crucial aspect of the MBE is the transfer of invisible rotation direction information from the inducing ring to test ring, and this attribute has no RRI counterpart because with the RRI display there is no inducing ring motion. The core measure used to measure the MBE — the degree of congruence between the inducing and test ring directions — is simply not a possible measure in the case of the RRI. The MBE can therefore be deemed to have two components: a direction biasing component that is unique to

(and can be taken to define) the MBE and an illusory test ring rotation, which is also generated by the RRI display and is the RRI's defining attribute. In addition, even when one sets aside considerations of direction the motion percepts seen with the MBE and RRI may not be absolutely identical. Data we report suggests that the clearness of the illusory test ring rotation is reliably stronger with MBE than RRI displays, suggesting that in the case of the MBE the inducing ring rotation serves to augment the motion percept that the MBE and RRI share.

Experiment 1

Following initial observations of the RRI in which we confirmed that an illusory rotation was seen when we replaced a stationary outline circle with a stationary pointed test ring, we conducted Experiment 1 to evaluate some characteristics of this new illusion. Specifically, we considered the effects of the number of points in the test ring, the ring diameter, the duration of the ring presentations, and the ISI between the inducing and test ring on participants' ratings of the clearness of the perceived test ring rotation.

Method

Participants. Twelve students of the University of Göttingen participated in the experiments with an average age of 26.4 years (8 females, 4 males). All participants had normal or corrected-to-normal vision as determined by the Landolt ring chart and received €7 per hour or student credits. Each participant completed two 1-hour sessions, which were run on separate days.

Apparatus. Stimuli were displayed on an analog HAMEG HM 400 cathode-ray oscilloscope controlled by a PC with a 12-bit Digital-Analog converter. The 8 × 10 cm oscilloscope screen was customized with a fast P15 phosphor (50 μs luminance decay time to 0.1%). Participants sat in a dark room with their head positions stabilized by a chin and forehead rest 57 cm from the oscilloscope screen. This was the same in all experiments of this study.

Stimuli. On each trial, a stationary outlined circle (the *inducing ring*) was followed by stationary ring of points (the *test ring*). The sequence of events is shown in Figure 1.

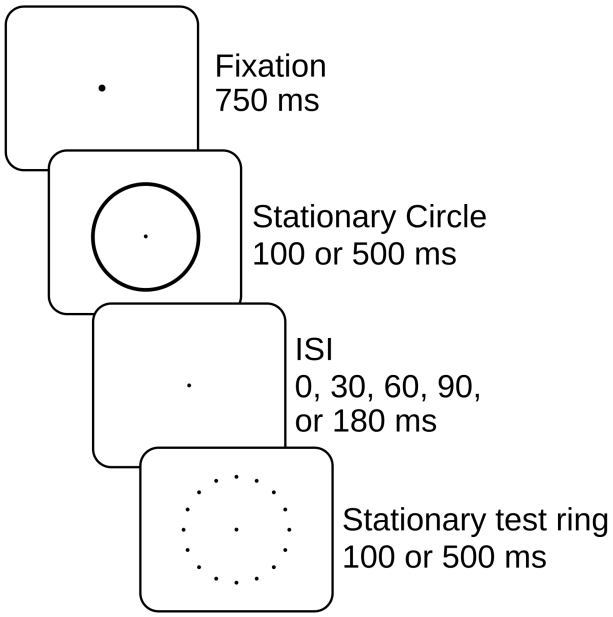

Figure 1. Sequence of events in Experiment 1. Note, the on the oscilloscope screen stimuli were bright on a dark background.

The stationary circle was constructed by displaying points around the inducing ring circumference in a random order 160 times per ms (plus 10 times to the position of the central fixation point). The resulting outline circle appeared completely continuous and conveyed no motion information.

When the diameter of the rings was not serving as an experimental variable their diameter was 6° of visual angle, and when the number of points in the test ring was not serving as a variable it was constructed of 16 equally spaced luminous points. These points were slightly out of focus because we previously found this strengthened the illusory motion percept being studied. The brightness of the stationary outlined circle was 0.099 cd/m², and the point brightness of the test ring was 1.20 cd/m² on a dark background. The methods employed to obtain these brightness measurements are described in Stein et al. (2019).

Procedure and Design. In the first session, the duration of each of the ring presentations was 500 ms and the ISI was 60 ms. In the first phase of this session, an initial practice block was followed by eight 48 trial experimental blocks. In the first 4 blocks we varied the number of points in the test ring within each block with 8, 12, 16, or 20 equally spaced points displayed. In

in the next four experimental blocks we varied the diameter of the two ring stimuli between blocks, with diameters of 2, 4, 6, and 8° of visual angle following a Latin Square design. In the second session, a practice block was followed by 10 experimental blocks of 50 trials. Within each block we quasi-randomly varied the ISI between the two stimuli with ISIs of 0, 30, 60, 90, and 180 ms. In addition, in the first half of the blocks the duration of the two stimuli was 500 ms and in the second half 100 ms.

Participants were instructed to report the clearness of the rotation that they perceived after the presentation of the two-stimulus displays on a modified computer keyboard with seven keys in a horizontal row, which had the numbers 3, 2, 1, 0, 1, 2, 3. The leftmost key was indicated a maximally clear counter-clockwise rotation, the rightmost key a maximally clear clockwise rotation. The middle key had the value zero and participants were instructed to use this key when they were not sure about the rotation direction. The remaining keys were introduced as indicating middle (value 2) or minimal (value 1) clearness of rotation in the direction indicated by their side. The space bar below this line of keys was used to start the next block of trials. Ratings were collapsed across clock-wise and counter-clockwise directions and the levels of clearness were assigned to values, with 0, 1, 2, and 3 for unclear, minimally clear, middle and maximally clear rotational percepts. The average of these reports was determined for each participant in each experimental condition.

Statistical Analyses. For statistical analyses there were 48 (50) trials in each condition of session one (two). The average rating of clearness of each participant in each condition were analyzed with three repeated measures analyses of variances (ANOVAs) with the within-subjects factors *Point Number*, *Diameter*, and the two independent variables *ISI* and *Stimulus Durations*. We corrected degrees of freedom using Greenhouse-Geisser estimates of sphericity. For the sake of readability, the uncorrected degrees of freedom are reported.

Results

The results of Experiment 1 are presented in Figure 2.

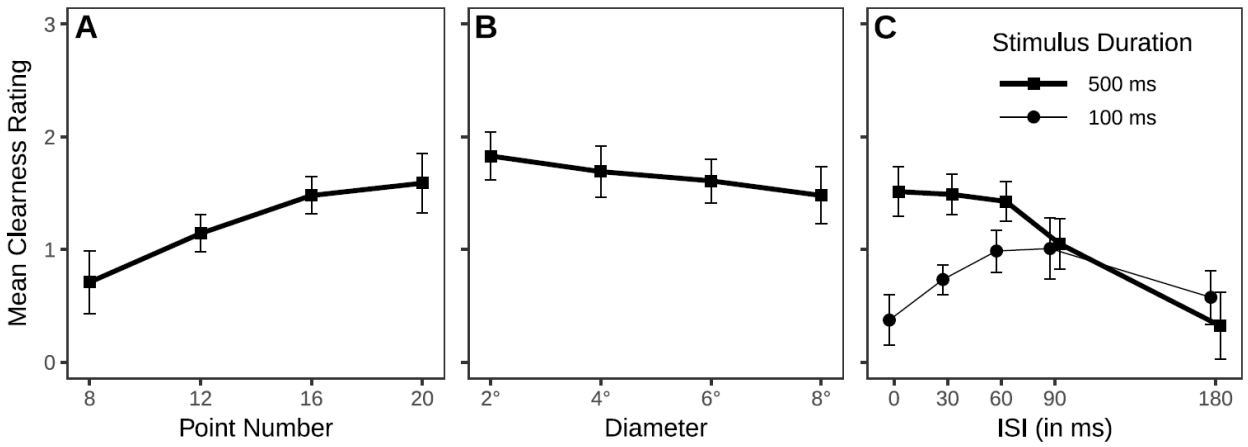

Figure 2. Mean clearness ratings of the Ring Rotation Illusion in Experiment 1. (A) Judged clearness as a function of the number of points in the test ring. (B) Clearness as a function of the diameter of the rings. In both A and B the duration of the rings was 500 ms. (C) Mean clearness ratings as a function of the interstimulus interval (ISI) between the inducing and test ring presentations for ring presentation durations of 100 and 500 ms. The error bars show 95% confidence intervals for the within-subject difference in means (Cousineau, 2005; Morey, 2008).

Point Number. The main effect of *Point Number* was significant, $F(3, 33) = 14.94$, $p = .002$, $\eta_p^2 = .576$, with the clearness of the rotation increasing as point number increased (see Figure 2A).

Diameter. It can be seen in Figure 2B that mean clearness ratings trended downward when the ring diameter increased, but this trend failed to reach statistical significance, $F(3, 33) = 2.13$, $p = .121$, $\eta_p^2 = .162$.

ISI. The main effects of *ISI* and *Stimulus Duration* were both significant, $F(4, 44) = 20.55$, $p < .001$, $\eta_p^2 = .651$, and $F(1, 11) = 18.64$, $p = .001$, $\eta_p^2 = .629$, respectively, and the interaction of these factors was significant, $F(4, 44) = 19.30$, $p < .001$, $\eta_p^2 = .637$ (Figure 2C). When the two stimuli were shown for 500 ms the RRI was clearer than it was with 100 ms durations. The clearness of the RRI was maximal with medium or short ISIs and it declined with increasing ISIs. With 500 ms stimuli durations, the clearness was maximal with a 0 ms ISI. With 100 ms stimuli durations the clearness followed an inverted u-shaped function over ISI with a maximum at 60–90 ms.

Discussion

Experiment 1 revealed that the clearness of the RRI varies with stimulus parameters, increasing as the number of points in the test ring increases and with longer exposure durations when the ISI between the inducing and test rings is less than 90 ms (all $p < .003$). However, the advantage produced by the increased duration vanished when the ISI was 90 ms ($p = .818$). With short stimulus durations, the clearness was modulated with ISI indicating an optimum with intermediate ISIs. A small progressive decrease in the clearness of the illusion was also observed when the ring diameter was increased but was non-significant. We note, however, that the effect of diameter was only examined with 500 ms stimulus durations. Subsequently, in Experiment 3, we investigated the effect of diameter with 121 ms stimulus durations, and it did reach significance.

While we cannot specify the source of these modulations, they may serve to guide future analyses of the illusion. Moreover, they provide a basis for comparing the MBE to the RRI. To the extent that if the motion percepts in the case of the two illusions are generated in an identical manner, it would be expected that the modulations observed with RRI displays would be identical with MBE displays. We evaluate this prediction in Experiment 3.

Experiment 2

We previously noted that observers might not be able to distinguish MBE displays in which the rate of rotation was high from RRI displays, since in both cases what is consciously visible is an outline circle followed by a ring of points. In this case, the illusory rotation generated by the two displays of the test ring might be identical. However, this would not necessarily be the case. We pointed out that the MBE entails a direction-biasing component, which is necessarily generated by the rapid rotation of the MBE inducing ring and cannot be present in RRI displays. Conceivably, the rapid rotation of the inducing ring, while not consciously perceived, might also contribute to the clearness of the illusory test ring motion. In Experiment 2, we evaluated this possibility by empirically determining the extent to which the MBE and RRI inducer displays were indistinguishable. In addition, we examined whether the illusory motion percepts generated by the two types of inducer were identical. To anticipate our results, we found that participants could not distinguish the rapidly rotating inducer and the stationary circle when these stimuli were shown alone. When presented together with the test

ring, however, similar percepts were reported but rotations were more often clearer and judged to have a greater spatial extent when the stimulus initially viewed was the rapidly rotating inducer rather that the stationary outline inducer.

Method

Participants. Twelve new University of Göttingen students (10 females, 2 males) with an average age of 24.1 years participated in the Experiment. All had normal or corrected-to-normal vision as determined by the Landolt ring chart and received €7 per hour or student credits. Each participant completed three 1-hour sessions, which were run on separate days.

Stimuli. The stimulus display sequence is shown in Figure 3. In all the experimental sessions, either the stationary outline circle or a rotating ring of points was initially presented for 91 ms. The diameter of the rings was 7.5° of visual angle. The stationary circle was created in the manner described in Experiment 1. The spinning inducing ring was rotated by advancing all 16 points every millisecond by a specified number of positions out of a total of 1440 positions so that it was updated with an effective frame rate of 1000 Hz. It was rotated clockwise or counterclockwise at angular velocities of 250 or 1500°/s, which entailed sequential point position progressions of 1 or 6 steps, respectively. At the high rotation speed, the inducing ring appeared to be a continuous solid circle. The time averaged brightness of inducing ring points was 0.017 and 0.099 cd/m² at the 250 and 1500°/s velocities respectively. Note that the location and timing of the point presentations in the spinning ring at the 1500°/s velocity was identical to that employed during the stationary circle presentation, with the only difference that the sequence of point positions in the stationary circle was scrambled. In session 2 and 3, after a 60 ms ISI, the stationary 16 point test ring followed the inducer for 500 ms. The test ring point brightness was 1.50 cd/m² on a dark background.

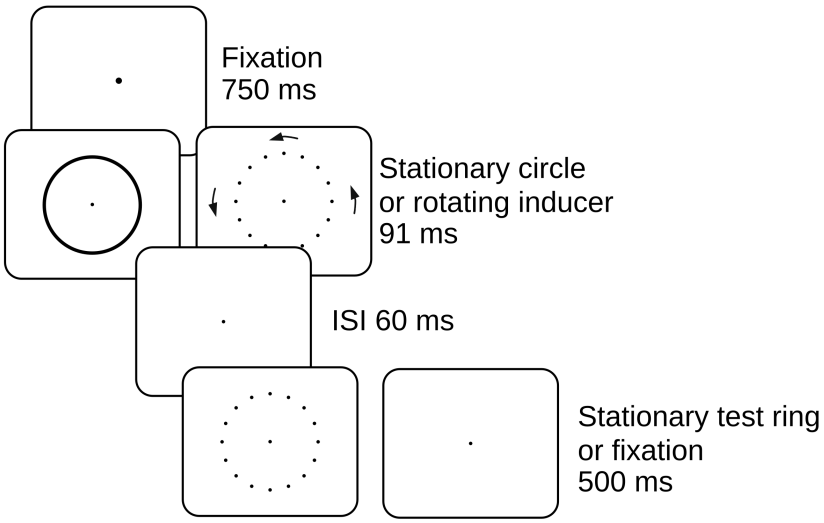

Figure 3. The stimulus sequence in Experiment 2. On a given trial the inducing ring rotated either counterclockwise (as shown in the figure) or clockwise. The points on the oscilloscope were bright on a dark background.

Procedure and Design.In the first session, we examined participants' ability to distinguish the rotating inducer from the stationary inducer in an initial session. Only the spinning or outline inducing ring was presented. Participants indicated whether the stimulus was stationary or rotating by pressing one of two keys. In the first four blocks the inducer rotated with a low velocity of 250°/s, in the following four blocks, the velocity was increased to 1500°/s. The first block of each group of four was considered practice and excluded from analysis. Across the six experimental blocks of 48 trials each, we gathered 72 trials for each of the four experimental conditions.

In session 2 and 3, the stationary ring of points (the *test ring*) followed the first stimulus (see Figure 3). The inducing stimulus was presented for 91 ms, the test ring for 500 ms. The stationary circle and rapidly rotating inducers were each shown on half the trials. On the half of trials in which the rapidly rotating inducer was presented it turned clockwise, on the other it turned counterclockwise. In one of the two sessions participants were asked to rate the clearness of rotation. In the other session, to obtain a second supporting measure of the strength of the perceived rotation, participants were asked to judge the covered distance of the perceived

rotation that they saw in terms of the distance traveled. The order of the two tasks was balanced across participants.

Ratings of clearness and of covered distance of the perceived rotation were given after the presentation of the second stimulus with five response keys that were arranged in a horizontal line on a modified computer keyboard. The leftmost key indicated a very clear (very far) rotation in counter-clockwise direction, the rightmost key a very clear (very far) rotation in clockwise direction, and the middle key was assigned to a rotation in both directions. The remaining two keys were assigned to rotations that were less clear (less far) in counter- and clockwise direction, respectively. Below this line of keys there was the space bar that was assigned to percepts of no motion. Following a practice block in each of the sessions, eight blocks of 48 trials each were run, providing data from 192 trials each with the stationary circle and the rotating inducer.

Statistical Analyses.We analyzed participants' sensitivity to distinguish the stationary circle from the rotating inducer in a two alternative forced-choice task by means of signal detection analyses (Macmillan & Creelman, 2005). "Rotating" responses to rotating inducers were considered hits and "Rotating" responses to stationary inducers were considered false alarms. Hit and false alarm rates were determined for each subject in each condition and the log-linear correction rule of Hautus (1995) was applied. To analyze the Ring Rotation Illusion, ratings were collapsed across clockwise and counter-clockwise directions and the responses were assigned to values 0, 1 and 2 for no motion / two motions, less clear (less far) and very clear (very far) rotational percepts, respectively. The average of these reports was determined for each participant and the effect of *Inducer Type* was analyzed. Moreover, to compare the RRI with the MBE, we compared the frequencies of reports of "no motion" and "two motions" between trials in which the test ring followed a stationary circle or a rapidly rotating inducer by using two-tailed Wilcoxon Signed-Rank Tests. Finally, to determine whether there was a MBE, we determined the frequency of congruent reports on trials with the rotating inducer.

Results

Participants' were able to perfectly distinguish the stationary circle from the rotating inducer when the velocity was 250°/s, $t(11) = 35.45$, $p < .001$, but performed at chance when making this distinction when the velocity was 1500°/s, $t(11) = 1.42$, $p = .09$ (mean $d' = 4.59$ and 0.25 respectively; see Figure 4A).

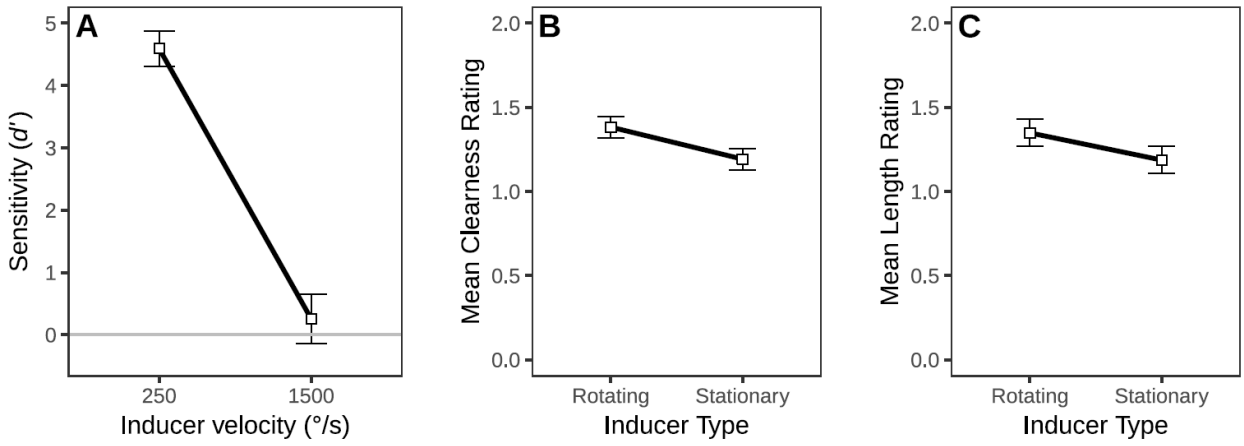

Figure 4. Strength of the Ring Rotation Illusion in Experiment 2. (A) Participants sensitivity to the difference between the rotating and stationary inducer when the rotation velocity was low or high. (B) Mean rating of the clearness of the rotation for a rapidly rotating and a stationary inducer. (C) Mean rating of the covered distance of the rotation as a function of Inducer Type. The error bars show 95% confidence intervals for single means in A and for the within-subject difference in means in B and C (Cousineau, 2005; Morey, 2008).

Mean ratings of the clearness of the RRI are shown in Figure 4B. Although clearness ratings were fairly similar with the rotating and stationary outline inducers (with mean clearness ratings of 1.38 and 1.19, respectively), the slightly greater clearness found with the rotating inducer proved to be statistically significant, $t(11) = 4.73$, $p < .001$. Additionally, we found that participants indicated they saw two directions or no movement at all significantly more often with the stationary outline inducer as compared to the rotating inducer, $W(11) = 56$, $p = .014$ and $W(11) = 28$, $p < .02$ for the two directions and no movement judgments, respectively.

Covered distance of motion ratings yielded a similar outcome (see Figure 4C): mean clearness ratings reached comparable levels with the rapidly rotating inducer and stationary inducers (with ratings of 1.35 and 1.19, respectively), but the small advantage with the rotating inducer proved to be statistically reliable, $t(11) = 3.11$, $p = .010$. Additionally, we found that participants indicated they saw two directions or no movement at all significantly more often in the condition with the stationary inducer as compared to the rotating inducer, $W(11) = 56.5$, $p = .013$ and $W(11) = 26$, $p < .05$ for the two directions and no movement judgments, respectively.

To confirm that our rapidly rotating inducer produced the MBE congruence effect, we examined the frequency of congruent responses on trials with the rotating inducer. Participants reported perceived rotations in the same direction as the rapid rotation on 67.9 and 69.1% of the trials in the clearness and the covered distance rating sessions, respectively. These correspond to mean d' values of 1.42 and 1.51, respectively.

Interestingly, the mean rating of clearness of rotation was only marginally increased on trials with congruent as compared to incongruent perceived directions (1.58 vs. 1.43), although this difference proved significant, $t(11) = 3.47$, $p = .005$. The mean rating of the covered distance of the illusory rotation was also only a little higher on trials with congruent as compared to incongruent perceived directions, and this difference was not significant (1.49 vs. 1.43; $t(11) = 1.09$, $p = .299$).

Discussion

Experiment 2 aimed to compare the Ring Rotation Illusion when the inducing stimulus was a stationary circle or a rapidly rotating ring of points. Initial observations indicated that participants could not distinguish between the stationary circle and the rapidly rotating inducing ring when these stimuli were presented without the test ring. In the following two sessions, we asked participants to rate the clearness and the covered distance of motion that they perceived in the test ring when it was presented after the inducer. Participants' rating of the degree of clearness and the covered distance of motion reached similar values with the two types of inducer. However, there was a small but significant increase in the reported clearness and covered distance of motion when the rapidly rotating inducing ring was shown. The increase in the ratings of clearness was greatest when the direction of the perceived rotation corresponded to the direction of the rapidly rotating inducer.

This finding suggests that the illusory motion of the test ring is to some degree dependent on the nature of the inducing stimulus. This was the case although participants could not distinguish the rotating and stationary inducers when the rotation was rapid. We see at least two possible ways of accounting for this finding. On the one hand, the motion signal that is conveyed by the rapidly rotating inducer might have access to the processes, which determine the clearness and covered distance of motion of the Ring Rotation Illusion. On the other hand, the inducing ring actually consists of the same regularly arranged points as the test ring. If the visual system is able to register this regularity in the rotating inducer, a matching process that supports the

perceptual hypothesis that the inducer is the rapidly rotating tetst ring might be facilitated. This facilitation could in turn affect the processes that generate the RRI.

Experiment 3

Experiment 2 provided evidence for a generally similar motion percept with the RRI (stationary outline circle) and MBE (rotating ring) displays. Participants could not distinguish the rapidly rotating ring, which was used in the MBE paradigm, from the stationary outlined circle used in the RRI paradigm. Ratings of both, clearness and covered distance of illusory test ring motion reached similar values, but were significantly stronger on trials in which the inducer was the invisibly rotating ring. A somewhat more stringent test of whether the motion percept is generated by the same process or processes with the two types of inducer can be implemented by examining whether the percept exhibits the same functional dependencies in the two cases. Some of the functional dependencies of the RRI were examined in Experiment 1: specifically, the effects of ring diameter, the number of points in the test ring, and the effect on ISI on the clearness of the perceived motion with different inducing and test ring display durations. Experiment 3 examined whether these dependencies were similar with the stationary outline and rotating point inducing ring displays.

In previous studies (Mattler and Fendrich, 2010; Stein et al., 2019) the measure of the MBE employed was the direction congruence between the invisible inducing ring rotation and illusory test ring rotation. This method cannot be used to compare the MBE and RRI because in the case of the RRI there is no direction congruence. In Experiment 3, our comparisons were therefore based on the motion clearness ratings utilized in our Experiments 1 and 2.

To facilitate the comparison between the RRI and MBE, within the trial blocks of Experiment 3 we randomly switched between trials in which the outlined circle and the rapidly rotating inducer were presented, and asked participants to rate the clearness of the perceived motion in the subsequent test ring. In this way, we were able to replicate findings of Experiment 1 while enabling a comparison of the functional dependencies of the RRI and MBE in a within-subjects design. In a final session, we also tested whether participants could distinguish the rapidly rotating inducer from the stationary inducer when the number of points was varied.

Method

Participants. Twelve new students from the University of Göttingen (12 females, 0 males) with an average age of 20.9 years participated in Experiments 3. All participants had normal or corrected-to-normal vision as determined by the Landolt ring chart and received €7 per hour or student credits. Each participant completed four 1-hour sessions, which were run on separate days.

Stimuli. On half of the trials, the stationary outlined circle was initially presented and on the other half a rotating ring of points. These stimuli were generated using the methods described in Experiments 1 and 2. When the rotating ring was presented its rotation direction was clockwise on half the trials and counterclockwise on the other half. The sequence of events corresponded to that used in Experiment 2 (cf. Figure 3) with the exception that both stimuli were presented for 121 ms. The standard parameters of the stimuli were 16 points, a diameter of 6° of visual angle, an inducing ring velocity of 1500°/s, and an ISI of 60 ms. The brightness of the test ring points was 1.2 cd\m² (as in Experiment 1). The stationary circle was created in the manner described in Experiment 1 and the motion of the rapidly rotating inducer was created in the manner described in Experiment 2 with the same values of averaged brightness.

In Session 1, we varied the number of points randomly between trials, (with point number set to 8, 12, 16, and 20 points). In a given trial, the inducing ring and the test ring always had the same number of points. In Session 2, we varied the diameter of the rings (with diameters set to 2, 4, 6, and 8° of visual angle). The diameter was varied block-wise and the order of conditions was balanced across participants according to a Latin square. In Session 3, we randomly varied the ISI (0, 30, 60, 90, and 180 ms) between trials. In Session 4, the stationary circle and the rotating ring were presented alone and the number of points forming the rapidly rotating ring varied randomly between trials (8, 12, 16, and 20 points). All other stimulus parameters except for the one being varied were set to the standard values. In all sessions, we considered the initial block of trials as practice and these trials were not included in the analyses.

Tasks. In the first three sessions, participants were asked to report the clearness of the perceived rotation after the presentation of the two-stimulus displays in the manner employed in Experiment 2. We used the instruction and the modified keyboard utilized in Experiment 1. In Session 4, participants were instructed to indicate whether the stimulus was stationary or rotating

by pressing one of the two arrow keys. We told them that the stationary stimulus was presented on half of the trials and the rotating stimulus on the other half.

Procedure and Design. There were eight experimental blocks of trials in each session. An additional first block of practice trials was excluded from analyses. Each experimental block comprised 48 trials except Session 3, where each block comprised 60 trials, so that we gathered 96 trials for each of the experimental condition in a session. The independent variable Inducer-Type (rotating vs. stationary) was varied randomly between trials in all sessions. This independent variable was combined with one other independent variable in different sessions: Point Number (8, 12, 16, and 20), Diameter (4, 6, 8, and 12° of visual angle), and ISI (0, 30, 60, 90, and 180 ms). The rating of clearness of the rotation in clockwise or counter-clockwise direction served as dependent variable for the strength of the Ring Rotation Illusion.

Statistical Analyses. In each experimental session, we analyzed participants' perception of the clearness of the Ring Rotation Illusion by collapsing ratings across clockwise and counter-clockwise directions. Responses were assigned values of 0, 1, 2, or 3, based on participants' key responses (see above) and average clearness ratings were determined in each stimulus condition. The effects of the independent variables on the averaged ratings were evaluated by two-factor repeated measures analyses of variance (ANOVAs) which combined the factor *Inducer-Type* (rotating vs. stationary) with either *Point Number*, *Diameter*, or *ISI*. Participants' ability to distinguish between the rapidly rotating inducer and the stationary inducer was analyzed by signal detection analysis (see Experiment 2). In addition, we determined the MBE on trials with the rotating inducer based on the congruency between the actual and reported directions and examined the effects of *Point Number, Diameter*, and *ISI* on the MBE.

In contrast to the results obtained in Experiment 2, the results of the final session of Experiment 3 indicated that participants could distinguish between rotating and stationary inducers at better than chance levels in the standard 16 point condition. We therefore performed additional analyses in which the data from the three initial sessions was reanalyzed with an ANOVA that included the between-subjects factor *Inducer Sensitivity*. These analyses are reported in the section on "Sensitivity to Inducer Motion" below. All reported ANOVA *p* values were Greenhouse-Geisser corrected, but for the sake of readability, we report the uncorrected degrees of freedom.

Results

Figures 5A-C show participants' average clearness ratings as a function of Inducer Type and the respective independent variables Point Number, Diameter, and ISI, respectively. Figures 5 D-F show the MBE as a function of Inducer Type and Point Number, Diameter, and ISI, respectively. Figure 5G shows how frequently participants' reported seeing a rotation as a function of whether the Inducer Type was rotating or stationary.

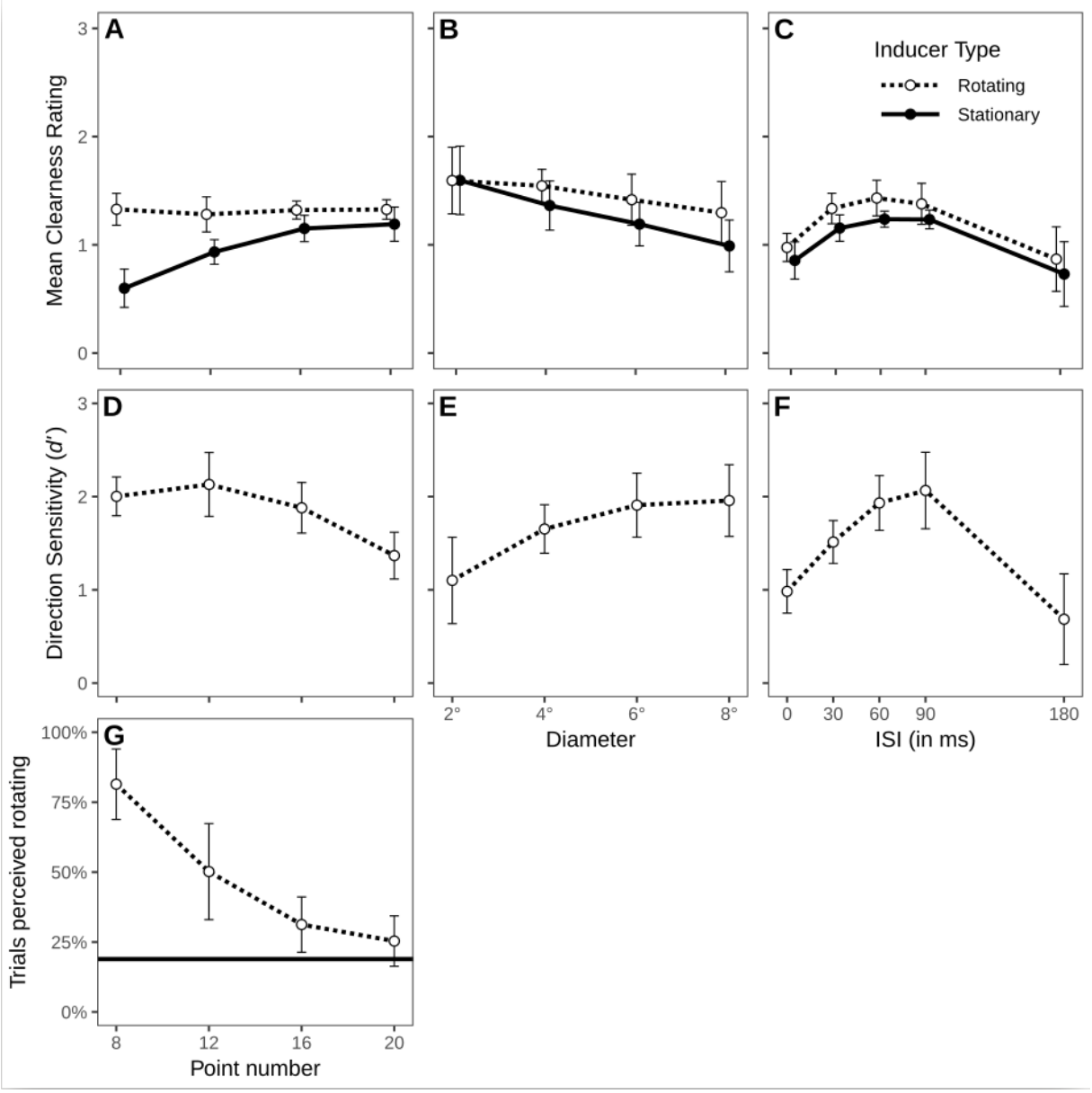

Figure 5. Measures of the Ring Rotation Illusion and the Motion Bridging Effect in Experiment 3. Top row: Mean rating of clearness of the illusionary rotation with rapidly rotating and stationary inducers as a function of (A) Point Number, (B) Diameter, and (C) the inducer-test ring ISI. Middle row: Sensitivity to the congruence of the rotating inducing ring and perceived test ring rotation directions (the MBE) as a function of (D) Point Number, (E) Diameter, and (F) the inducer-test ring ISI. Bottom row: (G) Mean frequency of perceiving the inducer as rotating or stationary as a function of Point Number. The black line indicates mean performance when the stationary inducer was presented. In A-F the stationary test ring followed the inducer. In G, the inducer appeared alone. Error bars in A-F show the 95% confidence intervals for the within-subject difference in means, in G for single means.

Point Number. The main effect of *Point Number* on the clearness of the test ring's perceived rotation was significant, $F(3, 33) = 16.82$, $p < .001$, $\eta_p^2 = .605$. The illusion becomes clearer as the number of points in the rings increased. The main effect of *Inducer Type* was also significant, $F(1, 11) = 17.51$, $p = .002$, $\eta_p^2 = .614$, indicating a clearer motion percept with the rapidly rotating ring than the stationary circle, an outcome also observed in Experiment 1. In addition, the interaction *Inducer Type* × *Point Number* was significant, $F(3, 33) = 17.65$, $p < .001$, $\eta_p^2 = .616$. Separate Post-hoc analyses confirmed what is apparent in Figure 5A: this interaction is produced by an improvement in motion clearness that occurs only with the stationary inducer, $F(3, 33) = 26.50$, $p < .001$, $\eta_p^2 = .707$. It can be attributed to a lack of clearness relative to the moving inducer condition when the number of points is low. This comparative lack of clearness diminishes as *Point Number* increases, so that *Inducer Type* has almost no impact at the highest *Point Number* value. There is no effect of *Point Number* on clearness when the rotating inducer is shown, $F(3, 33) = 0.32$, $p = .739$, $\eta_p^2 = .029$.

The effect of *Point Number* on the MBE when the rotating inducer was presented was quantified in terms of *d'*-values for compatible opposed to incompatible responses (Figure 5D). The ANOVA confirmed that the main effect of *Point Number* was significant, $F(3, 33) = 7.30$, $p = .002$, $\eta_p^2 = .399$, with the MBE decreasing as the number of points increases. This finding replicates a previous finding by Stein et al. (2019) but contrasts with the null-effect of *Point Number* when the rotating inducer is shown and clearness rather than congruence is used as the

dependent variable (Figure 5A). We also note that visual inspection of Figure 5D suggests a possible inverted u-shaped function with a maximum MBE at about 12 points.

Diameter. Visual inspection of Figure 5B suggests the clearness of the illusion of a test ring rotation gradually diminished as the diameter of the rings increased, but the main effect of *Diameter* did not reach statistical significance, $F(3, 33) = 2.99$, $p = .075$, $\eta_p^2 = .213$. However, the main effect of *Inducer Type* was once again significant, $F(1, 11) = 5.82$, $p = .035$, $\eta_p^2 = .346$, indicating that there was a clearer illusion with the rapidly rotating inducer (Figure 5B), and this effect significantly interacted with *Diameter*, $F(3, 33) = 5.75$, $p = .007$, $\eta_p^2 = .343$. Separate post-hoc analyses revealed this interaction occurred because *Diameter* did produce a significant reduction in the motion clearness when the stationary inducer was employed, $F(3, 33) = 5.03$, $p = .015$, $\eta_p^2 = .314$, but not with rotating inducers $F(3, 33) = 1.31$, $p = .285$, $\eta_p^2 = .107$. Note a comparable but non-significant trend toward a reduction in the clearness of the RRI was found with 500 ms stimulus durations in Experiment 1 (cf. Figure 2B).

Figure 5E suggests the MBE increased as a function of *Diameter* in a slightly bowed curve, reaching its maximum value at the largest (8° of visual angle) diameter tested. The ANOVA indicated this increase with increasing diameter was significant, $F(3, 33) = 5.46$, $p = .025$, $\eta_p^2 = .332$. This finding replicates a previous finding (Stein et al., 2019) but contrasts with the null-effect of Diameter on the clearness of the perceived motion when a rotating inducer was employed (see Figure 5B).

ISI. The main effect of *ISI* on the clearness of the test ring motion was significant, $F(4, 44) = 9.57$, $p = .003$, $\eta_p^2 = .465$. Figure 5C shows a clear inverted u-shaped function that indicates the illusion was maximal with a 60 ms ISI and decreased with shorter and longer ISIs. The main effect of *Inducer Type* was once again significant, $F(1, 11) = 9.01$, $p = .012$, $\eta_p^2 = .450$, indicating the rotating inducer produced a clearer motion percept than the stationary inducer. Importantly, the interaction *Inducer Type* × *ISI* did not reach significance, $p = .77$, indicating that the effect of ISI was the same with either type of inducer.

Figure 5F shows the MBE as a function of ISI. ANOVA results confirmed a significant main effect of *ISI*, $F(4, 44) = 14.34$, $p < .001$. An inverted u-shaped function is again evident, with a maximum MBE when the ISI is 90 ms. This finding accords with a previous finding (Mattler & Fendrich, 2010) and parallels with the effect of ISI on the clearness of the RRI (see Figure 5C).

Sensitivity to Inducer Motion. Figure 5G shows the frequency participants reported seeing a rotation as a function of *Point Number* when the inducer was the stationary circle or the rapidly rotating ring. The main effect of *Point Number* on *d′* was significant, $F(3, 33) = 52.41$, $p < .001$, $\eta_p^2 = .827$, with mean values of $d' = 2.22$, $d' = 1.07$, $d' = 0.52$, and $d' = 0.33$ for 8, 12, 16, and 20 points, respectively. Post hoc one-tailed t-tests revealed that mean sensitivity was above chance in all cases (all $p < .01$). This evidence for participants' ability to distinguish the stationary from the rotating inducer in the 16 point condition raises the possibility that perceptual differences in the detection of motion contributed to the pattern of results on the clearness ratings reported above where the 16 points where used as standard value.

To asses this possibility, first, we examined the correlation between each participants sensitivity to the inducer motion in terms of *d′* and the differece between their clearness ratings on trials with a rotating vs. a stationary inducer. We reasoned, if the interaction between *Inducer Type* and *Point Number* on the clearness of the RRI (Figure 5A) is at least in part due to perceptual differences caused by the type of inducer (Figure 5G), it should lead to a correlation between the two measures. Across participants, *d′*-values of motion sensitivity and clearness rating differences correlated with r = .57, .41, -.03, and -.11 with $p = .05$, .19, .92, and .74 for trials with 8, 12, 16, and 20 points respectively.

In addition, we divided our participants into two subgroups based on their ability to distinguish the inducer types in the 16 points condition: a poor performance subgroup ($d' = 0.205$) and a good performance subgroup ($d' = 0.841$). Then, we conducted additional ANOVAs, which included the between-subjects factor *Inducer Sensitivity* (poor vs. good), to see, whether the effects of our indipendent vairables differ in the two subgroups. However, regarding the *Point Number*, neither a main effect of Inducer Sensitivity on clearness ratings ($p = .56$), nor any interaction with Point Number ($p = .14$), Inducer Type ($p = .90$), or the interaction *Point Number* × *Inducer Type* ($p = .08$) reached significance. Regarding Diameter, neither the main effect of Inducer Sensitivity on clearness ratings reached significance ($p = .51$), nor any interaction with Diameter ($p = .67$), Inducer Type ($p = .95$), or the Diameter × Inducer Type interaction ($p = .77$). Regarding ISI, neither a main effect of Inducer Sensitivity reached significance ($p = .11$), nor any interaction with ISI ($p = .63$), Inducer Type ($p = .34$), or the ISI × Inducer Type interaction ($p = .29$). To sum up, there was no evidence for an effect of perceptual differences between

stationary and rotating inducers on the effect of the clearness rating regarding the RRI in the initial three sessions.

Post-hoc analysis of the effect of stimulus duration across experiments. Visual inspection of the RRI with stationary inducers in Figures 2A and 5A, and Figures 2B to 5B suggests that the mean clearness ratings of the RRI reach higher values in Experiment 1 as compared to Experiment 5. One crucial difference between the experiments is the stimulus duration of the inducer and the test ring. Durations of 500 ms were used in Experiment 1, 121 ms in Experiment 3. A within-subjects comparison in Experiment 1 already revealed a significant main effect of stimulus duration (see Figure 2C). To examine whether stimulus duration increases the RRI in the other conditions as well, we compared the conditions with the stationary inducer across Experiment 1 and 3 in a post-hoc analysis. However, the main effect of stimulus duration was only tentatively significant in the session where Point Number ($F(1, 22) = 3.91$, $p = .061$) and in the session where Diameter was ($F(1, 22) = 3.43$, $p = .077$) varied. Thus, findings are not decisive for the effect of stimulus duration but suggest that future research might examine this potentially effective variable.

Discussion

Experiment 3 examined the RRI with the stationary circle and the rapidly rotating ring as inducers and compared these effects to the MBE, which occurs only with the rotating inducer. Replicating Experiment 2, we found an RRI with both types of inducer. Above that, the clearness of the RRI was larger with the rotating inducer than the stationary inducer. Our measure of clearness indicated an increase in the RRI when Point Number increases and the RRI decreases with increasing Diameter with the stationary inducer. We note that the effect of Diameter did not reach significance in Experiment 1 where the duration of the two stimuli was 500 ms, rather than 121 ms in the present experiment. Thus, the RRI seems to depend on stimulus durations. With the rotating inducer, the RRI did not vary with Point Number and Diameter. The ISI, in contrast, modulated the RRI in the same way with either type of inducer.

The MBE reflects the effect of the motion direction of the inducer on the direction of the perceived RRI. The MBE was reduced by increasing Point Number and it increased with increasing Diameter. Visual inspection, however, suggests that the MBE has a curvilinear relationship to Point Number and Diameter similar to the curvilinear relationship to ISI where we found a clear maximum with 90 ms ISI. Beyond replicating previous reports of the MBE

(Mattler & Fendrich, 2010; Stein et al., 2019) the extended range of Point Numbers from 8 to 20, and Diameter between 2° and 8° of visual angle, the present findings point to curvilinear dependencies of the MBE. Findings suggests the MBE might break down with extreme values of Point Number, Diameter and ISI. We note that the ISI effect was found with 90 ms inducer and 500 ms test ring by Mattler & Fendrich (2010) whereas the effects of Point Number and Diameter were found with with 121 ms inducer and 500 ms test ring by Stein et al. (2019). In the present study, the duration of both stimuli was 121 ms. Therefore, these effects on the MBE appear to be robust against changes in stimulus durations.

Our comparison of the two illusions suggests that the appearance of the MBE might be due to an RRI in respect of the clearness of the perceived rotation. According to this view, the yoked rotation of the points of the stationary test ring might be caused by the same mechanism with both types of inducers. However, we also found a dissociation between the effects of Point Number and Diameter on measures of the clearness of the RRI (Figure 5A and 5B), and the effects of Point Number and Diameter on measures of the MBE (Figure 5D and 5E). This dissociation suggests that the source of the MBE cannot be equated with the source of the RRI.

In the last session, we found data suggesting that participants could distinguish the stationary outline inducer from the rapidly rotating inducer. This surprising finding provides an alternative account for differences on the clearness measures of the RRI with the two types of inducers. We have addressed this possibility by a re-analysis of our findings, which did not provide evidence for such an alternative account. In addition, we doubt that the findings in the last session are informative for the effects in the previous sessions. First, extensive pilot studies with the present stimuli did not provide evidence for a perceptual difference between the stationary and the rotating inducer. Second, findings of Experiment 2 showed that participants could not distinguish the two types of inducer when stimulus durations were 90 ms (see Figure 4A). Third, we speculate that participants might have developed special strategies to improve their performance in the final session, which they did not employ in the previous sessions. One of these strategies might include eye-movements, which can provide information to distinguish the rotating inducer from the stationary inducer. In consequence, we suggest to control eye movement in future studies.

General Discussion

This study describes a new illusory motion we term the "Ring Rotation Illusion" (RRI). The RRI occurs when the outline of a circle (which we term the Inducing Ring) is replaced by a ring of stationary points (the Test Ring). This produces the percept of a transient clockwise or counter clockwise rotation of the Test Ring. Three experiments are reported. In Experiment 1, we examined the functional dependencies of the RRI, using judgments of the clearness of the perceived motion as a measure of its strength. We found the RRI increased as the number of points forming the Test Ring was increased from 8 to 20, diminished when the diameter of the Inducing and Test Ring was increased from 2 to 8° of visual angle, and was modulated by the ISI between the Inducing and Test Ring in a manner that depended on the duration of the ring displays. When that duration was 100 ms the RRI followed an inverted U shaped function as the ISI was increased from 0 to 180 ms, peaking at 60 to 90 ms. When the duration was 500 ms, the RRI was stable with ISIs from 0 to 60 ms, then declined as it was increased to 180 ms.

The RRI is closely related to the Motion Bridging Effect (MBE), an illusion previously described by Mattler & Fendrich (2010) and Stein et al. (2019). The MBE and RRI displays are identical except that in the case of the MBE the Inducing Ring is a rapidly rotating ring of points. When the speed of this rotation is sufficiently high the Inducing Ring appears to be a continuous outline circle with no visible rotation, so observers perceive the RRI and MBE displays as identical. Both displays produce an illusory rotation of the test ring points, but the MBE is distinguished by the fact the rotation direction of the Inducing and Test Rings tend to be congruent. This congruence is measured to assess the MBE. In the case of the RRI congruence is not a meaningful idea since there is no Inducer rotation. However, Stein et al. (2019) have argued that processes that mediate congruence in the MBE are dissociable from processes that actually produce the illusion of motion in the Test Ring. In this case, it seems sensible to posit that the mechanism or mechanisms that produce the percept of a Test Ring motion are the same in the RRI and MBE. Our Experiments 2 and 3 evaluated this hypothesis.

In Experiment 2, we compared the clearness and estimated covered distance of the perceived test ring rotation when the stationary and rapidly rotating inducers were employed. Although these were similar for the two inducer types, there was a small but significant improvement in the scores for both measures when the rotating Inducer was shown. This was the case although participants could not discriminate the two inducer types.

In Experiment 3, clearness estimates were used to investigate whether the functional dependences observed in Experiment 1 (the effects of ISI, point-number and ring diameter) were the same with the two inducer types. The duration of the ring presentations was set to 121 ms. As the ISI was increased the identical inverted U shaped function first observed in Experiment 1 was found irrespective of the type of inducer, though as in Experiment 2 the clearness of the motion was slightly better when the rotating inducer was shown. With the rotating inducing ring, clearness was unaffected by the number of points that formed the rings, but with the stationary inducing ring clearness improved, like in Experiment 1, as point number increased, starting well below the level found with the rotating inducer but matching that clearness when 20 points were used. With the smallest ring diameter, clearness was identical with the two inducer types and declined slightly as diameter increased, but declined more rapidly with the stationary inducer.

Overall, the data appear compatible with the view that the motion percept of the MBE and RRI have at least a common basis in part, but the inducer rotation in the MBE display serves to augment this motion percept. Moreover, the inducer rotation appears to alter the way the motion percept is modulated by the stimulus attributes point number and diameter. It should be noted in this regard that we found point number and diameter modulated the MBE congruence effect in the opposite way that they modulated RRI clearness and perceived rotation distance: Congruence declined with increasing point number and increased with larger diameter rings. We will return to these findings, which replicate Stein et al. (2019), later in this discussion.

What produces the RRI?

In their 2019 paper Stein and colleagues pointed out that the MBE display bears a similarity to the displays used to produce another illusion, which has been variously termed Singularbewegung (Wertheimer, 1912), polarized gamma movement (Kanizsa, 1979), line-motion illusion (e.g., Hikosaka et al., 1993a), motion induction (e.g., von Grünau & Faubert, 1994), or illusory line motion (e.g., Kawahara et al., 1996). We will adopt the designation “line-motion illusion” with its “LMI” acronym. This similarity also applies to the RRI, perhaps even more so since in the case of both the RRI and LMI two genuinely static stimuli are exchanged. In LMI experiments, when the presentation of a flashed square on a screen is followed by the presentation of an adjacent line, the line is perceived to rapidly grow outward from the square. Thus, with both the LMI and RRI displays switching between an extended coherent stimulus (the line in the case of the LMI and outline circle in the case of the RRI) and a localized nonlinear

stimulus (the square in the case of the LMI and ring of points in the case of the RRI) creates an illusory motion. It therefore seems appropriate to ask if these illusions are generated by similar mechanisms.

Contemporary research on the LMI was initiated by Hikosaka et al. (1993a) who regarded it as an attention related phenomenon. These investigators argue, based on their own and previous temporal order experiments (e.g., Stelmach & Herdman, 1991), that sensory information that is attended is processed faster than unattended information. In the case of the LMI, they posit that attention is initially directed to the location of the square. Based on the evidence that there is a gradient of diminishing attention around an attentional focus (e.g., Mangun & Hillyard, 1988, Sagi & Julesz, 1986; Shulman, Sheehy, & Wilson, 1986) these authors propose that when the line appears the attentional gradient is stronger for the parts of the line closer to the square, so those parts reach consciousness more rapidly than more distal parts, causing the line to appear to grow outward. Commensurate with this view, von Grünau and Faubert (1994) found the LMI does not just occur when the square and line are differentiated from the background by luminance but also when they are defined by a wide variety of other attributes including isoluminant colors, texture, and stereoscopic depth, albeit sometimes with reduced strength. Von Grünau and Faubert concluded that the LMI is primarily mediated by a "high-level attention-related" process, although low level sensory processes can modulate this high level effect.

Downing and Treisman (1997), on the other hand, found that if they reversed the order of the line and square participants continued to perceive a smooth illusory motion, with the line now contracting into the square. This result cannot be accounted for by attention because no cue to bias attention to a specific location is presented. Other studies have demonstrated that the LMI can occur at multiple locations simultaneously (Faubert & von Grünau, 1995; Kawahara et al., 1996; Tang, Dickinson, Visser, Edwards, & Badcock, 2013), a finding difficult to reconcile with an account based on focal attention.

Low-level processes based on shifts in luminance or contrast profiles that are not dependent on attention have been proposed to explain the LMI (Hock and Nichols, 2010; Zanker, 1994). However, low-level models of this kind cannot easily account for instances with complex LMI displays where motions are perceived that violate the predictions made by motion energy models (e.g., Tse and Logothetis, 2002; see the review in Han, Zhu, Corballis, & Hamm, 2016).

Downing and Treisman (1997) offered a high-level alternative to the attention based account of LMI, which relates the illusion to apparent motion, and suggest it represents a case of an "impletion" process that fills in the missing intermediary positions of objects undergoing apparent motion. The authors regard the LMI as "a progressive transformation of shape induced by the binding of the dot and the line as successive states of one moving object" (p. 777), in which a dot transforms into a line (or vice-versa). They suggest the impletion process reflects a visual inference that interprets a stimulus sequence in terms of the real-world state of affairs likely to produce it. Tse and colleagues regard the LMI as an instance of transformational apparent motion (TAM, Tse et al.,1998; Tse & Logothetis, 2002). These authors distinguish TAM from standard types of apparent motion due to a set of unique rules that are applicable only to TAM. These include a parsing and matching process over successive scenes of spatiotemporally overlapping figures, which contributes to the smooth shape change that is the defining characteristic of TAM. Hsieh et al. (2005) expand on this idea and speak of visual "heuristics", one of which adjusts motion percepts to reflect the fact that in the external world object features change progressively rather than instantaneously.

The motion percept in the case of the RRI and MBE can be viewed as a global version of the LMI in which multiple segments of the outline of the circular inducer contract in unison into the circular array of points that form the test ring. According to this view, the inducer segments overlain by the test ring points and the points themselves correspond to two components of a conventional LMI display. The visual system integrates motion signals generated by these local units to form a global percept of rotation. It is apparent, however, the RRI cannot be regarded as direct extension of the version of the LMI presented by Hikosaka et al. (1993a) since in that version the square precedes the line while in the case of the RRI, the line precedes the points. However, as noted above, versions of the LMI display where a line is presented first and replaced by a square at one of its ends were examined by Downing and Treisman (1997) and Faubert and von Grünau (1995). In these cases, the line is perceived as contracting into the square. This version of the LMI display is the one to which the present RRI display can be likened. We note, however, even this version of the LMI differs in a fundamental way from the RRI. In all cases of the LMI, it is the line stimulus that hosts the motion percept. In the case of the RRI, the motion percept is hosted by the points.

A study by Tang et al. (2013) provides a possible way of addressing this discrepancy. These investigators studied circular arrays of various synchronous TAM stimuli of the LMI type. It was found that multiple TAM stimuli could integrate to yield a coherent global motion percept, sometimes dependent on the motion energy associated with shifting luminance centroids in the TAM elements but sometimes based on "high-level TAM-related motion signals" rather than motion energy. The displays in the Tang et al. experiments differ from ours because in theirs the global motion is generated by detectable local motions occurring in the array of discrete TAM elements. With our stimuli, in contrast, the initial display is a continuous outline and no local TAM generated motions are evident when the transition to a ring of points occurs. Nevertheless, the fact that grouped TAM arrays can generate global motion percepts raises the possibility that in the case of the RRI the hypothesized local contraction of inducer line segments into test ring points could generate a global percept of rotation.

This viewpoint, however, raises the additional problem of explaining why all the points in the test ring yoke and rotate together in a common direction. The global motion percepts reported by Tang et al. (2013) are rotational twists but in their case, the local TAM elements provide directional cues to support the rotation percept. In the case of the RRI, these directional cues are missing. If the RRI inducer line segments were contracting into the test ring points a plausible prediction would be that the inducer line segments between each pair of test ring points would split in the middle and contract symmetrically into the points being bridged. This counterfactual possibility is supported by a finding by Downing and Treisman (1997). When a line presentation was followed by two squares, one at each of its ends, the line was in fact seen to vanish outward in two directions from the center. If this is what happens with the RRI display, each of the test ring points would be associated with two opposing line movements that would cancel so that no percept of rotation would be expected. Why then does the RRI occur?

Another variant of the LMI demonstrated by Downing and Treisman (1997) bears on this issue. When two horizontal lines were followed by two points that occurred at the ends of one line, both lines were seen as shrinking toward a point with the same direction (see also Faubert & von Grünau, 1995). This effect indicates that the illusion takes geometrical arrangements into account and demonstrates a yoking of motion directions. In addition, an apparent motion yoking effect has been reported by Ramachandran and Anstis (1983). These investigators presented bi-stable pairs of points that could be seen to be undergoing either a horizontal or vertical

oscillation when repetitively switched between their alternative states. When groups of these point-pairs were presented and switched simultaneously, the same perceived direction of the oscillation was entrained into all the pairs. Ramachandran and Anstis (1986) suggest that their finding provides support for the view that their display is perceptually interpreted as a single object moving through space. This interpretation could also be applied to the RRI test ring display, and would provide a plausible account for our finding of a common direction of the rotation of all the test ring points. It does not, however, explain why any rotation is seen. Accounting for the RRI therefore remains a challenge.

The RRI also differs from the LMI in terms of its temporal characteristics. The clearness of the RRI increases with an increasing ISI between the inducing and test rings, to a maximum with 60 – 90 ms ISI, and decreases with an ISI of 180 ms. The LMI is typically examined with two sequential displays with an ISI of zero. However, Hikosaka, Miyauchi, and Shimojo (1993b) have reported that following a 17 ms presentation of the first frame, the LMI reaches a maximum with an SOA of 50 ms (i.e., ISI of 34 ms) and then continues to be seen with SOAs as long as 2176 ms. Similarly, Hikosaka and colleagues (1993a) used a 2 ms initial square and found an LMI that was maximal with 100 ms SOA but remained at this level in most subjects for 400 ms and was still above chance for 1s. The difference in the profiles of the LMI and RRI with increased ISIs suggests that the two illusions might not have a common basis.

In general, we think the RRI might be best accounted for by the inferential process suggested by Downing and Treisman (1997) and the visual "heuristics" model proposed by Hsieh et al. (2005). Some examples of possible "heuristics" provided by Hsieh and colleagues are that objects tend to change shape continuously, rarely appear out of nowhere, and rarely disappear into thin air. A "heuristic" of this kind might be involved in the generation of the RRI: specifically, one that holds that the most likely interpretation when a ring of points that follows an outlined circle is that a ring of points rotated very rapidly in one direction and decelerated to a halt.

We note that Han and colleagues (2016) compared instances of LMI that differ in aspects of the displays but nonetheless produce similar percepts of apparent motion. Changes of the order of the two displays that affected the instances of LMI differentially and the absence of within subjects' correlations between their measures of the illusion suggest that the different

instances of LMI may actually be mediated by different mechanisms. Therefore, we think it is worthwhile to examine the relation between different instances of the LMI and the RRI.

The relation between the RRI and the MBE

It is important to bear in mind that the MBE differs from the RRI in its defining attribute: The global rotation of the test ring constitutes the RRI, while the MBE is measured by the congruence between the direction of the actual (but not necessarily consciously visible) motion of the inducing ring and the test ring illusory motion. Nevertheless, the displays that produce the two illusions as well as the apparent test ring rotations they generate can appear indistinguishable. Moreover, both illusions exhibit a comparable inverted U shaped function as the ISI between the Inducing and test ring is increased (Figure 5C and 5F). It therefore seems reasonable to conclude that the motion percept in the case of the two illusions reflects in part a common mechanism. However, the fact that the measures of the MBE congruence and measures of the RRI motion clearness vary in opposing ways as the number of points in and diameter of the rings are manipulated, indicates the mechanism responsible for the congruence is not the same as the mechanism that produces the RRI rotation.

The fact that the clearness of the motion percept is consistently judged to be higher with the rotating inducer than the stationary inducer nevertheless indicates that the rotation of the inducer can facilitate the RRI. This could be because it serves to disambiguate the direction of the test ring motion or because it actually serves to boost the strength of that motion. In the latter case, the test ring rotation seen with the MBE display may reflect both the mechanism that produces the rotation in the RRI display and an additional motion signal. Additional research is needed to evaluate these alternatives.

Measures of the strength of illusory motion

It is always a challenge to measure the strength of subjectively perceived illusions. Here we employed a subjective rating measure that has been used in previous research on apparent motion (e.g., Kahneman, 1967) and the line-motion illusion (e.g., Christie & Klein, 2005; Downing and Treisman, 1997; Hubbard & Ruppel, 2011; 2018) and it has been shown to be statistically robust (Norman, 2010) and superior to two-alternative force-choice responses (e.g., Hikosaka et al., 1993 and the critique of Downing & Treisman, 1997). We are nevertheless aware of limitations that result from using this method. Anecdotally, participants reported that they compared the strength of the illusion on a given trial with the strength on previous trials,

which points to an involvement of memory and attention. In addition, it points to serial dependencies of the ratings because the rating of an illusory motion in one and the same condition depends on which condition occurred in the previous trials. These problems call for a replication of the present study with less subjective psychophysical measures of the strength of the illusion. However, since we found systematic variations of the ratings in Experiment 1 which were replicated in Experiment 3, we think our use of the ratings to measure the clearness of the illusory motion is justified in the current context.

We are currently working to develop alternative approaches to quantifying the strength of motion percepts produced by the RRI and the MBE displays. One class of possible measures takes advantage of the fact that moving stimuli shift the positions of stationary shifts (e.g., Durant & Johnston, 2004; Faubert & von Grünau, 1995; Scarfe & Johnston, 2010; Whitney, 2006). In these procedures, observers judge the relative spatial offset of a pair of stimuli. The displacement that is necessary to compensate the motion induced displacement of the two stimuli can be used as an implicit measure to quantify perceived motion. Whitney (2006) has used this approach to study illusory line motions.

Alternatively, a cancellation technique could be employed to quantify the illusionary motion (e.g., Blake & Hiris, 1993; Han, Zhu, Corballis & Hamm, 2016; Steinman, Steinman & Lehmkuhle, 1995; Wright & Johnston, 1985). Han and colleagues used real motion to cancel the illusionary motion and to quantify the illusion (see also Ha & Hamm, 2019). In our future research on the RRI and MBE we expect to employ measures of this kind.

Conclusion

We report evidence for a new illusion, the “Ring Rotation Illusion” that results when an inducer with a circular outline is followed by a ring of points, which appear to rotate unitarily in one direction to a halt. We quantified the strength of this illusion by subjective ratings of the clearness of the rotation. Mean clearness was modulated by the number of points, the diameter of the rings, the ISI between rings, the duration of the rings, and the type of inducer. We compare the RRI with the Motion Bridging Effect, which consists in a general unitary rotation in the direction of a rapidly rotating inducer, which precedes the ring of points. Similarities between the two illusions suggest that the RRI is part of the MBE. Differences between the two illusions suggest that the MBE cannot be reduced to the RRI. We suggest that the RRI is a variant of

apparent motion, which results from a heuristic interpretation of the stimulus sequence according to a corresponding sequence of events in the real world.

Acknowledgments

The authors thank Jana Baden, Alexander Kraut, and Sofie Soujon for their valuable support in recruiting participants and collecting data. The authors declare that the research was conducted in the absence of any commercial or financial relationships that could be construed as a potential conflict of interest.

References

Blake, R., & Hiris, E. (1993). Another means for measuring the motion aftereffect. *Vision Research*, *33*, 1589–1592. https://doi.org/10.1016/0042-6989(93)90152-M

Christie, J., & Klein, R. M. (2005). Does attention cause illusory line motion? *Perception & Psychophysics*, *67*, 1032–1043. https://doi.org/10.3758/BF03193629

Cousineau, D. (2005). Confidence intervals in within-subject designs: A simpler solution to Loftus and Masson's method. *Tutorials in Quantitative Methods for Psychology*, *1*, 42–45. https://doi.org/10.20982/tqmp.01.1.p042

Downing, P. E., & Treisman, A. M. (1997). The line-motion illusion: Attention or impletion? *Journal of Experimental Psychology: Human Perception and Performance*, *23*, 768–779. https://doi.org/10.1037/0096-1523.23.3.768

Durant, S., & Johnston, A. (2004). Temporal dependence of local motion induced shifts in perceived position. *Vision Research*, *44*, 357–366. https://doi.org/10.1016/j.visres.2003.09.022

Faubert, J., & von Grünau, M. (1995). The influence of two spatially distinct primers and attribute priming on motion induction. *Vision Research*, *35*, 3119–3130. https://doi.org/10.1016/0042-6989(95)00061-4

Ha, H., & Hamm, J. P. (2019). Comparisons of flashILM, transformational apparent motion, and polarized gamma motion indicate these are three independent and separable illusions. *Attention, Perception, & Psychophysics*, *81*, 517–532. https://doi.org/10.3758/s13414-018-1632-6

Han, S., Zhu, Z., Corballis, M. C., & Hamm, J. P. (2016). Illusory line motion in onset and offset bars. *Attention, Perception, & Psychophysics*, *78*, 2579–2611. https://doi.org/10.3758/s13414-016-1170-z

Hautus, M. J. (1995). Corrections for extreme proportions and their biasing effects on estimated values of *d'*. *Behavior Research Methods, Instruments, & Computers*, *27*, 46–51. https://doi.org/10.3758/BF03203619

Hikosaka, O., Miyauchi, S., & Shimojo, S. (1993a). Focal visual attention produces illusory temporal order and motion sensation. *Vision Research*, *33*, 1219–1240. https://doi.org/10.1016/0042-6989(93)90210-N

Hikosaka, O., Miyauchi, S., & Shimojo, S. (1993b). Voluntary and Stimulus-Induced Attention Detected as Motion Sensation. *Perception*, *22*, 517–526. https://doi.org/10.1068/p220517

Hock, H. S., & Nichols, D. F. (2010). The line motion illusion: The detection of counterchanging edge and surface contrast. *Journal of Experimental Psychology: Human Perception and Performance*, *36*, 781–796. https://doi.org/10.1037/a0016876

Hsieh, P.-J., Caplovitz, G. P., & Tse, P. U. (2005). Illusory rebound motion and the motion continuity heuristic. *Vision Research*, *45*, 2972–2985. https://doi.org/10.1016/j.visres.2005.02.025

Hubbard, T. L., & Ruppel, S. E. (2011). Effects of temporal and spatial separation on velocity and strength of illusory line motion. *Attention, Perception, & Psychophysics*, *73*, 1133–1146. https://doi.org/10.3758/s13414-010-0081-7

Hubbard, T. L., & Ruppel, S. E. (2018). Does Allocation of Attention Influence Relative Velocity and Strength of Illusory Line Motion? *Frontiers in Psychology*, *9*, 1–13. https://doi.org/10.3389/fpsyg.2018.00147

Kahneman, D. (1967). An onset-onset law for one case of apparent motion and metacontrast. *Perception & Psychophysics*, *2*, 577–584. https://doi.org/10.3758/BF03210272

Kanizsa, G. (1979). *Organization in vision: Essays on gestalt perception*. New York, NY: Praeger.

Kawahara, J., Yokosawa, K., Nishida, S., & Sato, T. (1996). Illusory line motion in visual search: Attentional facilitation or apparent motion? *Perception*, *25*, 901–920. https://doi.org/10.1068/p250901

Macmillan, N. A., & Creelman, C. D. (2005). *Detection theory: A user's guide* (2nd ed.). Mahwah, NJ: Lawrence Erlbaum Associates.

Mangun, G. R., & Hillyard, S. A. (1988). Spatial gradients of visual attention: Behavioral and electrophysiological evidence. *Electroencephalography and Clinical Neurophysiology*, *70*, 417–428. https://doi.org/10.1016/0013-4694(88)90019-3

Mattler, U., & Fendrich, R. (2010). Consciousness mediated by neural transition states: How invisibly rapid motions can become visible. *Consciousness and Cognition*, *19*, 172–185. https://doi.org/10.1016/j.concog.2009.12.015

Morey, R. D. (2008). Confidence intervals from normalized data: A correction to Cousineau (2005). *Tutorials in Quantitative Methods for Psychology*, *4*, 61–64. https://doi.org/10.20982/tqmp.04.2.p061

Norman, G. (2010). Likert scales, levels of measurement and the "laws" of statistics. *Advances in Health Sciences Education*, *15*, 625–632. https://doi.org/10.1007/s10459-010-9222-y

Sagi, D., & Julesz, B. (1986). Enhanced detection in the aperture of focal attention during simple discrimination tasks. *Nature*, *321*, 693–695. https://doi.org/10.1038/321693a0

Scarfe, P., & Johnston, A. (2010). Motion drag induced by global motion Gabor arrays. *Journal of Vision*, *10*, 1–15. https://doi.org/10.1167/10.5.14

Shulman, G. L., Sheehy, J. B., & Wilson, J. (1986). Gradients of spatial attention. *Acta Psychologica*, *61*, 167–181. https://doi.org/10.1016/0001-6918(86)90029-6

Stein, M., Fendrich, R., & Mattler, U. (2019). Stimulus dependencies of an illusory motion: Investigations of the Motion Bridging Effect. *Journal of Vision*, *19*, 1–23. https://doi.org/10.1167/19.5.13

Steinman, B. A., Steinman, S. B., & Lehmkuhle, S. (1995). Visual attention mechanisms show a center—Surround organization. *Vision Research*, *35*, 1859–1869. https://doi.org/10.1016/0042-6989(94)00276-R

Stelmach, L. B., & Herdman, C. M. (1991). Directed attention and perception of temporal order. *Journal of Experimental Psychology: Human Perception and Performance*, *17*, 539–550. https://doi.org/10.1037/0096-1523.17.2.539

Tang, M. F., Dickinson, J. E., Visser, T. A. W., Edwards, M., & Badcock, D. R. (2013). The shape of motion perception: Global pooling of transformational apparent motion. *Journal of Vision*, *13*, 1–20. https://doi.org/10.1167/13.13.20

Tse, P., Cavanagh, P., & Nakayama, K. (1998). The role of parsing in high-level motion processing. In T. Watanabe (Ed.), *High-level motion processing: Computational, neurobiological, and psychophysical perspectives* (pp. 249–266). Cambridge, MA: MIT Press.

Tse, P. U., & Logothetis, N. K. (2002). The duration of 3-D form analysis in transformational apparent motion. *Perception & Psychophysics*, *64*, 244–265. https://doi.org/10.3758/BF03195790

von Grünau, M., & Faubert, J. (1994). Intraattribute and Interattribute Motion Induction. *Perception*, *23*, 913–928. https://doi.org/10.1068/p230913

Wertheimer, M. (1912). Experimentelle Studien über das Sehen von Bewegung [Experimental studies on seeing movement]. *Zeitschrift für Psychologie*, *61*, 161–265.

Whitney, D. (2006). Contribution of bottom-up and top-down motion processes to perceived position. *Journal of Experimental Psychology: Human Perception and Performance*, *32*, 1380–1397. https://doi.org/10.1037/0096-1523.32.6.1380

Wright, M. J., & Johnston, A. (1985). Invariant tuning of motion aftereffect. *Vision Research*, *25*, 1947–1955. https://doi.org/10.1016/0042-6989(85)90019-7

Zanker, J. (1994). Modeling human motion perception I. Classical stimuli. *Naturwissenschaften*, *81*, 156–163. https://doi.org/10.1007/BF01134534

Spatiotemporal alignment and the Motion Bridging Effect.

Maximilian Stein
University of Goettingen
Robert Fendrich
Dartmouth College
Uwe Mattler
University of Goettingen

Author Note

Maximilian Stein, Department of Experimental Psychology, University of Goettingen; Robert Fendrich, Department of Psychological and Brain Sciences, Dartmouth College; Uwe Mattler, Department of Experimental Psychology, University of Goettingen.

Correspondence concerning this article should be addressed to Uwe Mattler, Georg-Elias-Mueller Institute of Psychology, Georg August University Goettingen, Gosslerstr. 14, 37073 Goettingen, Germany. E-mail: uwe.mattler@psych.uni-goettingen.de

Abstract

When a ring of points spins with sufficient rapidity it appears to be an unbroken outline circle with no visible rotational motion. When the rotating ring is followed or preceded by a stationary ring of points, however, the stationary ring is perceived to undergo a brief illusory spin, that generally matches the direction of the actual spin of the rotating ring. This allows observers to judge the spin direction of the rotating ring at above chance levels, an effect that has been termed the Motion Bridging Effect (MBE). We replicated the MBE when start and stop positions of points in rotating ring matched the point locations in the stationary ring, as has been the case in all previous studies. However, when the start and stop positions of the rotating ring were progressively displaced across the space between the points of the stationary ring, the MBE decreased as the displacement increased, vanishing when the displacement was 25% and then reversing so that the direction of the stationary ring's illusory spin was opposite the spinning rings direction. This reverse motion peaked when the start and stop positions of the points in the rotating ring were midway between the points of the stationary ring. As further displacements brought the final point positions of the rotating ring back into alignment with the points of the stationary ring the MBE shifted back to normal, crossing a null when the displacement of 75%. We argue that the MBE is not solely determined by the rotation direction of the inducing ring because it is generated by an interaction between the inducing ring and test ring points whose spatiotemporal distance is the factor that determines the perceived direction of the illusory motion.

Keywords: motion aftereffects, motion perception, unconscious perception, apparent motion, temporal frequency

Spatiotemporal alignment and the Motion Bridging Effect.

The motion bridging effect (MBE, Mattler & Fendrich, 2010) is an illusion in which a rotating ring of points (*the inducing ring*) is preceded or followed by a stationary point ring (*the test ring*). The stimulus sequence produces an illusory movement of the test ring points, that is mainly perceived to be in the direction of the inducing ring spin. This occurs although the speed of the inducing ring is so high that its direction cannot be distinguished when it is presented on its own: All that is seen is a continuous outline circle (Mattler & Fendrich, 2010; Stein, Fendrich, & Mattler, 2019). This absence of a motion percept is attributable to the fact that at the reported high velocities all point positions on the circumference of the rotating ring are refreshed at rates that exceed the human flicker fusion threshold (e.g., 125 Hz with 16 rotating points and a velocity of 2250°/s (Stein et al., 2019).

Two approaches have been proposed to explain the MBE. One is the velocity updating hypothesis of Mattler and Fendrich. They propose that the rapid rotation and spin direction of the inducing ring is stored at some neural processing level. When the rapidly rotating inducer is suddenly replaced by the stationary test ring a transition stage is generated that represents an intermediate velocity, bridging the two stimulus states and enabling perceptual continuity. The stored direction information represented in the interim stage produces the direction correspondence of the MBE. Evidence favoring this approach comes from phenomenological reports of participants, who often describe a percept of deceleration when the test ring follows the inducing ring. When the test ring is presented first, many participants report an acceleration of the test ring.

An alternative approach was proposed by Stein et al. (2019). This approach speculates that the transition from the visually unbroken inducing ring outline to the dotted test ring produces a transformational apparent motion that would be perceived even if the spinning inducing ring was replaced by a truly continuous stationary outline circle. This account posits that the MBE reflects the joint action of two processes, one that registers the direction of the inducing ring's rotation direction and one that generates the illusory test ring spin. Data gathered by Mattler, Stein and Fendrich (in preparation) support this multiple process account by demonstrating a test ring motion is in fact seen when the inducing ring is an actual outline circle that does not convey any rotational information. Note that the transitional velocity hypothesis

and the two-process approach share the premise that the direction of the inducing ring (clockwise vs. counter-clockwise) is encoded in the visual system and can bias the perceived direction of the illusory test ring spin despite the fact that this direction is not consciously visible in the inducing ring itself.

It was previously shown by Mattler and Fendrich (2010) that the MBE depends on the spatial and temporal separations between the inducing ring and test ring points. The authors varied the inter-stimulus interval (ISI) between the inducing ring and the test ring starting with an ISI of 0 ms. The MBE showed a significant increase as the ISI was increased with an optimum at 90 ms and a drop at 180 ms. Additionally, the MBE declined quickly as the position of the test ring was displaced by small spatial distances from the inducing ring. When the authors increased the test ring size to 6° while keeping the inducing ring size constant at 5° of visual angle, participants perceived a rotation in the test ring that matched the inducing ring direction on 55% of the trials, an opposite rotation on 35% of the trials, and no rotation on 10% of the trials. This contrasts with a finding of better than 75% direction congruence when there was no spatial displacement. When the test ring size was increased to 8° of visual angle participants responded with the inducing ring direction in 35% of trials, the opposite direction in 31% of trials, and a report of no rotation in 34 % of trials. This contrasts with a finding of better than 75% direction congruence and a nearly complete absence of no rotation reports when there was no spatial displacement. Note that the appearance of no motion reports in this data fits with the Stein et al. (2019) hypothesis that the illusory motion that allows the MBE direction congruence to be seen is generated by the inducing ring–test ring transition since transformational apparent motions require close spatial proximity (Tse, Cavanagh, & Nakayama, 1998).

In summary, the results of Mattler and Fendrich (2010) argue that the MBE is dependent on the spatial and temporal distances between the inducing and test ring, and in particular critically dependent on their spatial proximity. However, in the Mattler and Fendrich study only the spatial and temporal separations between the full inducing and test rings were considered. We were interested in whether the MBE would also be dependent on the spatiotemporal relationship of the point positions of the inducing and test ring — i.e., the spatial and temporal distances separating the individual inducing ring and test ring points — when the ring circumferences overlapped perfectly. We investigated this by shifting the start and stop position of the inducing ring along the circumference of the test ring. In all previous investigations this

spatiotemporal relationship was kept constant since the start and stop position of the inducing ring always corresponded to the position of the test ring.

Overview

In the present study, we report three experiments that investigate the dependence of the MBE on the start and stop position of the inducing ring. In Experiment 1 we displaced the start and stop positions of the inducing ring points across the spaces separating the points of the test ring that followed the inducing ring. This had the effect of changing the spatiotemporal distance between inducing and test ring point positions while leaving the inducing ring's direction information and subjective appearance unchanged. In Experiment 2, we investigated whether information about the onset and offset positions were the major cause of the effects found in Experiment 1 by temporally embedding the inducing ring between two stationary masks. In Experiment 3 was similar to experiment 1, but we reversed the presentation order of the two rings, so that the test ring was presented first.

General Methods

Participants

Participants were students of the University of Goettingen with an average age of 22.6 years, and were paid at €7 per hour or received student credits. All were tested with a Landolt ring chart prior to their first session and found to have normal or corrected to normal vision. In Experiment 1 and 3 participants completed four 1 hour sessions. In Experiment 2, they completed three 1 hour sessions. We examined 12 students in each experiment. No student participated in more than one of the experiments.

Apparatus

Displays were presented on an analog HAMEG HM 400 cathode-ray oscilloscope controlled by a PC with a 12-bit digital-to-analog converter. The 8 × 10 cm oscilloscope screen was customized with a fast P15 phosphor (50 μs luminance decay time to 0.1%). Participants sat in a dark room with their head positions stabilized by a chin and forehead rest 57 cm from the oscilloscope screen.

Stimuli

The stimuli were similar to those used in our previous study (Stein, Fendrich, & Mattler, 2019). A rotating ring (the *inducing ring*) and a stationary ring (the *test ring*) were displayed. Both rings were 7.5° of visual angle in diameter and constructed from 16 equally spaced luminous points. These points were slightly blurred because we previously found this strengthened the illusory motion percept being studied. The position of the points could be adjusted in increments of 0.25 angular degrees, allowing them to be placed in 1440 potential positions along the ring circumference. The inducing ring was rotated by advancing all of its points every millisecond by a specified number of positions so that it was updated with an effective frame rate of 1000 Hz. This ring could be rotated clockwise or counter-clockwise at angular velocities of 250, 750, 1500 and 2250°/s, which entailed sequential point position progressions of 1, 3, 6, and 9 steps. At the higher rotation speeds (above 250°/s) the inducing ring appeared to be a continuous solid circle. To eliminate visible switching artifacts, the oscilloscope electron beam was turned off during its transition between the successive point positions. The time averaged brightness of inducing ring points was 0.017, 0.050, 0.099, and 0.149 cd/m² at the 250, 750, 1500 and 2250°/s velocities respectively, and the test ring point brightness was 1.50 cd/m² on a dark background. The methods required to obtain these brightness measurements are described in Stein et al. (2019). Data reported in Stein et al. (2019) indicate the velocity dependent differences in luminance were unlikely to have any impact of the MBE.

In one of the reported experiments an 18 ms mask was presented immediately before and after the inducing ring was displayed. These masks were constructed by displaying points around the inducing ring circumference in a random order (and at the position of the central fixation point). For each inducing ring velocity, the location and timing of the point presentations in the associated mask was identical to that employed during the inducing ring presentation. Consequently, the inducing ring and mask had the same apparent brightness, but because the sequence of point positions in the mask was scrambled it did not convey a coherent motion direction. Like the inducing ring the mask appeared to be a continuous outline circle. Informal observations indicated that the presentation of these masks did not alter the appearance of the inducing ring. In all the experiments sessions of two types were run.

The Standard Alignment Session

In the first session of each experiment the rotation of the inducing ring always started and stopped with points placed at the same set of ring circumference positions. These were the positions of the test ring points when the test ring was presented. Fourteen trial blocks were run with the first two treated as practice and excluded from the data analysis. There were 48 trials in each block. Blocks in which only the inducing ring was presented were alternated with blocks in which both the inducing ring and the test ring were presented. The angular velocity and the rotation direction of the inducing ring was varied quasi-randomly within each block. The combination of two test ring states (present, absent) and four angular inducing ring velocities (250, 750, 1500, 2250°/s) produced eight experimental conditions. There were 72 trials in each of these conditions: 36 with a clockwise inducing ring rotation and 36 in counter-clockwise rotation.

Displacement Sessions

In the displacement sessions of each experiment the lowest velocity (250°/s) was not employed and the test ring was always present. The start and stop position of the inducing ring was displaced relative to the point positions in the test ring across the 22.5° distance separating the points forming these rings in 11 equal steps of approximately 1.88° angular degrees starting with a displacement of 0°. This displacement is illustrated in Figure 1 and was always in the rotation direction of the inducing ring (i.e., clockwise with a clockwise rotation, counter-clockwise with a counter-clockwise rotation). Actual displacements employed in each experiment and sequence of trial blocks run are described in the experiment specific methods sections below.

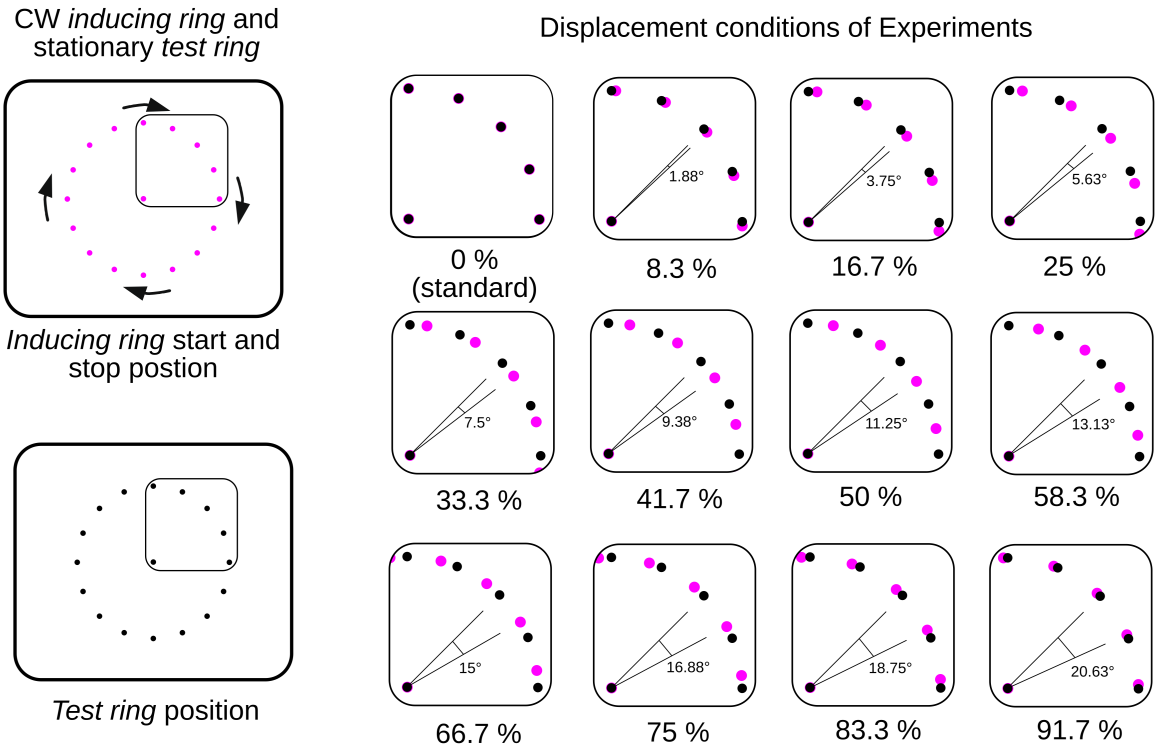

Figure 1. All conditions of the displacement sessions with a clockwise (CW) rotating inducing ring. Test ring point positions are shown in black, inducing ring start and stop positions in yellow. The inducing ring start and stop position was displaced in 11 steps across the 22.5° angular distance separating the test ring points. All the displayed points were identically bright on a dark background: In this figure we color the inducing ring position only to distinguish it from the test ring position.

Statistical Analysis

We used signal detection methods to analyze performance (Macmillan & Creelman, 2005). Hits were defined as clockwise responses to a clockwise rotation direction and false alarms as clockwise responses to a counter-clockwise direction. Hit and false alarm rates were estimated separately for each subject in each condition and corrected with the log-linear rule (Hautus, 1995). In the standard alignment sessions we evaluated *d′* measures of the discrimination ability of participants with repeated measures analyses of variances (ANOVAs). All degrees of freedom were corrected using Greenhouse-Geisser estimates of sphericity but for the sake of readability, the uncorrected degrees of freedom are reported.

Note that contrary to classical signal detection analysis the d' measures in our analyses do not represent the distance between the means of the noise and signal distributions but the distance between the means of two distributions that correspond to the two motion directions. D' has a high positive value if the rate of clockwise responses to a clockwise rotation when all clockwise rotations are considered (hit rate) is higher than the rate of clockwise responses to a counter-clockwise rotation when all counter-clockwise rotations are considered (false alarm rate). This also implies that d' values below zero cannot just be interpreted as chance occurrences when analyzing a small number of trials (e.g., Macmillan & Creelman, 2005) but also as a reversal of the relationship between hit and false alarm rates. If participants perceive a counter-clockwise rotation when the inducing ring is in fact rotating clockwise and vice versa the false alarm rate will be higher than the hit rate and this entails a negative d' value.

Because we observed that the effect of the inducing ring displacements on d' has an apparently sinusoidal profile, a sinusoidal function was fitted to each participant's d' values at each inducing ring velocity using least squares regression. D' variations were measured over the periodic interval that begins and ends with a 0° displacement of the inducing ring start and stop positions relative to the test ring point positions. The mean fit and amplitude of each sinusoidal function was calculated and amplitude estimates were evaluated across participants with Greenhouse-Geisser corrected repeated measures ANOVAs.

Experiment 1

In all previous investigations of the MBE the start and stop positions of the points in the inducing ring matched the positions of the points in the associated test ring. In this experiment we investigated the MBE when the start and stop positions of the inducing ring points were displaced across the 22.5° angular gap that separated the test ring points (see Fig. 1). This displacement manipulation makes it possible to investigate the influence of the spatiotemporal distances between the point positions of the inducing ring and test ring, while keeping the direction signal of the inducing ring untouched.

Method

See Figure 2. Participants reported the rotation direction of the inducing ring (clockwise or counter-clockwise). Responses were registered with the arrow keys of a conventional computer keyboard, with the right arrow indicating a clockwise rotation and the left arrow a

counter-clockwise rotation. Trial blocks were started with a press of the space key. No feedback was given about the correctness of responses.

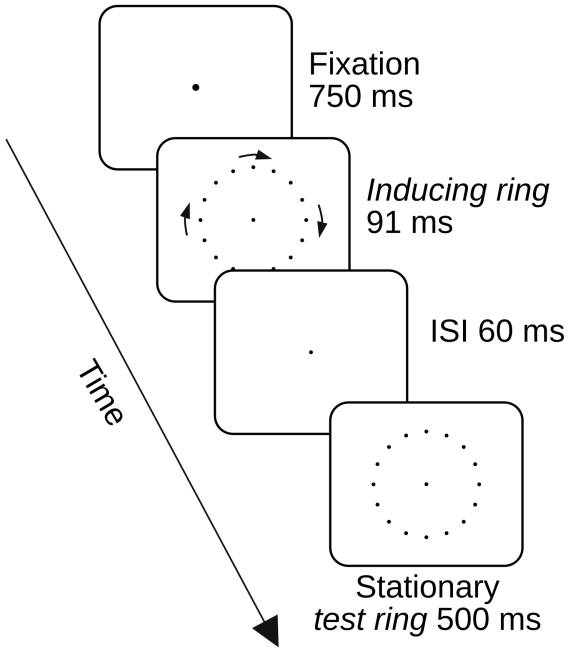

Figure 2. Display sequence in Experiment 1. The inducing ring rotated either clockwise (as shown in the figure) or counter-clockwise. In the standard session no test ring was presented in half of the trials and the inducing ring start and end point positions coincided with the test ring point positions when one was. In the displacement conditions the test ring was always presented and inducing ring start and stop positions fell between the test ring points.

Participants were instructed to maintain their gaze on a central fixation point during the trials. This fixation point brightened for 750 ms at the start of each trial to indicate that the inducing ring was about to appear. In the conditions in which the test ring was presented it followed the inducing ring after a 60 ms interstimulus interval (ISI) and remained visible for 500 ms. Subject's reports of the inducing ring direction were recorded starting 300 ms after the offset of the test ring. A response was required for the experiment to proceed. A new trial started 1 second after the response. In the standard alignment session (first session) no test ring was present in half of the blocks. In the displacement sessions (second to fourth sessions) only blocks in which the inducing ring was followed by the test ring were presented and the beginning and

position of the inducing ring points was displaced relative to the point positions of the test ring in 11 steps (with the standard condition providing a 0 displacement 12th step). In each displacement session nine trial blocks were run with the first treated as practice and excluded from the data analysis. There were 72 trials in each block. The angular velocity, the degree of displacement and the rotation direction of the inducing ring were varied quasi-randomly within each block. The combination of 12 displacements (0, 1.88, 3.75, 5.63, 7.5, 9.38, 11.25, 13.13, 15, 16.88, 18.75, and 20.63° across the 22.5° angular point-distance) and three angular inducing ring velocities (750, 1500, 2250°/s) produced 36 experimental conditions. There were 48 trials in each of these conditions: 24 with a clockwise inducing ring rotation and 24 in counter-clockwise rotation.

Results: The Standard Alignment Session

For the standard alignment session the across subject mean sensitivity (d') to the inducing ring's direction was calculated for each condition and examined with a two-way 2 × 3 ANOVA that evaluated the effect of presenting the additional test ring and the effect of the inducing ring's angular velocity. We will refer to these factors as *Test ring* (inducing ring only vs. inducing ring + test ring condition) and *Velocity*.

Results and confidence intervals are presented in Figure 3. Additionally, we report mean percent responses in inducing ring direction in Table 1. The occurrence of the MBE was confirmed by a higher sensitivity to the inducing ring rotation direction when the test ring was present than when it was absent, $d' = 2.66$ vs. $d' = 1.25$, $F(1, 11) = 90.05$, $p < .001$. There was also a significant main effect of *velocity,* $F(3, 33) = 295.69$, $p < .001$, with mean sensitivity declining as angular velocities increased ($d' = 4.20$, $d' = 1.92$, $d' = 1.08$, and $d' = 0.62$ for the 250, 750, 1500, and 2250°/s velocities respectively). However, the magnitude and character of this decline was quite different for the two *Test Ring* conditions, producing a significant interaction between *Test ring* and *Velocity*, $F(3, 33) = 32.81$, $p < .001$. When the inducing ring was presented alone, performance is high in the 250°/s velocity condition but drops steeply to near zero or zero at the other three levels of velocity ($d' = 4.17$, $d' = 0.67$, $d' = 0.16$, and $d' = -0.01$ at 250, 750, 1500, and 2250°/s, respectively). In contrast to the inducing ring only condition, accuracy falls of linearly when the inducing ring was followed by a test ring, with d' staying above zero even at the highest velocity condition ($d' = 4.22$, $d' = 3.17$, $d' = 2.00$, and $d' = 1.24$ at 250, 750, 1500, and 2250°/s, respectively).

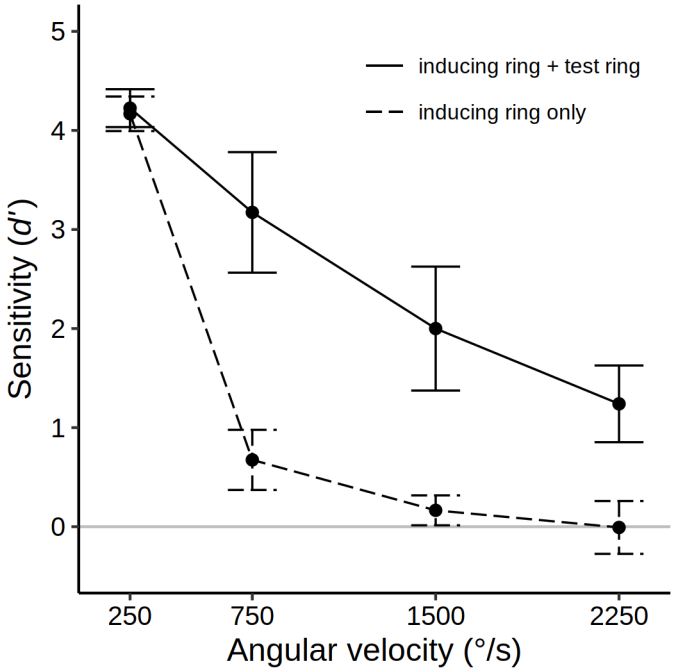

Figure 3. Mean sensitivity (*d'*) for 12 participants in the standard alignment session of Experiment 1 for each velocity in the inducing ring only conditions (the dashed line), and the inducing ring + test ring conditions (the solid line). Error bars show 95% confidence intervals. The solid gray line indicates the chance level of accuracy (*d'* = 0). Data are also presented in % correct format in Table 1.

Table 1

Mean percentage of reports in inducing ring direction for the standard alignment and displacement sessions of Experiment 1. Note that 50% represents chance performance, and values less than 50% indicate a bias to report motion opposite the actual inducing ring direction.

Standard Alignment Session of Experiment 1				
	Angular velocity (in °/s)			
Test ring condition	250	750	1500	2250
Inducing ring only	99.2	62.6	53.0	50
Inducing ring + test ring	99.3	93.2	81.4	72.0
Displacement Sessions of Experiment 1				
		Angular velocity (in °/s)		
Displacement (as % of 22.5°)		750	1500	2250
0		93.8	77.6	71.5
8.3		89.8	75.9	68.8
16.7		79.9	64.6	55.4
25		44.8	44.1	45.7
33.3		23.1	30.2	33.5
41.7		11.1	24.3	30.0
50		11.6	24.1	29.9
58.3		14.4	26.7	30.9
66.7		26.9	35.9	40.1
75		60.6	52.1	49.5
83.3		84.7	68.8	63.0
91.7		90.6	78.8	70.8

The presence of the MBE at each of the inducing ring velocities was evaluated by four paired one-tailed *t* tests, that compared the inducer-only and test ring present conditions. At all velocities higher than 250°/s, accuracy rates were significantly higher when the test ring was shown ($p < .001$). There was no significant MBE in the 250°/s velocity condition ($p > .1$) because accuracy rates were at ceiling irrespective of the test ring condition.

One striking characteristic of the MBE is that the improvement in accuracy produced by the test ring presentation can occur even when subjects perform at chance in the inducing ring only condition. To determine if this was the case with the present data we conducted 4 one-tailed *t* tests with a Bonferroni adjusted alpha level of .0125 that compared the performance of participants at each velocity in the inducing ring only condition to a chance level of 50% ($d' = 0$).

In addition to the obvious above chance performance in the 250°/s condition, we found that mean sensitivity was significantly greater than zero at 750°/s, $t(11) = 4.89$ ($p < .001$), but not at the two highest velocities. When we employed an uncorrected alpha level of .05 performance in the 1500°/s condition was also slightly better than chance, $t(11) = 2.41$, $p = .017$, but not in the 2250°/s condition, $t(11) = 0.06$, $p > .05$.

Results: Displacement Sessions

Mean d' values and confidence intervals for all the conditions of the displacement sessions are presented in Figure 4. Additionally, Table 1 presents the results as the mean percent of correct reports of the inducing ring direction in each condition. As can be seen in Figure 4, the displacement manipulation had a strong impact on the MBE. Mean sensitivity is high ($d' = 1.95$) with 0% displacement of the inducing ring start/stop positions relative to the test ring point positions (the standard alignment condition), gradually drops to near zero at 25% displacement ($d' = -0.26$), builds in an inverse direction (i.e., produces reports of a motion in the reverse direction of the actual inducing ring rotation) as the displacement continues to increase and reaches a negative peak with displacements around of 41.7% and 50% ($d' = -1.73$ for both). Then, as the displacement is increased further mean sensitivity steadily shifts back to its initial value, crossing the chance level of accuracy again at a displacement of 75% ($d' = 0.21$).

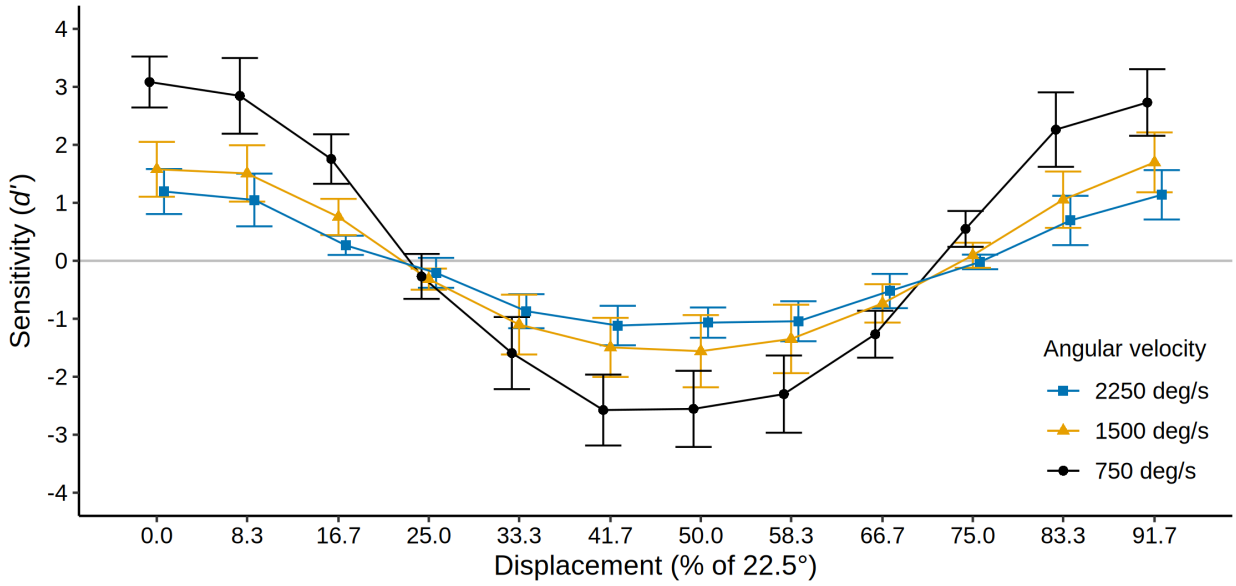

Figure 4. Mean sensitivity (*d'*) for 12 participants in the displacement sessions of Experiment 1 for each level of velocity and displacement. Error bars show 95% confidence intervals. Points and confidence intervals are slightly offset horizontally to improve their visibility. The solid gray line indicates the chance level of accuracy ($d' = 0$). Note that negative *d'* values indicate a bias to report motion opposite the actual inducing ring direction. Data are also presented in % correct format in Table 1.

Because of the sinusoidal profile of the data, we choose to model it with a sinusoidal function that resembles the change of *d'* over the various levels of displacement. The appropriateness of doing this was supported by a high mean fit between a sinusoid and participant's *d'* measure of discrimination ability ($R^2 = .96$, $R^2 = .88$, $R^2 = .85$ at 750, 1500, and 2250°/s, respectively). The amplitude of the fitted sinusoid indicates the strength of the positive and negative MBE. The amplitude of each subject's sinusoid in each velocity condition was therefore calculated and examined with a one-way ANOVA with angular velocity [750, 1500, 2250°/s] as the factor. The velocity effect was highly significant, $F(2, 22) = 111.26$, $p < .001$, with the sinusoid amplitude declining as velocity increased (M = 3.04, M = 1.72, and M = 1.22 at 750, 1500, and 2250°/s, respectively), indicating the strength of the MBE is modulated by velocity. As can be seen in Figure 4, an increase in velocity leads to a reduction in the mean sensitivity when the MBE is positive (e.g., $d' = 3.08$, $d' = 1.58$, $d' = 1.19$ at 750, 1500, and 2250°/

s, respectively at 0% displacement), but to an increase in mean sensitivity when the MBE is negative (e.g., $d' = -2.55$, $d' = -1.56$, $d' = -1.07$ at 750, 1500, and 2250°/s, respectively at 50% displacement). Note that in either case, an increase in velocity brings the MBE closer to chance performance.

Summary

In the standard session of Experiment 1 we replicate the MBE and its dependence on angular velocity (Mattler & Fendrich, 2010; Stein et al., 2019). When the rapidly rotating inducing ring was presented alone, participants perceived a stationary outline at the higher velocities and discrimination ability was at chance level. When the test ring succeeded the inducing ring performance was substantially above chance level because participants perceived an illusory motion in the same direction as the inducing ring was rotating. The most frugal explanation of this and previous investigations of the MBE is to assume the rotation direction of the inducing ring is registered by the visual system and subsequently determines the direction of the illusory motion.

However, the displacement sessions of Experiment 1 demonstrate that the perceived direction of motion was highly dependent on the inducing ring start and stop position. The MBE decreases when these positions are displaced from the test ring point positions and inverts when the displacement is greater than 25% of the inter-point distance, reaching a maximum negative value when it is midway between the test ring points. Neither the premise that the MBE reflects a neural transition between two velocity states of the same stimulus (Mattler & Fendrich, 2010) nor that it reflects the encoding of direction information that biases the direction of an illusory apparent motion (Stein et al., 2019) can readily account for this reversal. If the direction of the MBE is solely determined by the rotation direction of the inducing ring the start and stop position of the inducing ring should have no influence on the direction of the illusory motion. The fact that this influence does occur argues the MBE is generated by an interaction between the inducing ring and test ring points. We will argue in our final discussion that the spatiotemporal distance between the inducing ring and test ring point positions is the factor that determines the perceived direction of the illusory motion.

Experiment 2

The fading luminance streak generated by the advancing inducing ring points is a potential source of information about the direction of the inducing ring rotation. The persisting activity at recently stimulated retinal locations will be greater than the activity at locations activated earlier. Thus, the persisting trace of points positioned just behind an actively displayed point will necessarily be stronger than the persisting trace of the point just ahead of it. The fading of the afterimage of a luminance gradient can in fact by itself result in an illusory perception of motion (Hsieh, Caplovitz, & Tse, 2006). While the luminance streak in the Hsieh et al. Study was clearly visible to the observer and this was not the case in the present and prior MBE studies this example gives credence to the possibility that a luminance streak that is present but not consciously visible could elicit a motion percept. In Experiment 2 we evaluated the hypothesis that invisible fading luminance streaks are a modulator of the MBE.

In Experiment 1 we found that a displacement of the start and stop position of the inducing ring reduced and even inverted the MBE. While we suggest that these results can be accounted for if the perceived direction of the MBE is determined by the spatiotemporal distances of the inducing ring and test ring point positions, they leave open the possibility that the luminance streaks generated at the onset of the inducing ring presentation and fading luminance streaks that follow its offset, although not consciously perceived, play a role in determining the perceived direction of the illusory motion. These result from the temporal distance of the offsets of the inducing ring points and lead to differences in persisting activity at successively presented point positions. To examine the possibility we extended the stimulus arrangement of Experiment 1 by adding two stationary masks, one immediately before and one immediately after the inducing ring. While the masks to do not alter any visible features of the inducing ring (cf., Mattler et al., in preparation), the mask following the inducing ring will overwrite the fading luminance streaks that reflect the advance of the ring's final points positions while the mask preceding the inducing ring will reduce the salience of the onset information conveyed by the initial streaks produced when the inducing ring first appears.

Method

Stimuli and procedures were similar to those described for Experiment 1 with the following changes: The inducing ring was preceded and followed by 18 ms circular masks which emulated the point presentations in each velocity condition but randomized the order of those

presentations so that there was no coherent motion direction (see Figure 5 and general methods). Additionally, the number of displacement levels was pared down to eight while keeping the number of trials per experimental condition constant.

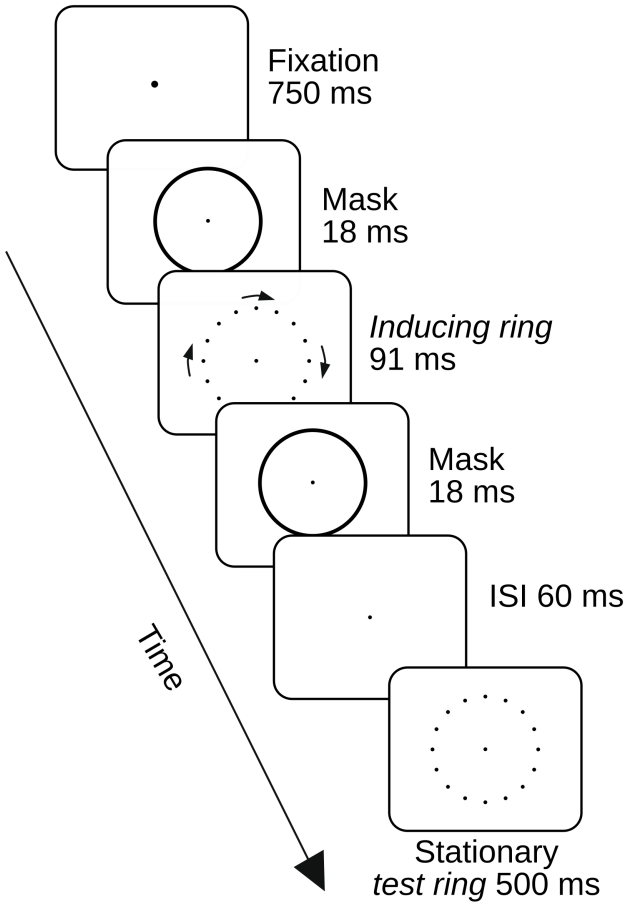

Figure 5. Display sequence in Experiment 2. The inducing ring rotated either clockwise (as shown in the figure) or counter-clockwise. In the standard session no test ring was presented in half of the trials and the inducing ring start and end point positions coincided with the test ring point positions when one was. In the displacement conditions the test ring was always presented and inducing ring start and stop positions fell between the test ring points.

In each displacement session thirteen trial blocks (48 trials per block) were run with the first treated as practice and excluded from the data analysis. The combination of 8 displacements (0, 1.88, 5.63, 9.38, 11.25, 13.13, 16.88, and 20.63° across the 22.5° angular point-distance) and three angular inducing ring velocities (750, 1500, 2250°/s) produced 24 experimental conditions.

There were 48 trials in each of these conditions: 24 with a clockwise inducing ring rotation and 24 in counter-clockwise rotation.

Results: The Standard Alignment Session

Results and confidence intervals for all conditions of the standard alignment session are presented as *d′* values in Figure 6. Mean percentage of responses in inducing ring direction are presented in Table 2. The data essentially duplicates the pattern found in the standard alignment condition of experiment 1. As in Experiment 1, the across subject sensitivity (*d′*) to the rotation direction of the inducing ring was calculated and examined with a 2 × 3 ANOVA with *Test ring* and *Velocity* as the factors. A significant main effect of *Test ring*, $F(1, 11) = 60.67$, $p < .001$, a significant main effect of *Velocity*, $F(3, 33) = 252.34$, $p < .001$, and an interaction between *Velocity* and *Test ring*, $F(3, 33) = 10.98$, $p < .001$. The interaction reflects the different response profiles found when the test ring is present and absent. Accuracy falls of linearly when the inducing ring was followed by a test ring, with *d′* staying above zero even at the high velocity conditions. When the inducing ring was presented alone, accuracy drops steeply to near zero with increasing velocities.

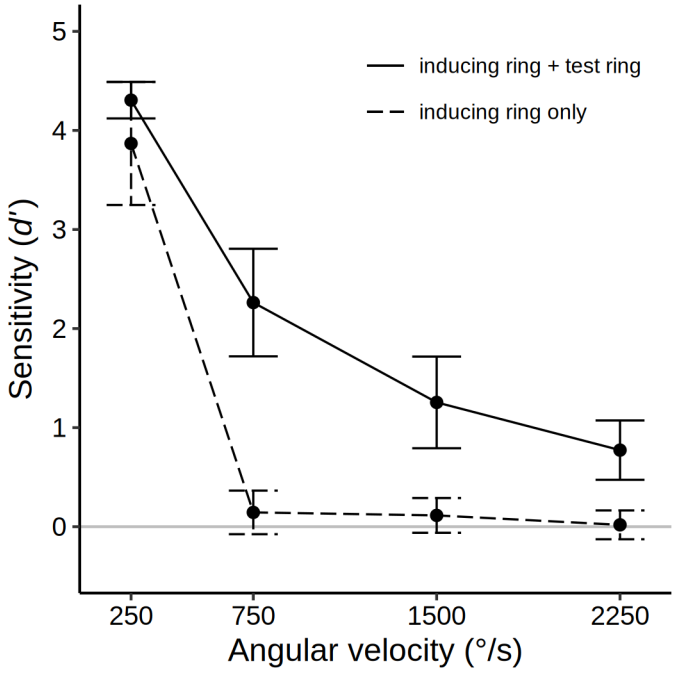

Figure 6. Mean sensitivity (*d′*) for 12 participants in the standard alignment session of Experiment 2 for each velocity in the inducing ring only conditions (the dashed line), and the

inducing ring + test ring conditions (the solid line). Error bars show 95% confidence intervals. The solid gray line indicates the chance level of accuracy ($d' = 0$). Data are also presented in % correct format in Table 2.

Table 2

Mean percentage of reports in inducing ring direction for the standard alignment and displacement sessions of Experiment 2. Note that 50% represents chance performance, and values less than 50% indicate a bias to report motion opposite the actual inducing ring direction.

Standard Alignment Session of Experiment 2				
	Angular velocity (in °/s)			
Test ring condition	250	750	1500	2250
Inducing ring only	96.6	52.9	52.2	50.3
Inducing ring + test ring	99.7	85.3	71.3	64.5
Displacement Sessions of Experiment 2				
		Angular velocity (in °/s)		
Displacement (as % of 22.5°)		750	1500	2250
0		87.3	74.7	64.8
8.3		80.9	67.2	60.6
25		45.1	46.9	48.8
41.7		24.1	36.8	36.5
50		24.7	35.1	37.2
58.3		24.5	35.4	39.4
75		48.3	50.7	46.5
91.7		83.2	72.2	65.1

As in Experiment 1, we directly compared the performance of participants in the inducing ring only condition to a chance level of 50% ($d' = 0$) using 1 tailed t-tests ($\alpha = .0125$). These tests confirmed the consistent above chance performance in the 250°/s velocity condition, $t(11) = 13.72$, $p < .001$, and chance performance in all the higher velocity conditions (all $p > .05$). Additionally, one-tailed t tests ($\alpha = .0125$) that compared the inducer only and inducer + test ring conditions at each level of velocity confirmed that the MBE was present in all conditions except the 250°/s velocity condition (all $p < .001$). There was no significant MBE for the 250°/s velocity condition even when an uncorrected alpha level of .05 was employed due to the high detection rates in the inducer only trials.

To investigate whether the MBE was influenced by the presentation of the ring masks we also calculated a mixed model ANOVA with *Test ring* and *Velocity* as within subjects factors and *Masking* [masks absent in Experiment 1 vs. masks present in Experiment 2] as a between subjects factor. In accord with the previous analyzes, the main effects of both within subjects factors were highly significant as was the interaction between them (all $p < .001$). A significant main effect of *Masking* $F(1, 22) = 7.24$, $p = .013$, indicates that mean sensitivity was reduced when the ring masks were added to the inducing ring ($d' = 1.95$ in the first vs. $d' = 1.59$ in the second experiment). However, due to a non-significant interaction between *Masking* and *Test ring*, $F(1, 22) = 2.08$, $p = .164$, it was not possible to conclude this reduction is solely due to a reduction in the MBE, as it also could be attributed to a general impairment in the perception of motion directions by the stationary masks (cf., Duyck, Wexler, Castet, & Collins, 2018). In general, these results indicate the presentation of the masks had little effect on the MBE.

Results: Displacement Sessions

Mean d' values and confidence intervals for all the conditions of the displacement sessions are presented in Figure 7. Additionally, we report mean percent responses in inducing ring direction in Table 2. The data shows the same pattern observed in Experiment 1. As can be seen in Figure 7 mean sensitivity is high with the standard alignment (0% displacement, $d' = 1.60$), drops as the inducing ring start/stop positions are displaced relative to the test ring point positions, crosses chance with an approximate 25% displacement, builds to a negative peak with a 50% displacement ($d' = -1.05$), then steadily shifts back to its initial positive value re-crossing chance at 75%.

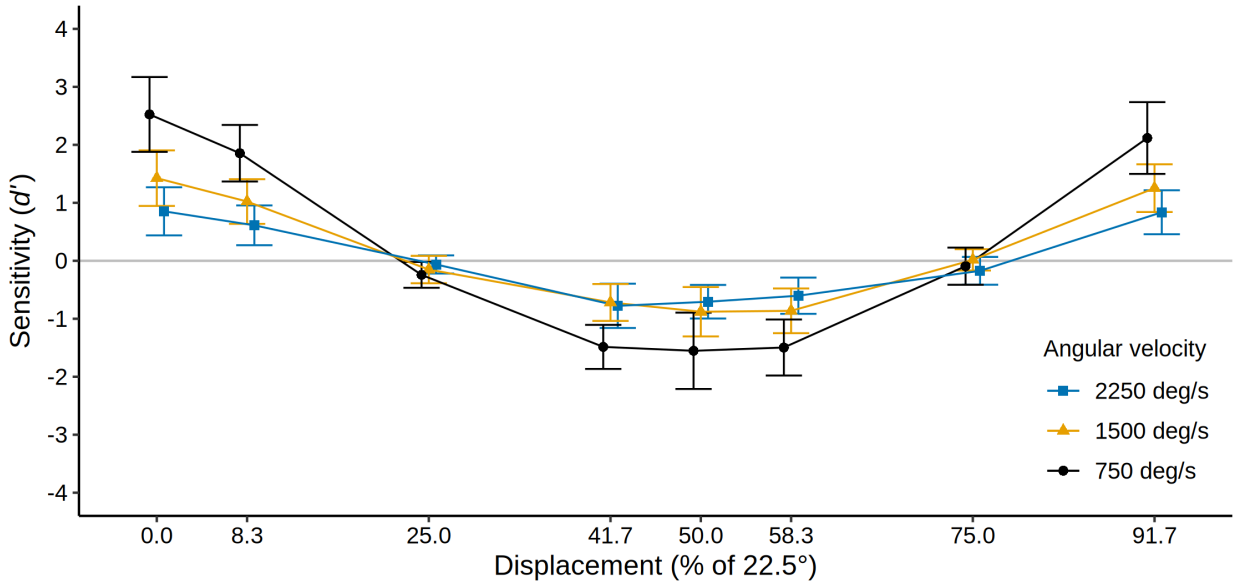

Figure 7. Mean sensitivity (*d'*) for 12 participants in the displacement sessions of Experiment 2 for each level of velocity and displacement. Error bars show 95% confidence intervals. Points and confidence intervals are slightly offset horizontally to improve their visibility. The solid gray line indicates the chance level of accuracy ($d' = 0$). Note that negative d' values indicate a bias to report motion opposite the actual inducing ring direction. Data are also presented in % correct format in Table 2.

As in Experiment 1 we fitted a sinusoid to the change of d' over displacement for each subject in each velocity condition and calculated the amplitude of the sinusoid. Once again, the fit of the observed variations in d' as a function of displacement with a sine function was excellent ($R^2 = .90$, $R^2 = .83$, $R^2 = .76$ at 750, 1500, and 2250°/s, respectively). The amplitude of the sinusoids was examined with one-way ANOVA with angular velocity [750, 1500, 2250°/s] as a factor. The effect of velocity was significant, $F(2, 22) = 54.14$, $p < .001$, with the amplitude of the sinusoid declining as velocity increased (M = 2.04, M = 1.15, and M = 0.83 at 750, 1500, and 2250°/s, respectively), indicating the MBE is modulated by velocity.

As can be seen in Figure 7, the increase in velocity leads to similar results as in Experiment 1: A reduction in the mean sensitivity when the MBE is positive (e.g., $d' = 3.08$, $d' = 1.58$, $d' = 1.19$ at 750, 1500, and 2250°/s, respectively at 0% displacement), but to an increase in mean sensitivity when the MBE is negative (e.g., $d' = -2.55$, $d' = -1.56$, $d' = -1.07$ at 750, 1500,

and 2250°/s, respectively at 50% displacement). Note that in either case, an increase in velocity brings the MBE closer to chance performance.

Summary

In Experiment 2 we once again replicated the MBE and in addition addressed possible explanations that relate to fading luminance streaks and a dependence of direction percepts on information gleaned during the onset and offset of the inducing ring. We found that embedding the inducing ring in two 18 ms masks had no distinct effect on the MBE and its reversal caused by displacements of the inducing ring start and stop position. As in Experiment 1, participants perceive a stationary outline at the higher inducer velocities and their ability to discriminate the inducer direction was near chance at these velocities when no test ring was presented. When the test ring was presented in the standard alignment condition participants perceived an illusory motion in the same direction as the inducing ring. As in Experiment 1, when the inducing ring start and end points were displaced across the spaces separating the tests ring points, the MBE was eliminated when the displacement reached 25% of the interpoint distance and then inverted with the inversion reaching a maximum with displacement of 50% (so that the inducing ring points stopped midway between the test ring points). This result appears to rule out any role of a fading luminance trace to the MBE motion percept.

Experiment 3

In their 2010 paper, Mattler and Fendrich reported a variant of the MBE display in which the test ring preceded the inducing ring. They found this display produced a percept of the inducing ring launching into motion in the direction of its actual rotation, although that rotation was undetectable when the inducing ring was presented alone. Despite the phenomenological differences between the conditions where the inducing ring preceded or followed the test ring, the authors assumed that the motion percepts they produced were instances of the same phenomenon. To further explore this assumption we were interested if the reversal of the MBE also occurs when the test ring precedes the inducing ring.

Method

In Experiment 3 the order of the test and inducing rings was changed in both the standard and the displacement sessions, as illustrated in Figure 8. As in Experiments 1 and 2, we ran a standard alignment sessions in which the start and stop position of the inducing ring points

corresponded to the position of the test ring points and displacement sessions in which those start and stop positions were shifted. In the standard alignment session the test ring was presented on half the trials. When present it was shown for 90 ms and was followed by a 90 ms ISI, after which the inducing ring was presented for 271 ms.

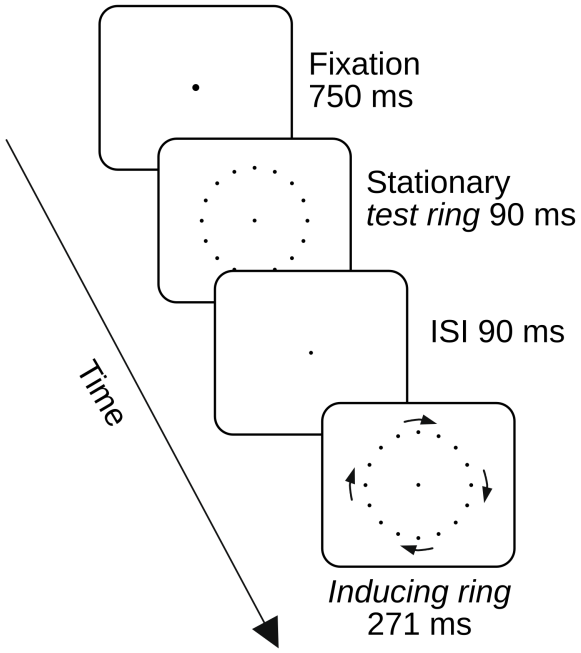

Figure 8. Display sequence in Experiment 3. The inducing ring rotated either clockwise (as shown in the figure) or counter-clockwise. In the standard session no test ring was presented in half of the trials and the inducing ring start and end point positions coincided with the test ring point positions when one was. In the displacement conditions the test ring was always presented and inducing ring start and stop positions fell between the test ring points.

In each displacement session nine trial blocks were run with the first treated as practice and excluded from the data analysis. There were 72 trials in each block. The angular velocity, the degree of displacement and the rotation direction of the inducing ring were varied quasi-randomly within each block. The combination of 12 displacements (0, 1.88, 3.75, 5.63, 7.5, 9.38, 11.25, 13.13, 15, 16.88, 18.75, and 20.63° across the 22.5° angular point-distance) and three angular inducing ring velocities (750, 1500, 2250°/s) produced 36 experimental conditions. There were 48 trials in each of these conditions: 24 with a clockwise inducing ring rotation and

24 with a counter-clockwise rotation. As in the previous Experiments, participants reported the direction of any perceived rotation.

Results: The Standard Alignment Session

Results and confidence intervals for all conditions of the standard alignment session of Experiment 3 are presented in Figure 9. Mean percentage of responses in the actual inducing ring direction are presented in Table 3. When the test ring preceded the inducing ring its effect was similar to that observed in the previous experiments in which it followed the inducing ring, with a higher mean sensitivity in the test ring + inducing ring condition vs. the inducing ring only condition (d' = 3.44 vs. d' = 1.32). A 2 × 3 ANOVA with *Test ring* and *Velocity* as the factors confirmed the main effect of *Test ring*, $F(1, 11) = 183.97$, and indicated there was a main effect of *Velocity*, $F(3, 33) = 243.48$ as well as a *Velocity* by *Test ring* interaction, $F(3, 33) = 43.73$ (all $p < .001$). The interaction reflects the steeper decline in performance in the inducing ring only (d' = 4.13, d' = 0.80, d' = 0.24, and d' = 0.11 at 250, 750, 1500, and 2250°/s, respectively) vs. the inducing ring + test ring condition (d' = 4.34, d' = 3.77, d' = 3.12, and d' = 2.55 at 250, 750, 1500, and 2250°/s, respectively).

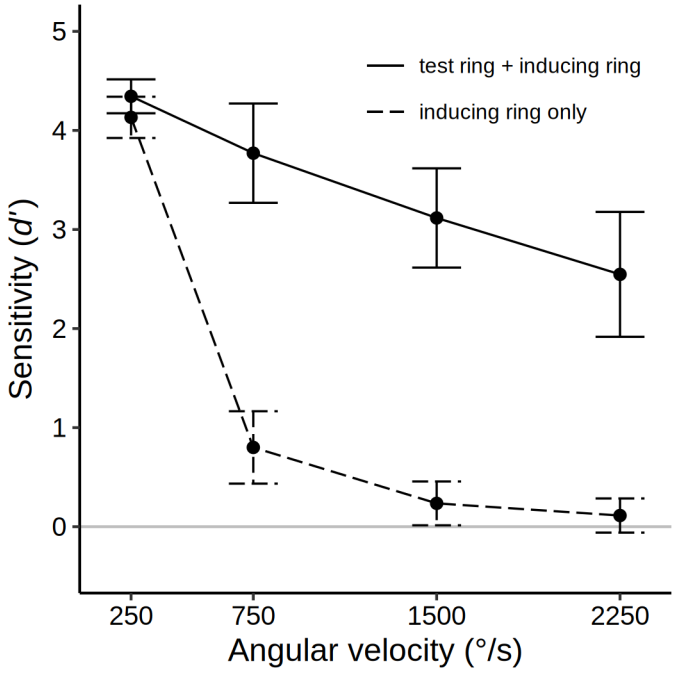

Figure 9. Mean sensitivity (d') for 12 participants in the standard alignment session of Experiment 3 for each velocity in the inducing ring only conditions (the dashed line), and the test

ring + inducing ring conditions (the solid line). Error bars show 95% confidence intervals. The solid gray line indicates the chance level of accuracy ($d' = 0$). Data are also presented in % correct format in Table 3.

Table 3

Mean percentage of reports in inducing ring direction for the standard alignment and displacement sessions of Experiment 3. Note that 50% represents chance performance, and values less than 50% indicate a bias to report motion opposite the actual inducing ring direction.

Standard Alignment Session of Experiment 3				
	Angular velocity (in °/s)			
Test ring condition	250	750	1500	2250
Inducing ring only	99.0	64.6	54.6	52.2
Test ring + inducing ring	99.8	97.1	93.2	87.8
Displacement Sessions of Experiment 3				
		Angular velocity (in °/s)		
Displacement (as % of 22.5°)		750	1500	2250
0		97.2	92.7	89.9
8.3		96.7	92.7	87.7
16.7		98.4	91.3	85.2
25		89.6	77.4	73.8
33.3		23.8	33.2	45.0
41.7		5.7	11.6	16.7
50		3.0	5.4	9.9
58.3		3.3	5.9	9.7
66.7		3.3	8.0	15.3
75		22.6	29.0	28.0
83.3		90.1	72.4	61.3
91.7		97.6	88.5	82.6

In the inducing ring only condition, Bonferroni corrected one-tailed *t* tests ($\alpha = .0125$) indicated sensitivity was significantly greater than zero in the 250°/s and 750°/s velocity condition, with respective $t(11)$ values of 43.67 and 4.82 (both $p < .001$). Performance did not differ from chance at the 1500°/s and 2250°/s velocity condition, but did exceed 0 in the 1500°/s condition when an uncorrected alpha was employed, $t(11) = 2.34$, $p = .020$. A comparison of the test ring present and absent conditions using 4 paired Bonferroni corrected one-tailed *t* tests (α

= .125) confirmed the MBE was present at all velocities except 250°/s, with $t(11)$ values of 13.60, 12.68, and 7.64 (all $p < .001$) for the 750, 1500, and 2250°/s velocities respectively. When employing an uncorrected alpha, there was also a small MBE in the 250°/s velocity condition, $t(11) = 1.90$, $p = .04$, although accuracy rates approached ceiling even when the test ring was absent.

Results: Displacement Sessions

When the test ring preceded the inducing ring, we found a pattern of data similar to that observed in the previous experiments. This is evident in the mean d' values of Figure 10 and mean percent correct values in Table 3. Mean d' changes from a peak in the standard alignment condition ($d' = 3.08$) to a negative peak at 50% displacement ($d' = -3.18$) and then back, crossing chance between a displacement of 25% ($d' = 1.93$) and 33.3% ($d' = -0.94$) and subsequently between 75% ($d' = -1.38$) and 83.3% ($d' = 1.55$). Similar to the previous experiments, the effect of velocity depends on the MBEs polarity. When the MBE is above chance level an increase in velocity decreases sensitivity (e.g., $d' = 3.52$, $d' = 2.94$, $d' = 2.78$ at 750, 1500, and 2250°/s, respectively at 0% displacement), and when the MBE is below chance level an increase in velocity increases sensitivity (e.g., $d' = -3.48$, $d' = -3.26$, $d' = -2.79$ at 750, 1500, and 2250°/s, respectively at 50% displacement).

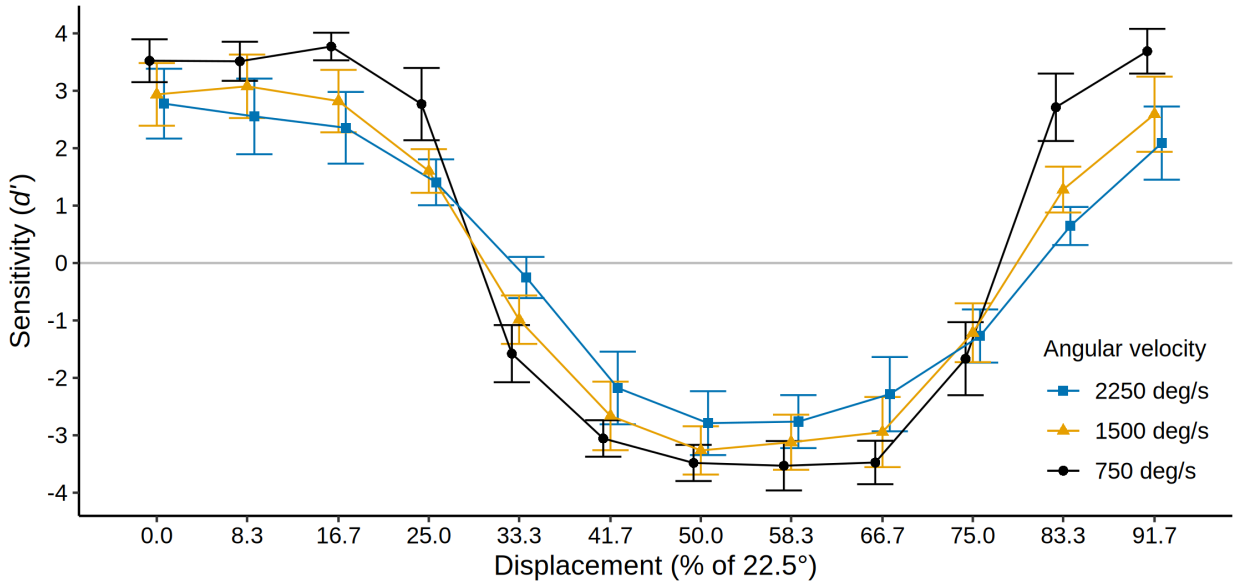

Figure 10. Mean sensitivity (*d'*) for 12 participants in the displacement sessions of Experiment 3 for each level of velocity and displacement. Error bars show 95% confidence intervals. Points and confidence intervals are slightly offset horizontally to improve their visibility. The solid gray line indicates the chance level of accuracy ($d' = 0$). Note that negative *d'* values indicate a bias to report motion opposite the actual inducing ring direction. Data are also presented in % correct format in Table 3.

We once again fitted a sinusoid to the change of *d'* over displacement for each subject in each velocity condition and calculated the sinusoid amplitudes, and once again the fit between a sinusoid and the mean *d'* functions was excellent ($R^2 = .91$, $R^2 = .96$, $R^2 = .96$ at 750, 1500, and 2250°/s, respectively). A one-way ANOVA indicated that the amplitude of the sinusoids varied significantly as a function of angular velocity, $F(2, 22) = 30.45$, $p < .001$, with the amplitude declining as velocity increased (M = 4.29, M = 3.52, and M = 2.98 at 750, 1500, and 2250°/s, respectively), indicating the MBE is modulated by velocity.

Summary

When the rapidly rotating inducing ring is presented alone, as in Experiment 1, the inducing ring looks like a stationary outline at the higher velocities and participant's discrimination ability is close to chance. When the test ring precedes the inducing ring, participants perceive the test ring as launching into motion in the same direction as the actual

inducing ring rotation, with its points fusing so that it becomes the inducing ring. This allows the inducing ring direction to be reported at levels well above chance. As in Experiments 1 and 2 the MBE diminishes and then reverses as the start and stop positions of the inducing ring points are displaced to positions between the test ring points. The pattern of this reversal is very similar to the pattern observed in Experiments 1 and 2, with the MBE becoming 0 with a 25% displacement, reaching its maximum reverse value at a 50% displacement and then reverting to normal, with a null effect at a 75% displacement.

General Discussion

In this study we once more replicated the MBE: When a stationary test ring of 16 points followed the rapidly rotating inducing ring at its start and stop position, participants perceived an illusory motion in the direction the inducing ring has been rotating. This was the case although participants were not able to distinguish the rotation direction of the inducing ring by itself due to the high temporal frequency of point presentations on the inducing ring circumference. Furthermore, we confirmed the MBE does not depend on the order of the two stimuli (Mattler & Fendrich, 2010). When the point positions of the inducing and test rings were aligned and the test ring preceded the inducing ring, there was an illusion of the test ring starting to spin and becoming the inducing ring. Both stimulus presentation orders produced similar effects on sensitivity (d') although the illusion they produce are phenomenologically different, with the test ring launching into motion in one case and spinning to a halt in the other. When only conditions where considered in which the inducing ring points start and stop positions were aligned with the test ring point positions, it seems that the inducing ring rotation direction must be encoded and acts to bias the illusory rotation direction.

To our surprise, however, when we displaced the inducing ring start and stop position on the test ring circumference, the effect on sensitivity (d') decreased with small displacements, vanished with displacements of 25% and then inverted so that the illusory motion was biased to the direction opposite inducing ring spin. The perceived reversal of the inducing ring motion was maximal when the start/stop position was halfway between the test ring points. One way to explain this reversal is to assume that the MBE is mediated by processes that encode motions in opposite directions.

Other visual phenomena have been reported in which a moving stimulus produces a subsequent illusory perception of movement or biases the perceived direction of a subsequent motion (e.g., Green, Chilcoat, & Stromeyer, 1983; Nishida & Sato, 1995; Pinkus & Pantle, 1997; Wohlgemut, 1911). The best known of these phenomena is the classic motion aftereffect (MAE): After watching a moving adapter stimulus for several seconds, observers perceive an illusory movement in the opposite direction in a subsequent static stimulus. Motion aftereffects are often explained by a temporary reduction in the base discharge rate of direction-specific motion tuned cells due to prolonged stimulation by the adapter, giving cells tuned to opposing directions a relative advantage (Anstis, Verstraten, & Mather, 1998). This advantage may occur at a processing stage as early as the retina (Barlow & Hill, 1963), but higher processing stages in V1 and extrastriate areas have also been implicated (see review by Niedeggen & Wist, 1998). Interestingly, when second order motion stimuli serve as the adapters little or no MAE is found with conventional static test stimuli, but second order motions do generate a pronounced MAE in in flickering test stimuli that have an intrinsic ambiguous motion direction (von Grünau, 1986; Nishida & Sato, 1995). Moreover, Nishida and Sato have shown that the same adapting stimulus can produce MAEs in opposite directions in static and flickering test stimuli, with these MAEs respectively reversing first and second order motion components in the adapting stimulus. These results can be interpreted as demonstrating of existence of multiple MAEs that occur at different stages of visual processing (Mather, Pavan, Campana, & Casco, 2008).

One approach to accounting for the variations in the direction of the MBE that we observed is to posit that our results reflect an interplay between the MAE and MBE. In terms of the velocity updating hypothesis of Mattler and Fendrich (2010) it may be consequential that the MBE only occurs when the last position of the inducing ring rotation is very close to the position of the stationary test ring because otherwise the visual system may not consider both rings as different states of the same stimulus. If the end position of the inducer is more and more displaced from the test ring point positions the direction information derived from the inducing ring may get lost and be overwritten by a countering MAE possibly produced by the reduced responsiveness of neurons in V1 that are adapted to the direction of motion (Niedeggen & Wist, 1998).

We deem the explanation of a countering MAE as unlikely, however, because the temporal frequencies of the stimuli presented in MBE experiments clearly exceeds the temporal

frequencies of adapter stimuli in MAE experiments. Pantle (1974) reports that the duration of the MAE is highest when the adapter frequency is 1-5 Hz, rapidly declines starting from 20 Hz, and no MAE occurs when the adapter is presented with a temporal frequency of 50 Hz. Performance in MBE experiments on the other hand is very high at 50 Hz, declines steadily as temporal frequency is increased and is still measurable even when the inducing ring is presented with temporal frequencies of up to 125 Hz (Stein et al., 2019). The MAE also tends to be independent of the start and stop position of the adapter and the position of the test stimulus and even occurs when no test stimulus in presented at all or the observers eyes are closed after the adapter stimulus was presented (Wohlgemut, 1911). Another defining characteristic of the MAE is the long adaptation period, clearly exceeding the presentation time of a 90 ms inducing ring (e.g., Hershenson, 1993). Kanai & Verstraten (2005) have reported a rapid form of the MAE that occurs after an adaptation period of 160 ms. However, these investigators used an ambiguous test stimulus instead of a stationary one and an inter stimulus interval (ISI) of 500 ms. In contrast, the MBE is found with a stationary test ring and will not occur with an ISIs of 500 ms, because it was already substantially reduced when Mattler and Fendrich (2010) employed an ISI of 180 ms. Moreover, when Kanai and Verstraten reduced their ISI to 40 or 120 ms, the MAE reversed and the ambiguous test stimulus was perceived in the same direction as the adapter when the adaptation period was less than 320 ms.

The MAE and the MBE also differ phenomenologically: While participants perceive a continuous motion over more than one second as an after effect when adapting to a MAE stimuli, in MBE experiments participants report that the dots rapidly spin to a halt (Mattler & Fendrich, 2010). While we did not measure the reports of participants in a way that could differentiate between different motion percepts, our own observations suggest that the reverse and normal MBE have a similar appearance. Green et al. (1983) have reported a MAE with a flickering sinusoidal patch as the test stimulus that was most prevalent with high temporal frequencies and appeared to be a “rapid motion in the direction opposite to the adapting motion” (p. 61). This effect, however, was only observed with low temporal frequencies (up to 16 Hz) and adaptation periods of multiple seconds. Lastly, we have shown a reverse MBE can occur when the test ring precedes the inducing ring, which cannot possibly be attributed to an MAE because the moving stimulus does not occur until after the stationary stimulus.

Therefore, the results of the experiments reported here force us to reconsider the role of the direction information provided by the inducing ring in the generation of the MBE (see Mattler & Fendrich, 2010 and Stein et al., 2019). While the direction of the perceived illusory motion does depend on the rotation direction of the inducing ring, this might only be the case because that rotation changes the spatiotemporal relationship between the inducing ring and test ring point positions. This relationship is determined by the spatial and temporal spacing of all point positions of the inducing ring and the test ring. The rotation direction of the inducing ring influences, for example, the spatial arrangement of points that are temporally closest (have the shortest temporal distance) to the test ring. Consider a test ring point located at 12 O'clock. If the inducing ring is rotating clockwise, the inducing ring points with the shortest temporal distance are on the left side of the test ring point position. On the other hand, when the inducing ring rotates counter-clockwise, the points with the shortest temporal distance are on the right side of the test ring point position. Consequently, when the inducing ring start and stop position is displaced half-way across the spaces between the test ring points, the inducing ring points with the shortest temporal distance are midway between two test ring point positions. Thus, the spatiotemporal distances between the inducing ring and test ring points are a function of the rotation direction, allowing this direction to generate the direction correspondence in the MBE, and are a function of the start and stop position of the inducing ring, allowing the displacement manipulation to affect the direction correspondence.

Because of the dependence of MBE's direction on the spatiotemporal relationship of the two rings, we are inclined to conclude that the illusory motion must be mediated by units that reflect the relationship between all the inducing and test ring point positions. We speculate that these units may be spatiotemporal receptive fields that detect movement from the inducing ring to the test ring, and further suggest that a combining weighting of these receptive fields could in theory predict opposing motions.

Spatiotemporal receptive fields

The existence of spatiotemporal receptive fields has been proposed among others by Adelson and Bergen (1985) and Burr, Ross, and Morrone (1986; see McLean, Raab, & Palmer, 1994 and Reid, Soodak, & Shapley, 1991 for neurophysiological evidence in cats). Adelson and Bergen suggested a moving stimulus (e.g., a square) can be conceptualized as a three-dimensional pattern in x-y-t space and movement is represented in case of the square by a

spatial-temporally tilted bar. By using separable temporal and spatial filters their motion energy model it is able to act as an opponent motion detector that responds to rightward or leftward motion. Burr et al. described the characteristics of these spatiotemporal receptive fields in humans and assumed that they are not constructed from separable filters, because the spatiotemporal tuning functions of theses receptive fields do not all peak at the same spatial frequency when the temporal frequency of the gratings used in their experiment was varied. Concerning the MBE there are multiple ways a spatiotemporal receptive field could detect movement. One of these possibilities is illustrated in Figure 11. Similar to Adelson and Bergen, we have reduced the spatial dimensions in this figure so that the ring of points effectively becomes a line of points. To further reduce complexity, only points between two test ring point positions are presented. The figure loosely resembles part of an 11 ms, 2250°/s velocity inducing ring located at 12 O'clock on the inducing ring circumference. During its rotation 9 point positions between the two test ring point positions are occupied, and a continuously illuminated test ring follows the inducing ring after a short ISI. The hypothetical spatiotemporal receptive field in Figure 11 encompasses points presented within the inducing ring motion and allows a cell to detect local motion that is consistent with the global direction of rotation. The existence of such receptive fields would be compatible with the velocity updating hypothesis (Mattler & Fendrich, 2010) and the two-process approach (Stein et al., 2019) and imply that the temporal limit for the detection of motion is substantially higher than it was previously proposed (e.g., Burr and Ross, 1982).

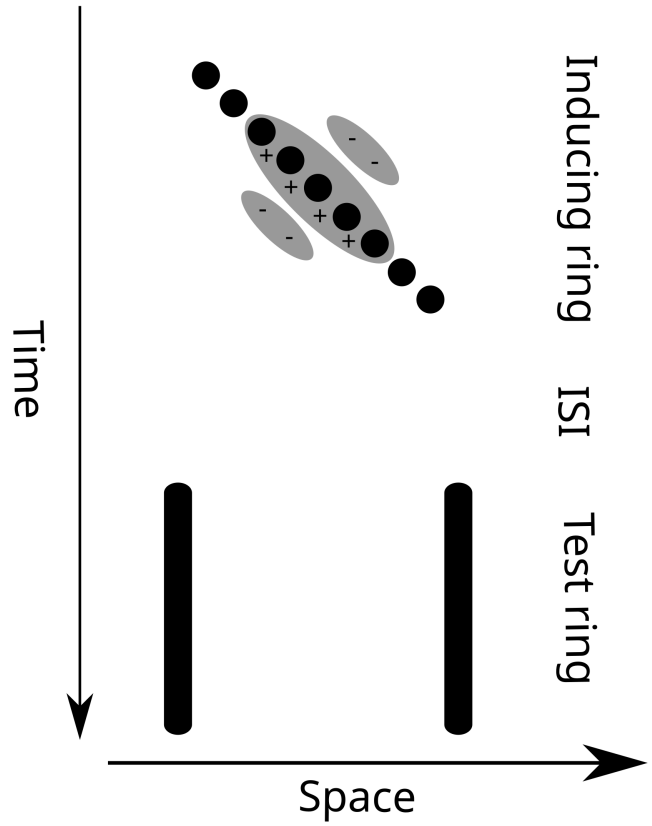

Figure 11. Spatiotemporal illustration of the inducing ring points presented between two test ring point positions at 12 O'clock on the inducing ring circumference. The stimulus sequence was reduced to one spatial dimension, so that a global clockwise rotation corresponds to a spatial shift to the right and a global counter-clockwise rotation to a spatial shift to the left. In the figure we depict a potential spatiotemporal receptive field similar to those of Burr et al. (1986) and Reid et al. (1991). This receptive field could potentially allow a cell to detect local motion in accordance with the clockwise rotation direction of the inducing ring. Note that the presented spatiotemporal receptive field, would require the visual system to have a temporal resolution far above the known limits of motion perception (above 100 Hz in case of the 2250°/s angular velocity inducing ring).

However, the strong dependence of the illusory motion direction on the spatiotemporal relationship of the inducing and test ring indicates that the MBE is most likely not caused by cells with receptive fields that only encompass the inducing ring points. The direction congruence of the MBE could, however, potentially result from cells that signal the inducing ring — test ring transition. These cells would essentially signal a motion starting from the inducing ring and stopping at the test ring points. In Figure 12 we illustrate two possible receptive fields that encompass both stimuli: the inducing and test ring. Most interestingly, the receptive fields proposed in Figure 12 could allow cells to detect local motion that correspond to both, a clockwise and a counter-clockwise rotation direction. Note that this approach would better integrate the MBE into existing theories of motion perception, because it is consistent with the temporal limits of visual perception (e.g., Holcombe, 2009). In order to be compatible with the temporal frequency limits of the visual system, which are about 40 Hz (Burr & Ross, 1982; Kelly, 1961), the spatiotemporal receptive fields would have to span over at least an interval of 25 ms. In the case of the MBE, this interval is ensured by the presentation time of the stimuli and the 60 ms ISI.

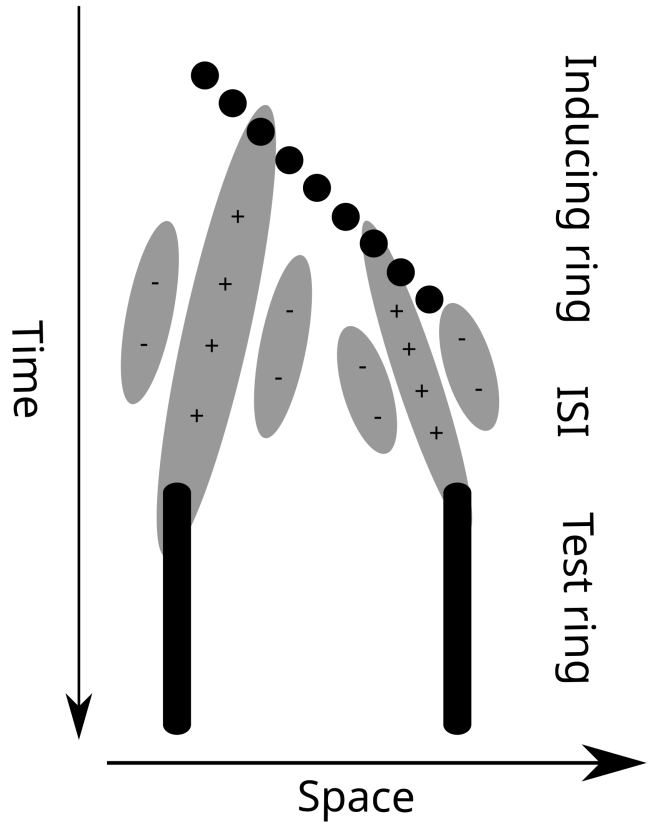

Figure 12. Spatiotemporal illustration of the inducing ring points presented between two test ring point positions at 12 O'clock on the inducing ring circumference. The stimulus sequence was reduced to one spatial dimension, so that a global clockwise rotation corresponds to a spatial shift to the right and a global counter-clockwise rotation to a spatial shift to the left. In the figure we depict a potential spatiotemporal receptive field similar to those of Burr et al. (1986) and Reid et al. (1991). These receptive field could potentially allow the detection of both, a spatial shift to the left and a spatial shift to the right. Note that the presented spatiotemporal receptive fields, would be well within the known limits of motion perception (in this case this is due to the increased temporal distance between inducing ring and test ring produced by the ISI).

Even though the assumption that spatiotemporal detectors mediate the MBE explains some aspects of the illusion, i.e., why movement is generally perceived when presenting the two stimuli, it does not yet explain why the perceived movement depends on the spatiotemporal relationship of the inducing and test ring points. For this reason we propose a highly speculative account that gives credence to the possibility that the direction correspondence of the MBE as

well as the effect of displacing the inducing ring start and stop position can be accounted for by the spatial and temporal distance of each inducing ring point position to the test ring point positions. For example, the visual system could preferentially process motion that is detected by cells whose receptive fields encompass low spatial and temporal distances. In Figure 13 we illustrate a two-stage weighing model of multiple receptive fields based on inducing and test ring point correspondences.

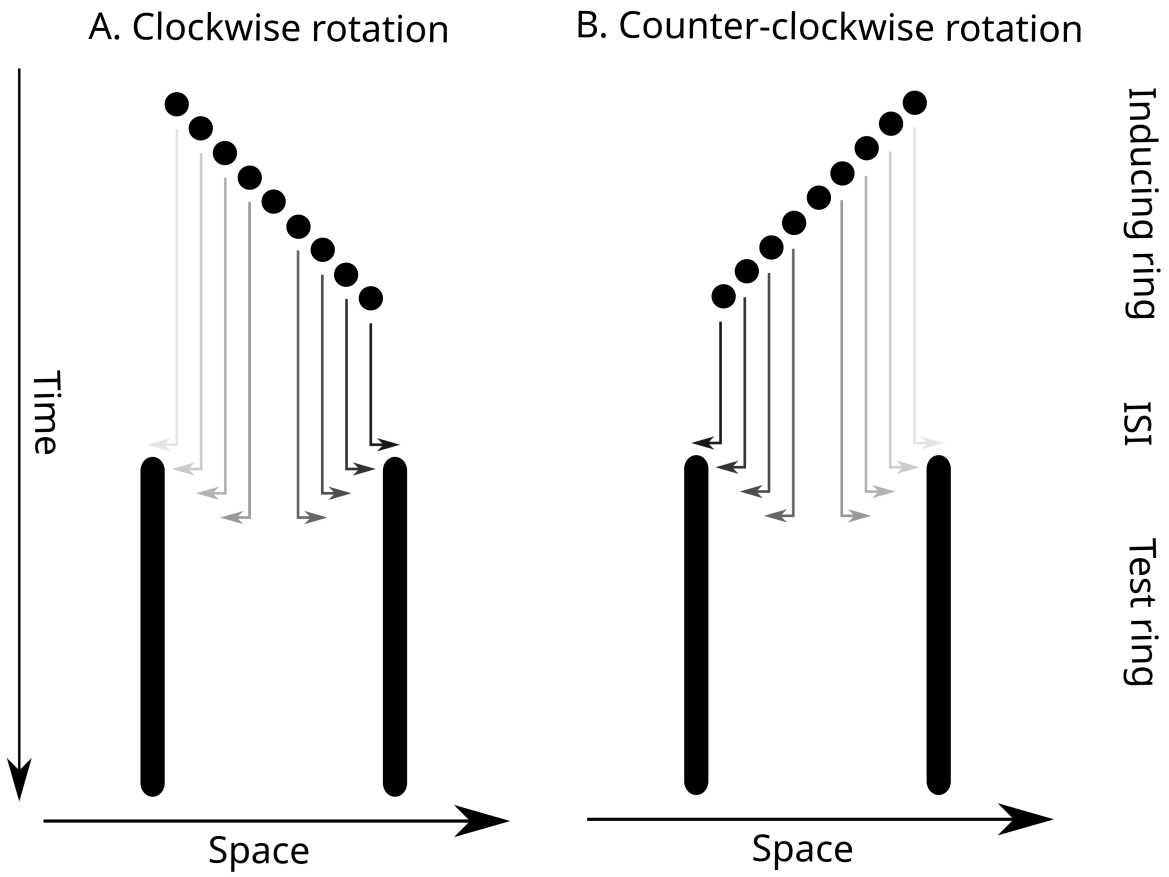

Figure 13. Spatiotemporal illustrations of the inducing ring points presented between two test ring point positions at 12 O'clock on the inducing ring circumference. The stimulus sequences were reduced to one spatial dimension, so that a global clockwise rotation corresponds to a spatial shift to the right and a global counter-clockwise rotation to a spatial shift to the left. The stimuli sequences correspond to an 11 ms inducing ring rotating in clockwise (A) or counter-clockwise direction (B) with a velocity of 2250°/s at 0% displacement. The arrows indicate the results from the first stage of the weighing model: Each inducing ring point is associated with its

closest test ring point. Inducing ring – test ring point correspondences with short temporal distances are printed black while correspondences with a large temporal distance are printed light gray.

At the first stage of this model it is assumed that two possible spatiotemporal receptive fields allow cells to detect the movement starting from each individual inducing ring point to the two neighboring test ring points. The cells are interconnected by a winner takes all opponent principle, so that only the movement with the smallest spatial distance is included into the calculation of the next stage. This first stage is represented in the figure by arrows that indicate in which direction each inducing ring point would move if the smallest spatial distance is preferred. On the second stage, cells that signal small temporal distances are weighted higher than those that signal large temporal distances. This is represented in the figure by the grey level of the arrows. Dark arrows have a short temporal distance and consequently a high weight, light grey arrows have a long temporal distance and a low weight. As can be seen in Figure 13A, when the inducing ring is rotating clockwise the cells signaling clockwise movement are weighted higher than the ones signaling counter-clockwise movement because of their small temporal distances. On the other hand, when the inducing ring rotates in a counter-clockwise direction, like it is illustrated in Figure 13B, this relationship is reversed. High weighted cells signal motion in a counter-clockwise direction while cells with low weights signal direction opposite the actual direction of the inducing ring.

Most importantly, this relationship of weights will be strongly influenced by the start and stop position of the inducing ring. Figure 14A presents the stimulus arrangement in the 50% displacement condition. In this condition the inducing ring starts and stops halfway between the test ring point positions. As a result, the inducing ring points that signal counter-clockwise motion have the smallest temporal distances and therefore the highest weights signaling a rotation opposite to the actual rotation direction of the inducing ring. Figure 13B on the other hand shows that in the 25% displacement condition, there would be a few strong and a few week signals in the direction opposite to the inducing ring rotation direction and multiple middle weighted signals in the inducing ring rotation direction. This ratio of weights could equalize and result in no more congruence between the direction of rotation of the inducing ring and the perceived direction of the illusory motion.

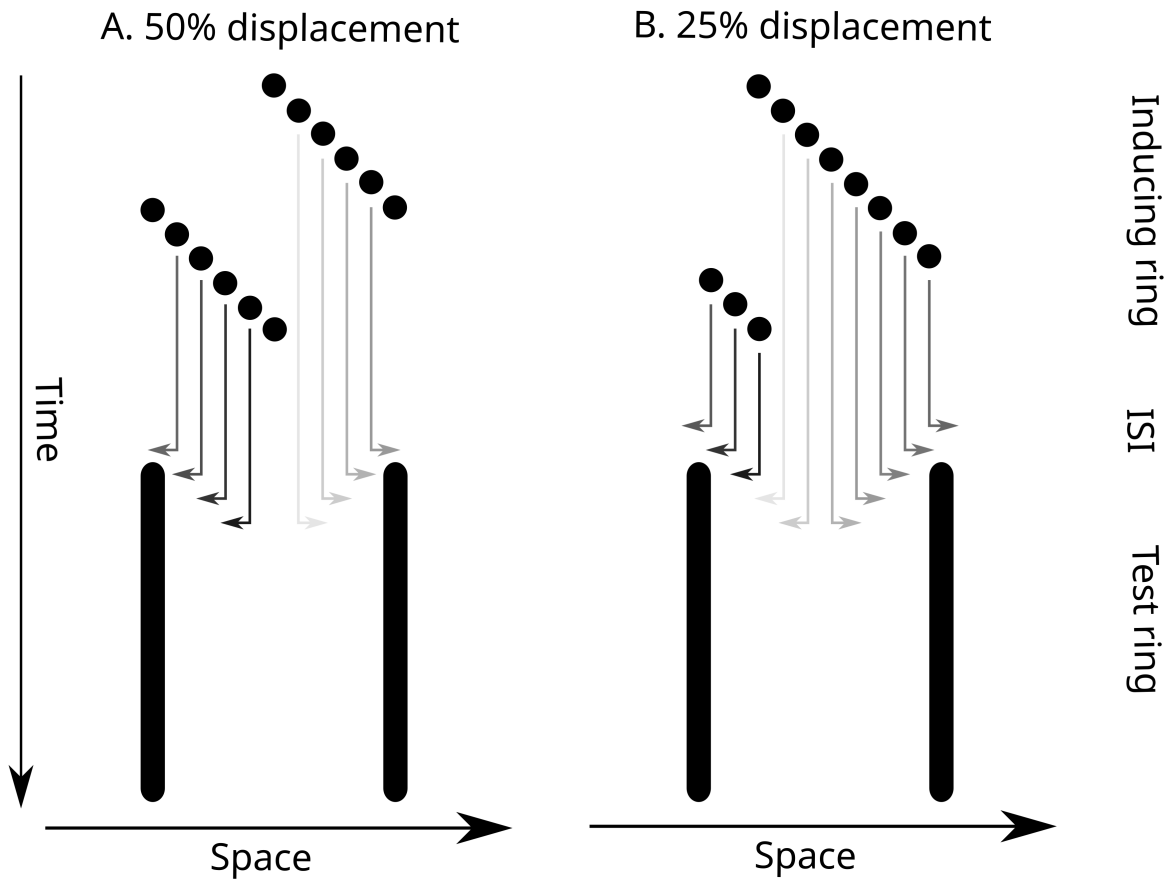

Figure 14. Spatiotemporal illustrations of the inducing ring points presented between two test ring point positions at 12 O'clock on the inducing ring circumference. The stimulus sequences were reduced to one spatial dimension, so that a global clockwise rotation corresponds to a spatial shift to the right and a global counter-clockwise rotation to a spatial shift to the left. The stimuli sequences correspond to an 11 ms clockwise rotating inducing ring at 50% (A) or 25% displacement (B) and a velocity of 2250°/s. The arrows indicate the results from the first stage of the weighing model: Each inducing ring point is associated with its closest test ring point. Inducing ring – test ring point correspondences with short temporal distances are printed black while correspondences with a large temporal distance are printed light gray.

By assuming that the receptive fields span from the test ring points to the inducing ring points, the proposed model can also be applied to the conditions in which the test ring preceded the inducing ring. As is illustrated in Figure 15, the prediction of the model matches the observed

effect. Interestingly, the MBE is not much affected by the presence of the ring masks in Experiment 2. It is difficult to say what prediction the model we presented makes about the presentation of the masks. On the one hand, the same spatiotemporal receptive fields should be activated, regardless of whether a ring mask is presented or not. It is therefore possible that the ring masks have no influence at all on the direction correspondence of the MBE. However, the presentation of the masks activate numerous spatiotemporal receptive fields spanning from the mask's point positions to the test ring points, which would not have been active in the standard condition, and these receptive fields could potentially affect the MBE.

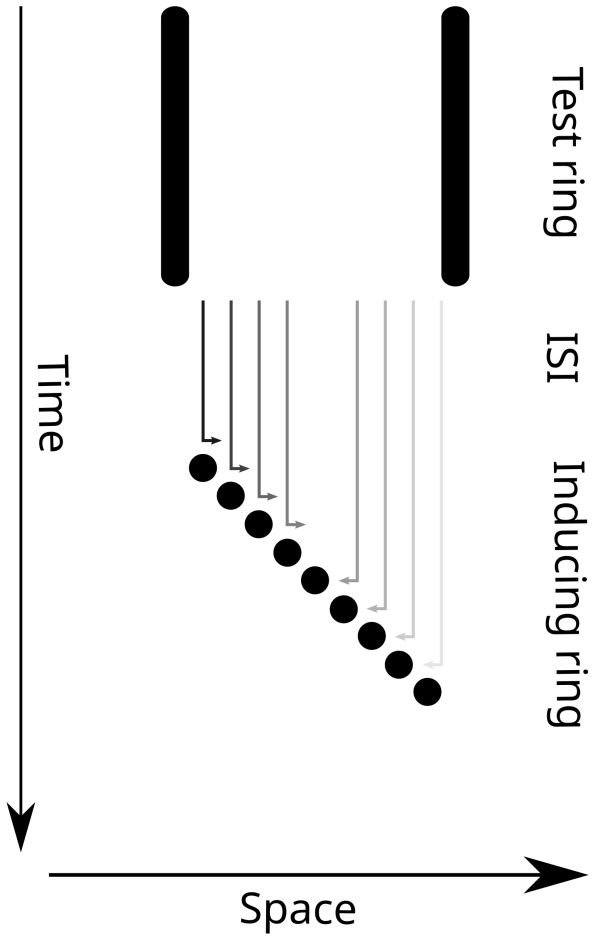

Figure 15. Spatiotemporal illustration of the inducing ring points presented between two test ring point positions at 12 O'clock on the inducing ring circumference. The stimulus sequence was reduced to one spatial dimension, so that a global clockwise rotation corresponds to a spatial

shift to the right and a global counter-clockwise rotation to a spatial shift to the left. The stimuli sequence corresponds to a test ring preceding an 11 ms clockwise rotating inducing ring with a velocity of 2250°/s. The arrows indicate the results from the first stage of the weighing model: Each test ring point is associated with its closest inducing ring point. Test ring – inducing ring point correspondences with short temporal distances are printed black while correspondences with a large temporal distance are printed light gray.

In summary, the proposed model is able to predict the displacement results of the experiments carried out as well as the direction correspondence of the MBE with both stimuli orders: the inducing ring preceding and following the test ring. However, the model has serious shortcomings in terms of its theoretical plausibility. While there is some evidence for the preference of short spatial distances coming from studies concerning the correspondence problem of motion perception (Burt & Sperling, 1981; Ullman, 1979), motion is most likely not preferably perceived across the shortest temporal interval. On the contrary, Weiss, Simoncelli, and Adelson (2002) and Dawson (1991), for example, suggest that the visual system prefers slow velocities that result from hight temporal distances. Clearly the model proposed above needs to be revised or extended to be in line with already known theories regarding the perception of movement. Nevertheless, the model underpins our argument that the MBE is not solely determined by the rotation direction of the inducing ring but by an interaction between the inducing ring and test ring points whose spatiotemporal relationship is the factor that determines the perceived direction of the illusory motion.

Conclusion

The MBE demonstrates the neural encoding of the spatiotemporal sequence of a spinning ring of points that rotates so rapidly its rotation direction is not consciously detectable (Mattler & Fendrich, 2010). When the spinning inducing ring is preceded or followed by a stationary test ring, participants report a test ring rotation in the same direction as the inducing ring was rotating. In this study we demonstrate that the MBE critically depends on the start and stop position of the inducing ring. When these positions are displaced across the test ring circumference, the MBE, indexed by the congruence of the perceived test ring and actual inducing ring rotation, vanishes and even reverses: When the inducing ring start and stop

position is displaced halfway across the test ring points, participants perceive a motion opposite to the actual inducing ring rotation direction. To account for this pattern of results, we propose that the directional congruence of the MBE is not caused by the direction of the inducing ring rotation itself but by the spatiotemporal distances between the inducing ring and test ring points. We propose a speculative model that predicts some aspects of the MBE by assuming that small spatial and temporal distances are preferably processed. Additional investigations are needed to further specify the effects of spatiotemporal distances on the MBE and produce a physiologically plausible model that explains its directional congruence.

Acknowledgments

The authors thank Johannes Bommes, Lotta Ottensmeyer, and Marilena Reinhardt for their valuable support in recruiting participants and collecting data. Data from Experiment 1 were presented at the Vision Sciences Society Annual Meeting 2018, St. Pete Beach, Florida, USA. The authors declare that the research was conducted in the absence of any commercial or financial relationships that could be construed as a potential conflict of interest.

References

Adelson, E. H., & Bergen, J. R. (1985). Spatiotemporal energy models for the perception of motion. *Journal of the Optical Society of America A*, *2*, 284–299. https://doi.org/10.1364/JOSAA.2.000284

Anstis, S., Verstraten, F. A. J., & Mather, G. (1998). The motion aftereffect. *Trends in Cognitive Sciences*, *2*, 111–117. https://doi.org/10.1016/S1364-6613(98)01142-5

Barlow, H. B., & Hill, R. M. (1963). Evidence for a physiological explanation of the waterfall phenomenon and figural after-effects. *Nature*, *200*, 1345–1347. https://doi.org/10.1038/2001345a0

Burr, D. C., Ross, J., & Morrone, M. C. (1986). Seeing objects in motion. *Proceedings of the Royal Society B: Biological Sciences*, *227*, 249–265. https://doi.org/10.1098/rspb.1986.0022

Burr, David C., & Ross, J. (1982). Contrast sensitivity at high velocities. *Vision Research*, *22*, 479–484. https://doi.org/10.1016/0042-6989(82)90196-1

Burt, P., & Sperling, G. (1981). Time, distance, and feature trade-offs in visual apparent motion. *Psychological Review*, *88*, 171–195. https://doi.org/10.1037/0033-295X.88.2.171

Dawson, M. R. (1991). The how and why of what went where in apparent motion: Modeling solutions to the motion correspondence problem. *Journal of Neurophysiology*, *52*, 1106–1130. https://doi.org/10.1037/0033-295X.98.4.569

Duyck, M., Wexler, M., Castet, E., & Collins, T. (2018). Motion masking by stationary objects: A study of simulated saccades. *I-Perception*, *9*, 1–11. https://doi.org/10.1177/2041669518773111

Green, M., Chilcoat, M., & Iii, C. F. S. (1983). Rapid motion aftereffect seen within uniform flickering test fields. *Nature*, *304*, 61–62. https://doi.org/10.1038/304061a0

Hautus, M. J. (1995). Corrections for extreme proportions and their biasing effects on estimated values of *d'*. *Behavior Research Methods, Instruments, & Computers*, *27*, 46–51. https://doi.org/10.3758/BF03203619

Hershenson, M. (1993). Linear and rotation motion aftereffects as a function of inspection duration. *Vision Research*, *33*, 1913–1919. https://doi.org/10.1016/0042-6989(93)90018-R

Holcombe, A. O. (2009). Seeing slow and seeing fast: Two limits on perception. *Trends in Cognitive Sciences*, *13*, 216–221. https://doi.org/10.1016/j.tics.2009.02.005

Hsieh, P.-J., Caplovitz, G. P., & Tse, P. U. (2006). Illusory motion induced by the offset of stationary luminance-defined gradients. *Vision Research*, *46*, 970–978. https://doi.org/10.1016/j.visres.2005.10.009

Kanai, R., & Verstraten, F. A. J. (2005). Perceptual manifestations of fast neural plasticity: Motion priming, rapid motion aftereffect and perceptual sensitization. *Vision Research*, *45*, 3109–3116. https://doi.org/10.1016/j.visres.2005.05.014

Kelly, D. H. (1961). Visual responses to time-dependent stimuli. I. Amplitude sensitivity measurements. *Journal of the Optical Society of America A*, *51*, 422–429. https://doi.org/10.1364/JOSA.51.000422

Macmillan, N. A., & Creelman, C. D. (2005). *Detection theory: A user's guide* (2nd ed.). Mahwah, NJ: Lawrence Erlbaum Associates.

Mather, G., Pavan, A., Campana, G., & Casco, C. (2008). The motion after-effect reloaded. *Trends in Cognitive Sciences*, *12*, 481–487. https://doi.org/10.1016/j.tics.2008.09.002

Mattler, U., & Fendrich, R. (2010). Consciousness mediated by neural transition states: How invisibly rapid motions can become visible. *Consciousness and Cognition*, *19*, 172–185. https://doi.org/10.1016/j.concog.2009.12.015

McLean, J., Raab, S., & Palmer, L. A. (1994). Contribution of linear mechanisms to the specification of local motion by simple cells in areas 17 and 18 of the cat. *Visual Neuroscience*, *11*, 271–294. https://doi.org/10.1017/S0952523800001632

Niedeggen, M., & Wist, E. R. (1998). The physiologic substrate of motion aftereffects. In G. Mather, F. Verstraten, & S. Anstis (Eds.), *The motion aftereffect: A modern perspective* (pp. 125–155). Cambridge, MA: MIT Press.

Nishida, S., & Sato, T. (1995). Motion aftereffect with flickering test patterns reveals higher stages of motion processing. *Vision Research*, *35*, 477–490. https://doi.org/10.1016/0042-6989(94)00144-B

Pantle, A. (1974). Motion aftereffect magnitude as a measure of the spatio-temporal response properties of direction-sensitive analyzers. *Vision Research*, *14*, 1229–1236. https://doi.org/10.1016/0042-6989(74)90221-1

Pinkus, A., & Pantle, A. (1997). Probing visual motion signals with a priming paradigm. *Vision Research*, *37*, 541–552. https://doi.org/10.1016/S0042-6989(96)00162-9

Reid, R. C., Soodak, R. E., & Shapley, R. M. (1991). Directional selectivity and spatiotemporal structure of receptive fields of simple cells in cat striate cortex. *Journal of Neurophysiology*, *66*, 505–529. https://doi.org/10.1152/jn.1991.66.2.505

Stein, M., Fendrich, R., & Mattler, U. (2019). Stimulus dependencies of an illusory motion: Investigations of the Motion Bridging Effect. *Journal of Vision*, *19*, 1–23. https://doi.org/10.1167/19.5.13

Tse, P., Cavanagh, P., & Nakayama, K. (1998). The role of parsing in high-level motion processing. In T. Watanabe (Ed.), *High-level motion processing: Computational, neurobiological, and psychophysical perspectives* (pp. 249–266). Cambridge, MA: MIT Press.

Ullman, S. (1979). *The interpretation of visual motion.* Cambridge, MA: MIT Press.

Von Grünau, M. W. (1986). A motion aftereffect for long-range troboscopic apparent motion. *Perception & Psychophysics*, *40*, 31–38. https://doi.org/10.3758/BF03207591

Weiss, Y., Simoncelli, E. P., & Adelson, E. H. (2002). Motion illusions as optimal percepts. *Nature Neuroscience*, *5*, 598–604. https://doi.org/10.1038/nn0602-858

Wohlgemuth, A. (1911). On the after-effect of seen movement. *The British Journal of Psychology: Monograph Supplements*, *1*, 1–117.

Encoding information from rotations too rapid to be consciously perceived as rotating: A replication of the motion bridging effect on a liquid crystal display

Maximilian Stein
University of Goettingen
Robert Fendrich
Dartmouth College
Uwe Mattler
University of Goettingen

Author Note

Maximilian Stein, Department of Experimental Psychology, University of Goettingen; Robert Fendrich, Department of Psychological and Brain Sciences, Dartmouth College; Uwe Mattler, Department of Experimental Psychology, University of Goettingen.

Correspondence concerning this article should be addressed to Uwe Mattler, Georg-Elias-Mueller Institute of Psychology, Georg August University Goettingen, Gosslerstr. 14, 37073 Goettingen, Germany. E-mail: uwe.mattler@psych.uni-goettingen.de

Abstract

The Motion Bridging Effect (MBE) is an illusion in which a motion that is not consciously visible generates a visible illusory motion in a preceding or succeeding stationary stimulus. In the initial study of the MBE (Mattler & Fendrich, 2010), a ring of 16 points was rotated as rapidly as 2250 angular °/s, and point positions on the rings circumference were refreshed at temporal frequencies as high as 100 Hz. Observers saw only an unbroken outline circle and performed at chance when asked to report the rotating ring's direction. However, when the rotating ring was replaced by a ring of 16 stationary points the stationary ring appeared to visibly spin to a halt, principally in the same direction as the initial ring's rotation. Thus, although the inducing ring rotation was not consciously perceived its rotation direction was somehow being encoded. Similar results were found when the stationary ring preceded the rotating ring: the stationary ring appeared to rapidly accelerate. Previously, the MBE could only be investigated using analogue oscilloscopes because conventional raster scan monitors cannot be updated at the temporal frequencies required to portray the rapid inducing ring rotation. Here we show that the MBE can be reproduced using a recent generation of LCD monitors with 240 Hz refresh rates. These findings replicate basic characteristics of the MBE, demonstrating robustness with a completely new display system and software, and in general demonstrate that LCD monitors provide a major new resource for the psychophysical investigation of rapid motions.

Keywords: motion aftereffects, motion perception, unconscious perception, liquid crystal display, temporal frequency

Encoding information from rotations too rapid to be consciously perceived as rotating: A replication of the motion bridging effect on a liquid crystal display

The conscious perception of spatial or temporal changes in the environment is limited by the visual system's ability to perceptually resolve high spatial and temporal frequencies. This limit is approximately 60 cycles per degree of visual angle when discriminating the orientation of fine grids (He & MacLeod, 1996), 30-60 Hz when observing flickering patches (Cornsweet 1970; Hartmann, Lachenmayr, & Brettel, 1979), and approximately 30 Hz when detecting the direction of sinusoidally moving gratings (Burr & Ross, 1982), depending on the luminance of the stimuli (Brown, 1958). These limits, however, apply to conscious perception. Some studies suggest that information can unconsciously be encoded even when these limits are exceeded. He and MacLeod (2001), for example, demonstrated that gratings indistinguishable from a uniform field can affect the magnitude of the tilt aftereffect and Shady, MacLeod, and Fisher (2004) showed that temporal frequency modulations above the critical flicker fusion frequency (CFF) can influence the sensitivity to subsequent flickering patches.

In 2010, Mattler and Fendrich published a study that indicated the human visual system can process motions so rapid they are not visually perceptible as motion. On an analog oscilloscope with an effective frame rate of 1000 Hz, they presented a 16-point ring (the *inducing ring*) that rotated at angular velocities of up to 2250°/s. These high velocities were achieved by advancing the points around the ring circumference at temporal rates up to 100 Hz. As the velocity and refresh rate of point positions along the ring circumference was increased participants' ability to judge the rotation direction of the ring drastically decreased, and the rotating points were seen as forming a static circular outline. However, when a stationary ring of 16 points (the *test ring*) preceded or followed the rotating ring, participants perceived an illusory motion of the test ring that was predominantly in the direction of the inducing ring. Mattler and Fendrich argued that this effect demonstrated that the rapid advance of the rotating points, though not consciously perceived by participants, conveyed a directional motion signal to the test ring points.

These findings were extended by Stein, Fendrich, and Mattler (2019), who showed how the MBE, indexed by the congruence of the inducing and test ring directions, was affected by variations in the diameter of the rings, the number of the points used to form those rings, and the

spacing of the points along the ring perimeters. Stein et al. proposed that the perceived rotation of the test ring might be related to apparent motion. According to this view, the MBE would reflect the joint action of two processes, one that registers the direction of the inducing ring's rotation and one that generates the illusory test ring spin. Data gathered by Mattler, Stein, and Fendrich (in preparation) support this dual process account by demonstrating a test ring motion is seen even when the inducing ring is an actual outline circle that does not convey any rotational information. However, the mechanism by which the rotating inducing ring acts to bias the direction of the illusory rotation of the test ring remains to be established.

Previous MBE studies have been conducted using analog oscilloscope displays with the point positions on the cathode ray tube (CRT) screen controlled by Digital-to-Analog converters and screens customized with a fast phosphor. Conventional computer monitors with screen refresh rates below 100 Hz, while widely employed for investigations of phenomena like visual attention, are unsuitable for displaying the controlled rapid ring rotations needed for MBE investigations. However, recent technical advances have made liquid crystal display (LCD) "gaming monitors" with refresh rates of up to 240 Hz readily available. These high refresh rate monitors allow display sequences to be updated more rapidly than has been possible with the standard CRT monitors. Moreover, LCD monitors avoid potential artifacts associated with the downward raster scans CRT monitors use to display each frame: all pixels are effectively replaced simultaneously. With CRT monitors, phosphor decay times impose an additional limitation on the speed with which displays can be updated. A corresponding limitation in LCD monitors is imposed by LCD switching times. Although in early LCD monitors these switching times were too slow to allow the use of these monitors in psychophysical research, technological advances have now overcome this problem (Wang & Nikolić, 2011; Zhang et al., 2018).

We wondered whether currently available LCD "gaming monitors" with 240 Hz would have sufficient speed and spatial resolution to be used to study the MBE. Pilot observations suggested that this was in fact possible. The experiments reported here formally confirm these observations. We replicate the MBE and certain of its characteristics with this technology and compare the MBE on an LCD monitor to the MBE on the oscilloscope CRTs.

Method

Participants

The participants were 12 students at the University of Göttingen with a mean age of 22.5 years. They were compensated €7 per hour for their participation or received student credits. Testing conducted with the Landolt ring chart confirmed all participants had normal or corrected-to-normal vision. After providing their written informed consent participants completed one session that took approximately one hour.

Apparatus

Stimuli were presented on a 240 Hz LCD monitor (Dell Alienware AW2518HF) controlled by a PC via the display port connector of a MSI GeForce GT 1030 graphics card. The experiment was run in a darkened room and participants had their head positions stabilized by a chin and forehead rest 107.87 cm from the LCD monitor. This resulted in a per-pixel display size of 0.015° of visual angle. The background luminance of the LCD was reduced to a minimum (0.02 cd\m²).

Stimuli

Stimuli are illustrated in Figure 1. Participants were presented with a rapidly rotating inducing ring and a stationary test ring constructed from 16 equally spaced dots. The diameter of both rings was 6° and the diameter of each dot was 0.12° of visual angle. The luminance of the test ring dots, measured with a Minolta LS-100 luminance meter with a close-up lens, was 3.0 cd\m² and the luminance of the inducing ring dots was 1.5 cd\m². Note that when running the monitor in 240 Hz mode, the luminance does not reach its maximum when only one frame is displayed. Since this was the case for the points that formed our inducing rings, we determined their luminance by presenting a flickering square with a one-frame (4.166 ms) on-off duty cycle and doubled the measured luminance of this square.

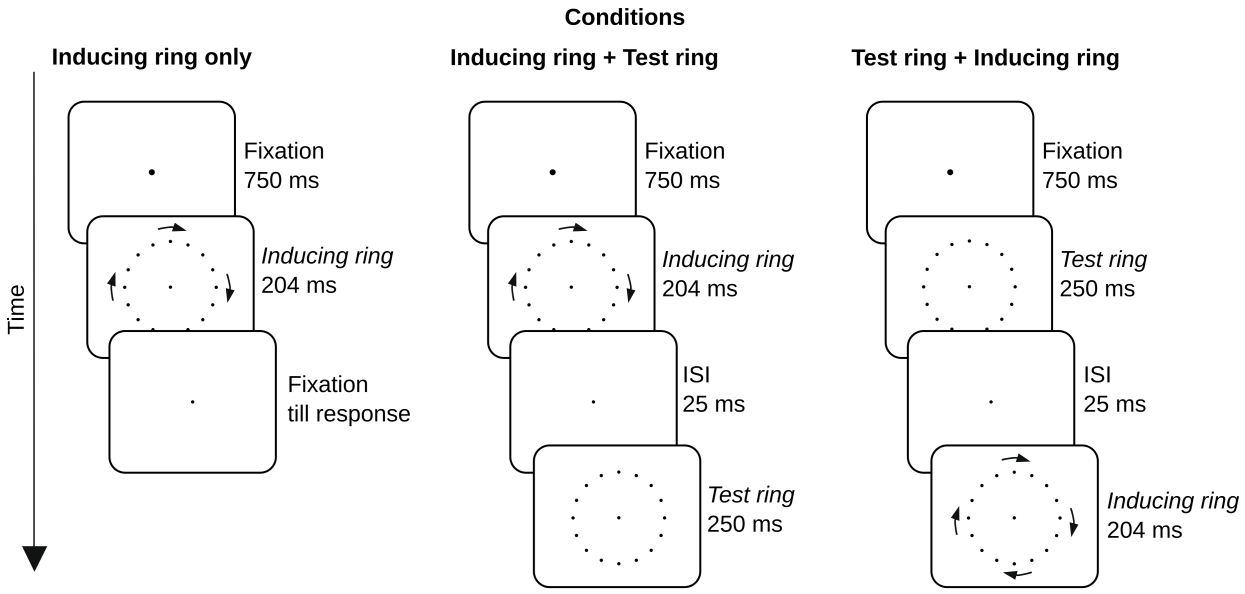

Figure 1. Display sequence in the three conditions of the experiment. On a given trial, the inducing ring rotated either clockwise (as shown in the figure) or counter-clockwise. In the inducing-ring-only condition, there was no test ring present while in the other two conditions the test ring either preceded or followed the inducing ring. The dots on the LCD appeared light gray on a dark gray background.

At the monitors 240 Hz rate, frames were updated every 4.166 ms. The inducing ring was rotated at angular velocities of 225, 675, 900, and 1350°/s by respectively advancing all of its dots by 0.9375, 2.8125, 3.75, and 5.625 angular degrees per frame in a clockwise or counter-clockwise direction. These distances respectively generated 384, 128, 96, and 64 dot positions along the ring circumference, which were refreshed at respective temporal frequencies of 10, 30, 40, and 60 Hz as successive dots crossed each display location. The rotation of the inducing ring always started and ended with dots placed at the same set of ring circumference positions. These were also the positions of the test ring dots when the test ring was presented. At 10 Hz temporal frequency, the inducing ring looked like a rotating outline circle formed by overlapping dots. At higher temporal frequencies, it appeared to be a circle of stationary dots, almost touching at 30 Hz but clearly separated at 40 Hz and more widely separated at 60 Hz.

Task

Participants reported the direction of any perceived rotation (clockwise or counter-clockwise). Responses were registered with the right and left arrow keys of a conventional computer keyboard, to indicate clockwise rotation and counter-clockwise rotation, respectively. Trial blocks were started by a press of the space key. No feedback was given about the correctness of responses.

Procedure

Participants were instructed to maintain their gaze on a central fixation point during the trials. This fixation point brightened for 750 ms at the start of each trial to indicate that the inducing ring or test ring was about to appear. In the conditions in which the test ring was presented it followed or preceded a 204 ms inducing ring presentation with a 25 ms inter-stimulus interval (ISI) and remained visible for 250 ms. Subject's reports of the perceived motion direction were recorded starting 300 ms after the offset of the last presented ring. A response was required for the experiment to proceed. A new trial started 1 second after the response.

Design

Fifteen trial blocks were run in each session with the first three blocks treated as practice and excluded from data analysis. There were 48 trials in each block. Blocks were run in a repeated sequence: a block with the inducing ring only was followed by a block with the inducing ring preceding the test ring, and a block with the test ring preceded the inducing ring. The temporal frequency and the rotation direction of the inducing ring was varied quasi-randomly within each block.

The combination of three *Test Ring* conditions (absent, preceding, and following the inducing ring) and four *Angular Velocities* of the inducing ring (225, 675, 900, and 1350°/s) produced 12 experimental conditions. There were 48 trials in each of these conditions: 24 with a clockwise inducing ring rotation and 24 in counter-clockwise rotation.

Statistical Analysis

We used signal detection methods to analyze performance (Macmillan & Creelman, 2005). We defined hits as clockwise responses to a clockwise rotation and false alarms as clockwise responses to a counter-clockwise rotation. Values of d' were estimated by measuring hit and false alarm rates separately for each subject in each condition and correcting these values

by applying the log-linear rule (Hautus, 1995). Across participants, mean *d′* measures were analyzed with a 2-way repeated measures analysis of variance (ANOVA) which evaluated the effect of angular velocity and test ring condition on observers' sensitivity to the inducing ring rotation. We will refer to these factors as *Angular Velocity* and *Test Ring*. All reported ANOVA *p*-values were corrected using Greenhouse-Geisser estimates of sphericity, but for the sake of readability, the uncorrected degrees of freedom are reported. Differences between specific conditions were evaluated with post hoc Bonferroni corrected two-tailed *t* tests. Performance levels in specific conditions were compared to a chance level of 50% with one-tailed Bonferroni corrected *t* tests that evaluated whether *d′* exceeded zero.

Results

Means and confidence intervals for sensitivity to the inducing ring rotation direction in the 24 conditions are shown in Figure 2. This data is also presented in terms of mean percent correct accuracy rates in Table 1. ANOVA outcomes are presented in Table 2. The main effects of both *Angular Velocity* and *Test Ring* were significant and there was a significant *Angular Velocity* × *Test Ring* interaction. Critically, mean sensitivity differed conspicuously in the three *Test Ring* conditions (see Figure 2). When the inducing ring was presented alone, mean sensitivity was high in the 10 Hz condition, but declined steeply to zero as *Angular Velocity* was increased (*d′* = 3.86, 0.37, 0.09, and 0.09 with 225, 675, 900, and 1350°/s, respectively). When the inducing ring was followed or preceded by the test ring, mean sensitivity declined linearly and stayed above zero even at the highest Angular Velocity employed. When the inducer preceded the test ring, *d′* values of 3.77, 2.60, 2.15, and 1.35 were observed with 225, 675, 900, and 1350°/s, respectively. When the test ring preceded the inducer, *d′* values of 3.85, 3.28, 2.41, and 1.31 were observed with these velocities. The contrast between the rapid decline to chance sensitivity in the inducer only condition and the gradual decline in conditions with the test ring is the source of the interaction *Angular Velocity* × *Test Ring* and reflects a basic characteristic of the MBE.

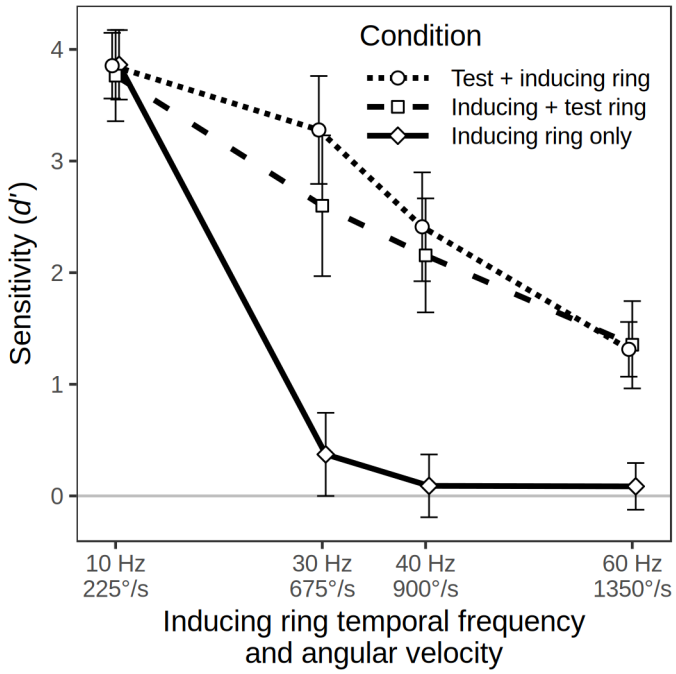

Figure 2. Mean sensitivity (*d'*) as a function of the angular velocity of the inducing ring in the inducing ring only condition (the solid black line), the condition where the inducing ring precedes the test ring (the dashed line), and the condition where the test ring precedes the inducing ring (the dotted line). The solid gray line indicates the chance level of accuracy (*d'* = 0). The error bars show 95% confidence intervals. Points and confidence intervals are slightly offset horizontally to improve their visibility.

Table 1

Mean percentage of correct direction reports.

	Angular Velocity (in °/s)			
Condition	225	675	900	1350
Inducing ring only	98.6	56.3	51.2	51.4
Inducing ring + Test ring	98.1	88.2	84.0	71.9
Test ring + Inducing ring	98.8	95.0	87.5	73.3

Table 2

ANOVA outcomes.

Effect	*Numerator df/Denominator df*	*F*	*p*
Angular Velocity	3/33	215.58	< .001
Test Ring	2/22	72.35	< .001
Angular Velocity × Test Ring	6/66	30.54	< .001

Note: The ANOVA was calculated on the d' values.

Importantly, the improvement in sensitivity to the inducing ring direction produced by the test ring presentation occurs even when subjects perform at chance in the inducing ring only condition. In the present investigation, four 1- tailed *t*-tests were run (one for each inducer velocity in the inducing ring only condition) to compare participants sensitivity to the inducing ring direction to a chance level of 50% ($d' = 0$). When a Bonferroni adjusted alpha level of .0125 was employed, the mean d' in the inducing ring only condition was significantly greater than zero only when the Angular Velocity was 225°/s ($p < .001$), and did not exceed zero in conditions with higher velocities ($p = .025$, $p = .248$, and $p = .194$, for 675, 900, and 1350°/s respectively). However, sensitivity was slightly better than chance with 675°/s when an uncorrected alpha level of .05 was employed, indicating in with this velocity it was sometimes possible for participants to detect the rotation direction. As can be seen in Figure 3, the pattern of results is very similar to that observed in the previous studies, which used oscilloscope displays (Matter & Fendrich, 2010; Stein, Fendrich and Mattler, 2019), and is consistent with Burr and Ross's study (1982), in which the detection of the motion of sinusoidal gratings starts to break down at around 30 Hz, which corresponds to an angular velocity of 675°/s.

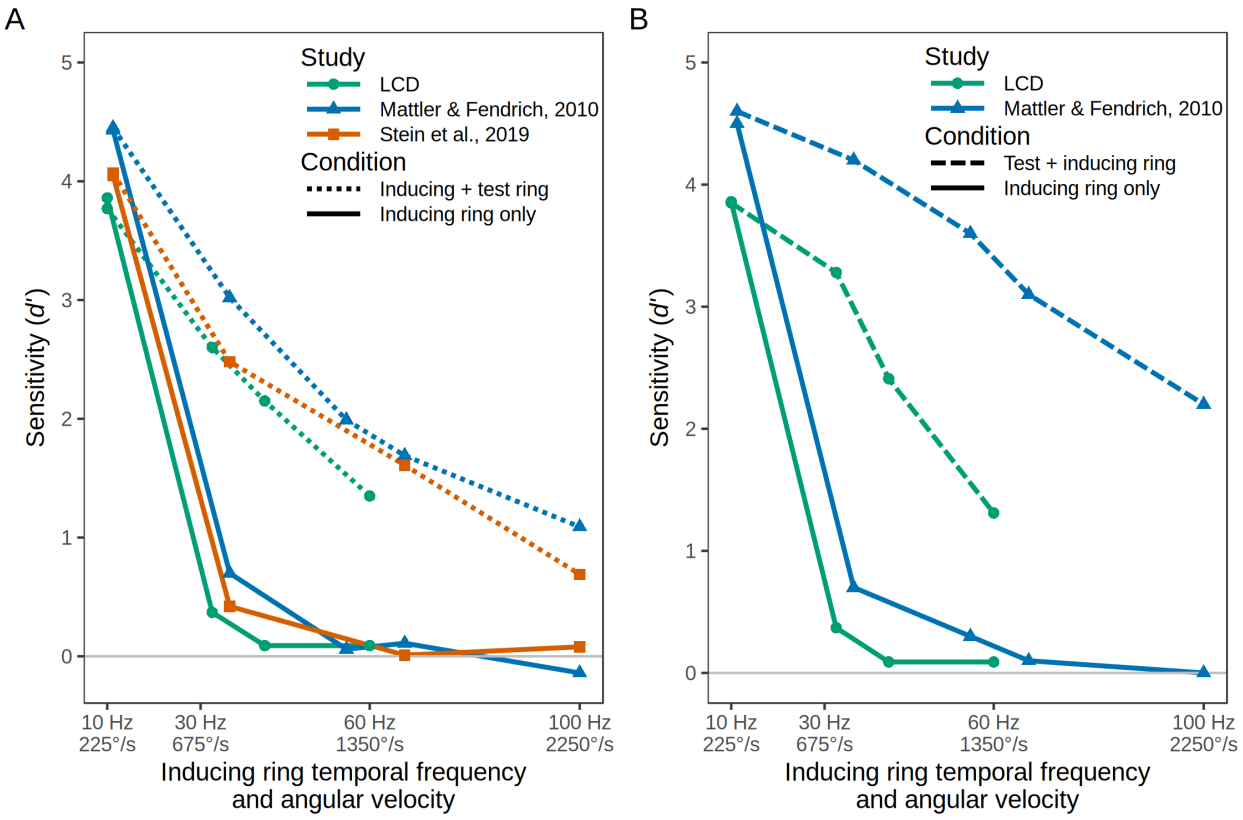

Figure 3. Mean sensitivity (*d'*) as a function of inducing ring angular velocity in the inducing ring only conditions (the solid black line) and the conditions where the test ring was presented (the dashed lines) in this study and its predecessors (Mattler & Fendrich, 2010. Stein et al., 2019). Panel A presents data from conditions where the test ring followed the inducing ring and panel B where it preceded the inducing ring. In all studies the mean sensitivity with a 16-point inducing ring is reported. The solid gray line indicates the chance level of accuracy ($d' = 0$).

While the contrast between the inducing-ring-only and the two test-ring-present conditions is the most striking aspect of Figure 2 and Figure 3, it can also be seen that the two test-ring-present conditions are not identical. Previously, Mattler & Fendrich (2010) reported that the MBE tends to be larger when the test ring precedes the inducing ring than when it follows the inducing ring. One-tailed post-hoc *t*-tests (with a Bonferroni adjusted alpha level of .0167) confirmed that a similar difference is also present in the current data when the Angular Velocity is 675°/s ($p < .005$), but not in the 900 and 1350°/s conditions. In addition, when the test ring precedes the inducing ring, participants sensitivity falls short in the present data when compared

to previous data (Figure 3). Both characteristics of the LCD screen and changes to the stimulus parameters used may have contributed to these differences.

Discussion

The ability of observers to perceive the motion of repetitive patterns is limited by the temporal frequency of the intensity modulations that those motions generate (Burr & Ross, 1982). The rapid rotations of the ring stimuli needed to demonstrate the MBE produce modulations too rapid to support conscious motion percepts, but not so rapid they prevent the encoding of information that can reveal the direction of the rotations. To study the processing of rapid motions of this kind requires a technology that enables screen displays to be updated at very rapid rates. This has previously been achieved by using analog oscilloscopes as the display device. Here we demonstrate that recent LCD monitors with 240 Hz frame rates can also be used to investigate these rapid motions.

In the present study participants could report the direction of an inducing ring rotation when the dots that formed the ring perimeter advanced at angular velocities of 225°/s and were refreshed at 10 Hz, but their performance decreased to near chance when the velocity was 675°/s (refresh rate 30 Hz), and completely to chance at velocities of 900°/s (refresh rate 40 Hz), and 1350°/s (refresh rate 60 Hz). The appearance of the inducing ring accords with this outcome: at refresh rates of 30 Hz and higher it is seen as a static circle of flicker-free dots. This ring of dots corresponds to the steady outline circle that was seen at high inducing ring velocities in previous MBE experiments conducted with oscilloscope screens. However, despite the static appearance of the inducing ring dots, when the inducing ring is followed by the veridically stationary 16-dot test ring, the test ring dots appear to briefly rotate, primarily in the same direction as the invisible inducing ring rotation. Similarly, when a stationary test ring precedes the inducing ring, that test ring appears to momentarily spin in the inducing ring direction when the inducing ring onsets. Mattler and Fendrich (2010) used the frequency of the reports in which the illusory test ring rotation matched the actual (although not consciously visible) direction of the inducing ring rotation as a quantitative measure of the MBE. The congruency rates obtained in the present study with comparable inducing ring velocities are similar to the rates they obtained.

The MBE demonstrates the human visual system can derive motion information from stimuli with temporal frequencies previously thought to exceed its processing capabilities. With

oscilloscope screens, this occurs with refresh rates of 100 Hz (Mattler & Fendrich, 2010) and higher (125 Hz in Stein et al., 2019). The present study shows that it is robust with an LCD screen when the inducing ring dots are refreshed at 60 Hz, which is at the upper limit of conventional CFF estimates (Kaufman, 1974) and exceeds the reported limits for the conscious detection of motion in repetitive stimuli (Burr & Ross, 1982; Kelly 1979). The MBE therefore extends the gamut of phenomena that reveal the visual system's processing of information that is not consciously visible.

The present study is the first to demonstrate that the MBE can be investigated with a readily available commercial system. It replicates the modulation of the MBE by the inducing ring's angular velocity both when the test ring precedes and follows the inducing ring (Mattler & Fendrich, 2010; Stein et al., 2019). This replication with new software and hardware gives added credence to previous descriptions of the MBE. Moreover, the differences between the LCD and oscilloscope display provide a demonstration of the MBE's generality. With the oscilloscope screen, the inducing and test rings were necessarily constructed from luminous points on a background close to totally black. On the LCD screen, however, slightly larger 0.12° dots were used and displayed on a dark gray background. In addition, the 240 Hz LCD frame rate remains well below the 1000 Hz "frame rate" used in the previous oscilloscope investigations. To achieve comparable inducing ring velocities with the lower frame rates, the dots had to be advanced in larger spatial steps. In consequence, the inducing ring looks like a chain of dots with the LCD rather than the continuous outline circle it appeared to be with the oscilloscope. Importantly, in both cases the inducing ring conveys no motion percept when the temporal frequencies exceed 30 Hz. We note, however, that the absence of any visible motion in the inducing ring strikes us as especially salient with the LCD screen because of the conspicuously static character of the inducing ring dots. We also note that although the motion illusion looks very similar on the two devices, our informal impression is that it appears to be briefer with a more abrupt start and stop on the LCD screen than on the oscilloscope. The display attributes that might produce differences in the appearance of the illusion of this kind remains to be determined.

In conclusion, the present study suggests that LCD monitors are a viable tool for the investigation of the MBE. Used in conjunction with MRI or EEG they may enable investigations of the physiological sources of the MBE. Although the frame rate of LCD monitors is still limited compared to that of the oscilloscope, they allow the effects of rapidly moving stimuli to

be examined using variables that cannot be readily manipulated on an oscilloscope. These include manipulations of shape and complexity, color, background luminance, contrast, and size. By uncovering new features of the MBE such studies could facilitate the development of new or more extensive theoretical accounts of the illusion.

Acknowledgments

The authors thank Marilena Reinhardt for their valuable support in recruiting participants and collecting data. We acknowledge support by the Open Access Publication Funds of the Goettingen University. The authors declare that the research was conducted in the absence of any commercial or financial relationships that could be construed as a potential conflict of interest.

References

Brown, R. H. (1958). Influence of stimulus luminance upon the upper speed threshold for the visual discrimination of movement. *Journal of the Optical Society of America*, 48, 125–128. https://doi.org/10.1364/JOSA.48.000125

Burr, D. C., & Ross, J. (1982). Contrast sensitivity at high velocities. *Vision Research*, *22*, 479–484. https://doi.org/10.1016/0042-6989(82)90196-1

Cornsweet, T. N. (1970). *Visual perception*. New York, NY: Academic Press.

Hartmann, E., Lachenmayr, B., & Brettel, H. (1979). The peripheral critical flicker frequency. *Vision Research*, *19*, 1019–1023. https://doi.org/10.1016/0042-6989(79)90227-X

Hautus, M. J. (1995). Corrections for extreme proportions and their biasing effects on estimated values of *d'*. *Behavior Research Methods, Instruments, & Computers*, *27*, 46–51. https://doi.org/10.3758/BF03203619

He, S., & MacLeod, D. I. A. (1996). Local luminance nonlinearity and receptor aliasing in the detection of high-frequency gratings. *Journal of the Optical Society of America A*, *13*, 1139–1151. https://doi.org/10.1364/JOSAA.13.001139

He, S., & MacLeod, D. I. A. (2001). Orientation-selective adaptation and tilt after-effect from invisible patterns. *Nature*, *411*, 473–476. https://doi.org/10.1038/35078072

Kaufman, L. (1974). *Sight and mind: An introduction to visual perception*. New York, NY: Oxford University Press.

Kelly, D. H. (1979). Motion and vision. II. Stabilized spatio-temporal threshold surface. *Journal of the Optical Society of America*, *69*, 1340–1349. https://doi.org/10.1364/JOSA.69.001340

Macmillan, N. A., & Creelman, C. D. (2005). *Detection theory: A user's guide* (2nd ed.). Mahwah, NJ: Lawrence Erlbaum Associates.

Mattler, U., & Fendrich, R. (2010). Consciousness mediated by neural transition states: How invisibly rapid motions can become visible. *Consciousness and Cognition*, *19*, 172–185. https://doi.org/10.1016/j.concog.2009.12.015

Mattler, U., Stein, M., & Fendrich, R. (2019). *Ring rotation illusion: A new type of apparent motion*. Manuscript in preparation.

Shady, S., MacLeod, D. I. A., & Fisher, H. S. (2004). Adaptation from invisible flicker. *Proceedings of the National Academy of Sciences of the United States of America*, *101*, 5170–5173. https://doi.org/10.1073/pnas.0303452101

Stein, M., Fendrich, R., & Mattler, U. (2019). Stimulus dependencies of an illusory motion: Investigations of the Motion Bridging Effect. *Journal of Vision*, *19*, 1–23. https://doi.org/10.1167/19.5.13

Wang, P., & Nikolić, D. (2011). An LCD Monitor with Sufficiently Precise Timing for Research in Vision. *Frontiers in Human Neuroscience*, *5*, 1–10. https://doi.org/10.3389/fnhum.2011.00085

Zhang, G.-L., Li, A.-S., Miao, C.-G., He, X., Zhang, M., & Zhang, Y. (2018). A consumer-grade LCD monitor for precise visual stimulation. *Behavior Research Methods*, *50*, 1496–1502. https://doi.org/10.3758/s13428-018-1018-7

Octave script

```
# This code was executed in Octave 5.1.0. Each of the following calculations, first creates an array containing
# the temporal distances in seconds between a point in the inducing ring and the beginning of the test ring. Then,
# for each condition, two more arrays are created which cover the spatial distances of the point in the inducing
# ring to the two nearest test ring points (in clockwise and counterclockwise direction) at the respective temporal
# distance. In the last step, each of the spatial distances is divided by the respective temporal distance to obtain
# the velocity, the average velocity for both directions (clockwise and counterclockwise) is determined and the
# difference between these velocities is calculated.

# The following code produces the differences in mean velocity of the conditions realized in Mattler and
# Fendrich (2010) The output values are shown in Figure 2 of the summary of this thesis.
isi=60;
temp_dist=([90:-1:0]+isi)/1000;
diameter=5;
point_dist=2*pi*diameter/2/16;

stepnumber=30;
spatial_dist_cw_750=[0,repmat(linspace(point_dist,0,stepnumber+1)(:,2:stepnumber+1),1,3)];
spatial_dist_ccw_750=[repmat(linspace(0,point_dist,stepnumber+1)(:,1:stepnumber),1,3),0];

stepnumber=18;
spatial_dist_cw_1250=[0,repmat(linspace(point_dist,0,stepnumber+1)(:,2:stepnumber+1),1,5)];
spatial_dist_ccw_1250=[repmat(linspace(0,point_dist,stepnumber+1)(:,1:stepnumber),1,5),0];

stepnumber=15;
spatial_dist_cw_1500=[0,repmat(linspace(point_dist,0,stepnumber+1)(:,2:stepnumber+1),1,6)];
spatial_dist_ccw_1500=[repmat(linspace(0,point_dist,stepnumber+1)(:,1:stepnumber),1,6),0];

stepnumber=10;
spatial_dist_cw_2250=[0,repmat(linspace(point_dist,0,stepnumber+1)(:,2:stepnumber+1),1,9)];
spatial_dist_ccw_2250=[repmat(linspace(0,point_dist,stepnumber+1)(:,1:stepnumber),1,9),0];

mean(spatial_dist_ccw_750./temp_dist)-mean(spatial_dist_cw_750./temp_dist)
mean(spatial_dist_ccw_1250./temp_dist)-mean(spatial_dist_cw_1250./temp_dist)
mean(spatial_dist_ccw_1500./temp_dist)-mean(spatial_dist_cw_1500./temp_dist)
mean(spatial_dist_ccw_2250./temp_dist)-mean(spatial_dist_cw_2250./temp_dist)
```

```
# The following code produces the differences of the mean velocity of the conditions realized in Experiment 1
# of Stein et al (2019). The output values are shown in Figure 3A of the summary of this thesis.

isi=60;
temp_dist=([120:-1:0]+isi)/1000;
diameter=5.5;
point_dist=2*pi*diameter/2/12;

stepnumber=40;
spatial_dist_cw_750_12=[0,repmat(linspace(point_dist,0,stepnumber+1)(:,2:stepnumber+1),1,3)];
spatial_dist_ccw_750_12=[repmat(linspace(0,point_dist,stepnumber+1)(:,1:stepnumber),1,3),0];
stepnumber=20;
spatial_dist_cw_1500_12=[0,repmat(linspace(point_dist,0,stepnumber+1)(:,2:stepnumber+1),1,6)];
spatial_dist_ccw_1500_12=[repmat(linspace(0,point_dist,stepnumber+1)(:,1:stepnumber),1,6),0];
stepnumber=12;
spatial_dist_cw_2250_12=[0,repmat(linspace(point_dist,0,stepnumber+1)(:,2:stepnumber+1),1,10)];
spatial_dist_ccw_2250_12=[repmat(linspace(0,point_dist,stepnumber+1)(:,1:stepnumber),1,10),0];

point_dist=2*pi*diameter/2/16;
stepnumber=30;
spatial_dist_cw_750_16=[0,repmat(linspace(point_dist,0,stepnumber+1)(:,2:stepnumber+1),1,4)];
spatial_dist_ccw_750_16=[repmat(linspace(0,point_dist,stepnumber+1)(:,1:stepnumber),1,4),0];
stepnumber=15;
spatial_dist_cw_1500_16=[0,repmat(linspace(point_dist,0,stepnumber+1)(:,2:stepnumber+1),1,8)];
spatial_dist_ccw_1500_16=[repmat(linspace(0,point_dist,stepnumber+1)(:,1:stepnumber),1,8),0];
stepnumber=10;
spatial_dist_cw_2250_16=[0,repmat(linspace(point_dist,0,stepnumber+1)(:,2:stepnumber+1),1,12)];
spatial_dist_ccw_2250_16=[repmat(linspace(0,point_dist,stepnumber+1)(:,1:stepnumber),1,12),0];

point_dist=2*pi*diameter/2/20;
stepnumber=24;
spatial_dist_cw_750_20=[0,repmat(linspace(point_dist,0,stepnumber+1)(:,2:stepnumber+1),1,5)];
spatial_dist_ccw_750_20=[repmat(linspace(0,point_dist,stepnumber+1)(:,1:stepnumber),1,5),0];
stepnumber=12;
spatial_dist_cw_1500_20=[0,repmat(linspace(point_dist,0,stepnumber+1)(:,2:stepnumber+1),1,10)];
spatial_dist_ccw_1500_20=[repmat(linspace(0,point_dist,stepnumber+1)(:,1:stepnumber),1,10),0];
stepnumber=8;
spatial_dist_cw_2250_20=[0,repmat(linspace(point_dist,0,stepnumber+1)(:,2:stepnumber+1),1,15)];
spatial_dist_ccw_2250_20=[repmat(linspace(0,point_dist,stepnumber+1)(:,1:stepnumber),1,15),0];
```

```
mean(spatial_dist_ccw_750_12./temp_dist)-mean(spatial_dist_cw_750_12./temp_dist)
mean(spatial_dist_ccw_1500_12./temp_dist)-mean(spatial_dist_cw_1500_12./temp_dist)
mean(spatial_dist_ccw_2250_12./temp_dist)-mean(spatial_dist_cw_2250_12./temp_dist)

mean(spatial_dist_ccw_750_16./temp_dist)-mean(spatial_dist_cw_750_16./temp_dist)
mean(spatial_dist_ccw_1500_16./temp_dist)-mean(spatial_dist_cw_1500_16./temp_dist)
mean(spatial_dist_ccw_2250_16./temp_dist)-mean(spatial_dist_cw_2250_16./temp_dist)

mean(spatial_dist_ccw_750_20./temp_dist)-mean(spatial_dist_cw_750_20./temp_dist)
mean(spatial_dist_ccw_1500_20./temp_dist)-mean(spatial_dist_cw_1500_20./temp_dist)
mean(spatial_dist_ccw_2250_20./temp_dist)-mean(spatial_dist_cw_2250_20./temp_dist)

# The following code produces the differences of the mean velocity of the conditions realized in Experiment 2
# of Stein et al (2019). The output values are shown in Figure 3B of the summary of this thesis.

isi=60;
temp_dist=([90:-1:0]+isi)/1000;
diameter=3.5;
point_dist=2*pi*diameter/2/16;

stepnumber=30;
spatial_dist_cw_750=[0,repmat(linspace(point_dist,0,stepnumber+1)(:,2:stepnumber+1),1,3)];
spatial_dist_ccw_750=[repmat(linspace(0,point_dist,stepnumber+1)(:,1:stepnumber),1,3),0];

stepnumber=15;
spatial_dist_cw_1500=[0,repmat(linspace(point_dist,0,stepnumber+1)(:,2:stepnumber+1),1,6)];
spatial_dist_ccw_1500=[repmat(linspace(0,point_dist,stepnumber+1)(:,1:stepnumber),1,6),0];

stepnumber=10;
spatial_dist_cw_2250=[0,repmat(linspace(point_dist,0,stepnumber+1)(:,2:stepnumber+1),1,9)];
spatial_dist_ccw_2250=[repmat(linspace(0,point_dist,stepnumber+1)(:,1:stepnumber),1,9),0];

mean(spatial_dist_ccw_750./temp_dist)-mean(spatial_dist_cw_750./temp_dist)
mean(spatial_dist_ccw_1500./temp_dist)-mean(spatial_dist_cw_1500./temp_dist)
mean(spatial_dist_ccw_2250./temp_dist)-mean(spatial_dist_cw_2250./temp_dist)

diameter=5.5;
point_dist=2*pi*diameter/2/16;
```

```
stepnumber=30;
spatial_dist_cw_750=[0,repmat(linspace(point_dist,0,stepnumber+1)(:,2:stepnumber+1),1,3)];
spatial_dist_ccw_750=[repmat(linspace(0,point_dist,stepnumber+1)(:,1:stepnumber),1,3),0];

stepnumber=15;
spatial_dist_cw_1500=[0,repmat(linspace(point_dist,0,stepnumber+1)(:,2:stepnumber+1),1,6)];
spatial_dist_ccw_1500=[repmat(linspace(0,point_dist,stepnumber+1)(:,1:stepnumber),1,6),0];

stepnumber=10;
spatial_dist_cw_2250=[0,repmat(linspace(point_dist,0,stepnumber+1)(:,2:stepnumber+1),1,9)];
spatial_dist_ccw_2250=[repmat(linspace(0,point_dist,stepnumber+1)(:,1:stepnumber),1,9),0];

mean(spatial_dist_ccw_750./temp_dist)-mean(spatial_dist_cw_750./temp_dist)
mean(spatial_dist_ccw_1500./temp_dist)-mean(spatial_dist_cw_1500./temp_dist)
mean(spatial_dist_ccw_2250./temp_dist)-mean(spatial_dist_cw_2250./temp_dist)

diameter=7.5;
point_dist=2*pi*diameter/2/16;

stepnumber=30;
spatial_dist_cw_750=[0,repmat(linspace(point_dist,0,stepnumber+1)(:,2:stepnumber+1),1,3)];
spatial_dist_ccw_750=[repmat(linspace(0,point_dist,stepnumber+1)(:,1:stepnumber),1,3),0];

stepnumber=15;
spatial_dist_cw_1500=[0,repmat(linspace(point_dist,0,stepnumber+1)(:,2:stepnumber+1),1,6)];
spatial_dist_ccw_1500=[repmat(linspace(0,point_dist,stepnumber+1)(:,1:stepnumber),1,6),0];

stepnumber=10;
spatial_dist_cw_2250=[0,repmat(linspace(point_dist,0,stepnumber+1)(:,2:stepnumber+1),1,9)];
spatial_dist_ccw_2250=[repmat(linspace(0,point_dist,stepnumber+1)(:,1:stepnumber),1,9),0];

mean(spatial_dist_ccw_750./temp_dist)-mean(spatial_dist_cw_750./temp_dist)
mean(spatial_dist_ccw_1500./temp_dist)-mean(spatial_dist_cw_1500./temp_dist)
mean(spatial_dist_ccw_2250./temp_dist)-mean(spatial_dist_cw_2250./temp_dist)
```

```
# The following code produces the differences of the mean velocity of the conditions realized in Experiment 3
# of Stein et al (2019). The output values are shown in Figure 3C of the summary of this thesis.

isi=60;
temp_dist=([120:-1:0]+isi)/1000;

diameter=4.125;
point_dist=2*pi*diameter/2/12;
stepnumber=40;
spatial_dist_cw_750_12=[0,repmat(linspace(point_dist,0,stepnumber+1)(:,2:stepnumber+1),1,3)];
spatial_dist_ccw_750_12=[repmat(linspace(0,point_dist,stepnumber+1)(:,1:stepnumber),1,3),0];
stepnumber=20;
spatial_dist_cw_1500_12=[0,repmat(linspace(point_dist,0,stepnumber+1)(:,2:stepnumber+1),1,6)];
spatial_dist_ccw_1500_12=[repmat(linspace(0,point_dist,stepnumber+1)(:,1:stepnumber),1,6),0];
stepnumber=12;
spatial_dist_cw_2250_12=[0,repmat(linspace(point_dist,0,stepnumber+1)(:,2:stepnumber+1),1,10)];
spatial_dist_ccw_2250_12=[repmat(linspace(0,point_dist,stepnumber+1)(:,1:stepnumber),1,10),0];

diameter=5.5;
point_dist=2*pi*diameter/2/16;
stepnumber=30;
spatial_dist_cw_750_16=[0,repmat(linspace(point_dist,0,stepnumber+1)(:,2:stepnumber+1),1,4)];
spatial_dist_ccw_750_16=[repmat(linspace(0,point_dist,stepnumber+1)(:,1:stepnumber),1,4),0];
stepnumber=15;
spatial_dist_cw_1500_16=[0,repmat(linspace(point_dist,0,stepnumber+1)(:,2:stepnumber+1),1,8)];
spatial_dist_ccw_1500_16=[repmat(linspace(0,point_dist,stepnumber+1)(:,1:stepnumber),1,8),0];
stepnumber=10;
spatial_dist_cw_2250_16=[0,repmat(linspace(point_dist,0,stepnumber+1)(:,2:stepnumber+1),1,12)];
spatial_dist_ccw_2250_16=[repmat(linspace(0,point_dist,stepnumber+1)(:,1:stepnumber),1,12),0];

diameter=6.875;
point_dist=2*pi*diameter/2/20;
stepnumber=24;
spatial_dist_cw_750_20=[0,repmat(linspace(point_dist,0,stepnumber+1)(:,2:stepnumber+1),1,5)];
spatial_dist_ccw_750_20=[repmat(linspace(0,point_dist,stepnumber+1)(:,1:stepnumber),1,5),0];
stepnumber=12;
spatial_dist_cw_1500_20=[0,repmat(linspace(point_dist,0,stepnumber+1)(:,2:stepnumber+1),1,10)];
spatial_dist_ccw_1500_20=[repmat(linspace(0,point_dist,stepnumber+1)(:,1:stepnumber),1,10),0];
stepnumber=8;
spatial_dist_cw_2250_20=[0,repmat(linspace(point_dist,0,stepnumber+1)(:,2:stepnumber+1),1,15)];
```

```
spatial_dist_ccw_2250_20=[repmat(linspace(0,point_dist,stepnumber+1)(:,1:stepnumber),1,15),0];

mean(spatial_dist_ccw_750_12./temp_dist)-mean(spatial_dist_cw_750_12./temp_dist)
mean(spatial_dist_ccw_1500_12./temp_dist)-mean(spatial_dist_cw_1500_12./temp_dist)
mean(spatial_dist_ccw_2250_12./temp_dist)-mean(spatial_dist_cw_2250_12./temp_dist)

mean(spatial_dist_ccw_750_16./temp_dist)-mean(spatial_dist_cw_750_16./temp_dist)
mean(spatial_dist_ccw_1500_16./temp_dist)-mean(spatial_dist_cw_1500_16./temp_dist)
mean(spatial_dist_ccw_2250_16./temp_dist)-mean(spatial_dist_cw_2250_16./temp_dist)

mean(spatial_dist_ccw_750_20./temp_dist)-mean(spatial_dist_cw_750_20./temp_dist)
mean(spatial_dist_ccw_1500_20./temp_dist)-mean(spatial_dist_cw_1500_20./temp_dist)
mean(spatial_dist_ccw_2250_20./temp_dist)-mean(spatial_dist_cw_2250_20./temp_dist)



# The following code produces the differences of the mean velocity of the conditions realized in the third
# manuscript of this thesis. The output values are shown in Figure 4 of the summary of this thesis.

for displacement = 0:9
isi=60;
temp_dist=([90:-1:0]+isi)/1000;
diameter=7.5;
point_dist=2*pi*diameter/2/16;

stepnumber=10;
spatial_dist_cw_2250=[repmat(linspace(point_dist,0,stepnumber+1)(:,2:stepnumber+1),1,9)];
spatial_dist_cw_2250=circshift(spatial_dist_cw_2250,-displacement);
spatial_dist_cw_2250=[spatial_dist_cw_2250(90),spatial_dist_cw_2250];
spatial_dist_ccw_2250=[repmat(linspace(0,point_dist,stepnumber+1)(:,1:stepnumber),1,9)];
spatial_dist_ccw_2250=circshift(spatial_dist_ccw_2250,-displacement);
spatial_dist_ccw_2250=[spatial_dist_ccw_2250,spatial_dist_ccw_2250(1)];

mean(spatial_dist_ccw_2250./temp_dist)-mean(spatial_dist_cw_2250./temp_dist)
end

for displacement = 0:14
stepnumber=15;
spatial_dist_cw_1500=[repmat(linspace(point_dist,0,stepnumber+1)(:,2:stepnumber+1),1,6)];
spatial_dist_cw_1500=circshift(spatial_dist_cw_1500,-displacement);
```

```
spatial_dist_cw_1500=[spatial_dist_cw_1500(90),spatial_dist_cw_1500];
spatial_dist_ccw_1500=[repmat(linspace(0,point_dist,stepnumber+1)(:,1:stepnumber),1,6)];
spatial_dist_ccw_1500=circshift(spatial_dist_ccw_1500,-displacement);
spatial_dist_ccw_1500=[spatial_dist_ccw_1500,spatial_dist_ccw_1500(1)];

mean(spatial_dist_ccw_1500./temp_dist)-mean(spatial_dist_cw_1500./temp_dist)
end

for displacement = 0:29
stepnumber=30;
spatial_dist_cw_750=[repmat(linspace(point_dist,0,stepnumber+1)(:,2:stepnumber+1),1,3)];
spatial_dist_cw_750=circshift(spatial_dist_cw_750,-displacement);
spatial_dist_cw_750=[spatial_dist_cw_750(90),spatial_dist_cw_750];
spatial_dist_ccw_750=[repmat(linspace(0,point_dist,stepnumber+1)(:,1:stepnumber),1,3)];
spatial_dist_ccw_750=circshift(spatial_dist_ccw_750,-displacement);
spatial_dist_ccw_750=[spatial_dist_ccw_750,spatial_dist_ccw_750(1)];

mean(spatial_dist_ccw_750./temp_dist)-mean(spatial_dist_cw_750./temp_dist)
end
```